2009-01-01

Multidisciplinary Modeling, Control, and Optimization of a Solid Oxide Fuel Cell/Gas Turbine Hybrid Power System

Atid Abbassi Baharanchi
University of Miami, aabbasibaharanchi@umiami.edu

UNIVERSITY OF MIAMI

MULTIDISCIPLINARY MODELING, CONTROL AND OPTIMIZATION OF A SOLID OXIDE FUEL CELL/GAS TURBINE HYBRID POWER SYSTEM

By

Atid Abbassi Baharanchi

A THESIS

Submitted to the Faculty
of the University of Miami
in partial fulfillment of the requirements for
the degree of Master of Science

Coral Gables, Florida

May 2009

UNIVERSITY OF MIAMI

A thesis submitted in partial fulfillment of
the requirements for the degree of
Master of Science

MULTIDISCIPLINARY MODELING, CONTROL AND OPTIMIZATION OF A SOLID OXIDE FUEL CELL/GAS TURBINE HYBRID POWER SYSTEM

Atid Abbassi Baharanchi

Approved:

_____
Zhenhua Jiang, Ph.D.
Professor of Electrical
and Computer Engineering

_____
Terri A. Scandura, Ph.D.
Dean of the Graduate School

_____
Michael Swain, Ph.D.
Professor of Mechanical Engineering

_____
Miroslav Kubat, Ph.D.
Professor of Electrical
and Computer Engineering

ABBASSI BAHARANCHI, ATID (M.S., Electical Engineering)

Multidisciplinary Modeling, Control and Optimization of a Solid Oxide Fuel Cell/ Gas Turbine Hybrid Power System

(May 2009)

Abstract of a thesis at the University of Miami.

Thesis supervised by Professor Zhenhua Jiang.
No. of pages in text. (105)

This thesis describes a systematical study, including multidisciplinary modeling, simulation, control, and optimization, of a fuel cell – gas turbine hybrid power system that aims to increase the system efficiency and decrease the energy costs by combining two power sources.

The fuel cell-gas turbine hybrid power systems can utilize exhaust fuel and waste heat from fuel cells in the gas turbines to increase system efficiency. This research considers a hybrid power system consisting of an internally reforming solid oxide fuel cell and a gas turbine. In the hybrid power system, the anode exhaust, which contains the remainder of the fuel, is mixed with the cathode exhaust as well as an additional supply of fuel and compressed air and then burned in a catalytic oxidizer. The hot oxidizer exhaust is expanded through the turbine section, driving an electric generator. After leaving the gas turbine, the oxidizer exhaust passes through a heat recovery unit in which it preheats the compressed air that is to be supplied to the fuel cell and the oxidizer.

This research concentrates on multidisciplinary modeling and simulation of the fuel cell-gas turbine hybrid power system. Different control strategies for the power sharing between the subsystems are investigated. Also, the power electronics interfaces and controls for the hybrid power system are discussed. Two different power sharing

strategies are studied and compared. Simulation results are presented and analyzed. Transient response of the hybrid energy system is studied through time-domain simulation. In addition, in this effort, Particle Swarm Optimization (PSO) is used to optimize the power sharing for the hybrid power system to increase the efficiency and decrease the fuel consumption.

To my beloved Parents

and

to my loyal husband

ACKNOWLEDGMENTS

First, I would like to express my sincere gratitude to all those who gave me the possibility to complete my thesis . Special thanks to my advisor Dr. Zhenhua Jiang who helped me during my study in University of Miami. He encouraged me to pursue novel ideas and provided me with exceptional experience and knowledge.

My thanks also go to the other members of the committee, Dr. Michael Swain, and Dr. Miroslav Kubat for their valuable comments and suggestions. In particular, I want to thank Dr. Michael Swain for his valuable support, comments, and encouragement during my research.

Also I have to indicate that this work was supported in part by the National Science Foundation under grants ECCS-0652300.

In addition, I want to thanks to Dr. James W. Modestino ,Dr. Abdel-Mottaleb and Dr. Kamal Premaratne for their supports during my study at UM.

More than everyone, I am indebted to my parents for their enthusiastic encouragement, prayers and unlimited support during all the stage of my life. Also, I must express my appreciation to my Loyal and kind husband Rooholah who helped me to finish my study and encouraged me to continue my research,

I would like to extend my thanks to the faculty and staff members of the Electrical and Computer Engineering Department at the University of Miami, especially Ms. Clarisa Alvarez, Ms. Rosamund Coutts, and Ms. Marisol Ternas for their role in my education and various resources made available to me to do my research.

Also, I wan to thank my fellow lab members, specially, Habibolah Rahimi, for their collaboration during the completion of this thesis.

Also I would like to thanks my friends, Dr. Beladi, Dr. Mohamad H. Mahor , Zahra Daftariyan and Maryam Vejdani who helped me to finish my thesis.

I grateful to my friends Naicy Sarduy and her family, Dr. Mohyedin Mesbahi and Dr. Hamid Serri for their kindness and help during last three years that I lived in Miami.

Contents

List of Figures

List of Tables

List of Acronyms

AC: Alternative Current

ACA: Ant Colony Algorithm

AFC: Alkaline fuel cell (AFC)

BA: Bees Algorithm

CHP: Combined Heat and Power

DC: Direct Current

GA: Genetic Algorithm

GT: Gas Turbine

MCFC: Molten carbonate fuel cell (MCFC)

PAFC: Phosphoric acid fuel cell (PAFC)

PEFC: Polymer electrolyte fuel cell (),

PEM: Proton Exchange Membrane (PEM)

PI: Proportional Integral

PSO: Particle Swarm Optimization

PWM: Pulse Width Modulation

SOFC: Solid Oxide Fuel Cell

U_z: Utilization Factor

Chapter 1

Introduction

In recent years, energy has become one of the most challenging aspects of human life. Developing the industry and improving the science world, has a challenge that renders much impact on the electrical power industry. In this respect various energy resources to produce the electricity, including renewable and nonrenewable resources, are introduced to the power industry. These energy resources have their own characteristics which limit them to use them in specific applications.

For instance, increasing use and diminishing resources of fossil fuels and concerns about environmental issues such as emissions and global warming are leading people to pay more attention to alternative resources of energy. Although renewable energy such as wind and solar power is promising in power generation, their resources are intermittent. Power generation from these resources is fluctuating with the wind or sunlight, and large-scale energy storage devices are needed. As a result, combining these resources of energy with other such as batteries or fuel cells will help to improve the reliability and efficiency of them. Therefore, to improve the use of the property of the energy resources, the combination of them is more appropriate. In this respect, the hybrid power system has been introduced to the electrical world.

1.1 Hybrid Power System

The hybrid power system, by definition, utilizes a combination of different energy recourses to produce electricity. The purpose of using hybrid power systems is to combine different properties of various power sources to get better advantages of them to achieve a global goal. High power density, fast transient response, maximum efficiency, minimum emission, and minimum costs are examples of the global goal for different applications.

One example of hybrid power systems is the combination of batteries with ultracapacitors. Chemical batteries have been used as electric energy storage devices for a long time. Batteries have relatively high energy densities and low power densities. But batteries have to be oversized to accommodate a peak power demand. On the other hand, the unique electrochemical characteristics of ultracapacitors are able to provide a much higher pulse current capability over the battery system. A combination of battery and ultracapacitor can improve the battery capability for power peak and also extend battery lifetime [3].

Fuel cell generators are considered to be an alternative power source for automotive propulsion, residential power systems, portable electricity generation, or back-up power supplies because of their clean and energy-efficient mode of operation. In most applications, it is very important to minimize the time needed to warm up the fuel cell system. For example, in a vehicle it is expected that after starting the vehicle customer can drive away immediately. However, even for low-temperature fuel cell systems it is a very hard to overcome the transient power limitations during warm-up (e.g., due to water flooding in the gas diffusion layers or reduced fuel cell efficiency). A good solution to

this problem is system hybridization. The hybrid system which is used in this case is a combination of the primary energy conversion devices (the fuel cell system) with an energy storage system, such as an electrochemical battery. In the case of a cold start, the energy storage system can be used to guarantee the power output demanded throughout this temperature-transient phase and, preferably in combination with an auxiliary heating device, to accelerate the system warm-up. A hybrid power system combining of these two energy resources can have benefits of high energy densities of the fuel cell as well as high power density of the battery and lead to longer battery life [4].

It is apparent that energy resources currently available to us in the form of nonrenewable fossil fuels (coal, oil, natural gas) and nuclear fuels are limited, and cannot be reproduced in short time spans. In addition, these resources produce the greatest amount of pollution in our atmosphere. Therefore, this growing energy consumption and depletion of fossil-fuel energy resources, in addition to the increasing concern for environmental issues such as global warming, have endorsed the use of renewable energy resources. Some examples include biomass resources (plant material or organic waste), geothermal (the natural heat in the earth), hydropower sources (the force of moving water from rivers or storage reservoirs), mechanical energy of ocean tides, currents, waves, as well as solar and wind energy.

Although use of renewable energy has become the center of attention, it is nonetheless expensive and unreliable. For instance, efficient use of wind energy is contingent on its availability and is dependent on the speed of the wind. Solar energy, as well is a resource that is not available at night. Therefore in order to get the maximum efficiency from these sources, it is best to use appropriate combinations of resulting in the

highest advantage. Therefore, recently designing most economic and reliable hybrid power system has been the center of attention.

The most common examples of hybrid power systems using renewable energy are as follows:

- Wind generation combined with diesel generation
- Photovoltaic generation joined with battery storage or diesel generation
- Combination of fuel cell with gas turbine generator

Among different configurations of the hybrid power system, the combination of gas turbine and fuel cells is very common to get the high efficiency. Therefore, interest in the hybrid system has grown with recent improvement of Gas Turbine (GT) technologies and maturity of fuel cells. A research program, Vision 21, was carried out by the United State's Department of Energy in 1997 for determining the conceptual feasibility of high-efficient fossil power plants [35]. The aim of this program was to develop a hybrid power system with minimum efficiency of 75%. As a result, the integration of fuel cell and GT was established to achieve the goals of the Vision 21 program due to its high-performance and low-emission. [1]

1.2 Fuel Cell - Gas Turbine Hybrid Power System

Fuel cells are well known sources of power generation, which produce electricity through an electromechanical process producing heat. They are considered as one of the most promising technologies for power production in stationary applications.

Fuel cells are attractive as energy sources because they are clean, reliable, and almost entirely nonpolluting. Also since they do not have any moving parts and the cells are

therefore vibration-free, the noise pollution associated with power generation is also eliminated. In addition, fuel cell systems can provide high efficiency (40%-60%).

A variety of fuel cells are in different stages of development. The most common classification of fuel cells is by the type of electrolyte used in the cells and includes proton exchange membrane (PEM), alkaline fuel cell (AFC), phosphoric acid fuel cell (PAFC), molten carbonate fuel cell (MCFC), and solid oxide fuel cell (SOFC). Broadly, the kind of electrolyte determines the operating temperature range of the fuel cell. The operating temperature and useful lifetime of a fuel cell dictate the physicochemical and thermo mechanical properties of materials used in the cell components (i.e., electrodes, electrolyte, interconnect, current collector, etc.). Aqueous electrolytes operate under temperature limitation of about 200 °C or lower because of their high vapor pressure and rapid degradation at higher temperatures. The operating temperature also has an important impact in determining the degree of fuel processing required. In low-temperature fuel cells, the fuel which is used in the fuel cell is hydrogen. Therefore, all the fuel must be converted to hydrogen prior to entering the fuel cell. In addition, the anode catalyst in low temperature fuel cells (mainly platinum) is strongly poisoned by CO. In high-temperature such as SOFC fuel cells, CO and even CH4 can be internally converted to hydrogen or even directly oxidized electrochemically [59]. Table 1.1 introduces some kind of existing fuel cells and their operational characteristics.

Type	Electrolyte material	Fuel	Operating temperature (°C)	Applications
PEM	Hydrated organic polymer	H_2	70-85	Transport
PAFC	Phosphoric acid	H_2	150-220	CHP (combined heat & power)
MCFC	Molten Li/Na/K carbonate	H_2,CO	600-700	CHP power generation
SOFC	Yttria-doped zirconia	H_2,CO	1000	CHP power generation

Table 1.1 Properties of fuel cells [77]

Since SOFCs' have high operating temperature and they can use currently available fossil fuels, thus reducing operating costs, most of the power generation applications have focused on solid oxide fuel cells (SOFC).

On the other hand, the transient response of SOFC is very slow. Therefore, another energy generator is used to improve the system behavior in transient situation. Gas turbine generators (GT), have a fast response to the step changes. As a result they could be an appropriate component to combine with SOFC.

Hybrid power plants combining SOFC with GT also can improve the total efficiency of the system. As long as SOFC's always can not use all the supplied fuel, the waste fuel can be injected to the gas turbine combustor. This fact increases the overall efficiency if the hybrid power system. In addition, SOFC works in high temperature. Since the fuel injected to the combustor needs to be preheated, using the heat produced in an SOFC increase the efficiency of the system.

1.3 System Modeling and Control

Both SOFC and gas turbine are very complex components. By combining these two generators together, due to the tight integration between them in a hybrid power system, dynamic operability and hence control of the process is a challenge. Therefore, modeling is the first and most important step in studying the behavior of these components individually and interdependently.

Considerable works have been done to model SOFC [6]-[11]. Some of these studies have been developed the dynamic model based on the pressure effect on the fuel cells [10],[7],[8]. Some of them have developed an electrical model for SOFC [9],[6].

The control issue is another important challenge in design of fuel cell systems. It is very important to design a control system to maintain the appropriate fuel and air flow rate to produce the desire output power. Several studies have been denoted to study the different control strategy for power and fuel control in fuel cell generators [55]-[56].

Furthermore, some studies have improved the gas turbine model [12]-[18]. Among them some presented the dynamic model of gas turbine [12] [14][18][15]. There are several researches, which have investigated the appropriate model for the advanced gas turbine [13]. Controlling gas turbine is also one of the important issues in this area. Since gas turbines perform in a very high speed designing a reliable control system is quit complex and important. In this respect some efforts have been done to investigate the control system for gas turbine [57]-[58].

Producing electrical energy from mechanical energy has been studied for many years. There have been many studies on different kind of generators such as synchronous machines, induction machines and their performance in the power grid. Among them, synchronous generators have been used as electric generators in power grids. In this respect there have been many researches to investigate the behavior of synchronous generators dependently and in a power generator system [46][51]. Also there have been many studies implementing and developing model of synchronous machines [50],[51]. One of the challenges in synchronous generator is control issue and stability of them. In this respect several studies have been investigate and design an appropriate control design system [52]-[54].

In hybrid power system area, also, many efforts have been done to investigate the model of SOFC-GT hybrid power system [19]-[30]. Some of these studies focused on the

various system layout of the power planet [21]. Some studies focused to improve the model of SOFC-GT for aerospace applications [19]-[20] some other researches have worked to improve the dynamic model of these hybrid power systems [22]. A number of researches have simulated the performance of several kinds of SOFC–GT systems, and analyzed their performance by paying special attention to the energy aspect [23], [24] [25]. More recently, a group of papers have investigated the electrochemical performances of the fuel cell stack [23], [24], [25] and [26]. Some of them, have studied the stack or simple system also using the exergy analysis [28],[29]. Some study focused on developing control strategy for specific SOFC-GT hybrid power system.

Although there have been many studies on SOFC and GT and combining these generators, there is a great need to investigate a systematical model for SOFC-GT hybrid power system. Also, having a reliable and simplified model for online optimization will help to improve the system optimality. In addition, it is important not only to design a good control system, but also to choose a process design that with an appropriate control structure allows satisfying disturbance rejection, and part load condition. Such design procedures have been conducted in previous research [1]-[2].

1.4 System Optimization

The desire for optimality or perfection is an inherent characteristic of every human being. The search for perfection motivates mountaineers, scientists, mathematicians, and the rest of the human race. A practical mathematical theory of optimization (i.e. search-for-optimum strategies) is developed since the sixties when computers came in to the world. The goal of the theory is the creation of reliable methods to achieve the optimum solution of a function by an intelligent arrangement of its evaluations (measurements).

This theory plays a very important role in the modern engineering and plans to apply optimization to each step of the complicated decision making process. In this respect various optimization methods introduced to the application area from many years ago. The first optimization technique, which is known as steepest descent, dates back to Gauss. Historically, the first term to be introduced was linear programming, which was invented by George Dantzig in the 1940s. Introducing complex problems to the optimization area has a very enormous impact on developing the optimization methods. Neural networks, genetic algorithms, ant colony, fuzzy logic, and particle swarm optimization are some examples of the advanced optimization methods.

Optimization methods based on implementing the nature behaviors are very common. The social sharing of information among individuals of a population, may present an evolutionary advantage and there are numerous examples coming from the nature to support this idea. Ant Colony Algorithm (ACA), Bees Algorithm (BA), and Particle Swarm Optimization (PSO) are some examples of these methods. These methods have been used for different optimization problems based on their complexity.

Compared with other optimization methods, PSO is easier to implement and there are less parameters to be adjusted. Also, PSO has a more effective memory capability, and can be used for nonlinear optimization problems. Considering these advantages, PSO is used in many applications such as economic, electrical industry, marketing, banking and so on [31]-[34].

One of the applications of PSO algorithm is power industry as well. Some applications is used PSO in control area [38]-[40].Some studies have been done for distribution system.

As it was mentioned, one of the goals of the Vision 21 program was to improve the hybrid power system combining SOFC and GT to achieve the maximum efficiency as well as minimum emission and cost. Optimum power generation of a hybrid system is critical in achieving an economically competitive and operationally reliable hybrid power system with high efficiency.

There are some efforts focused on optimization of the hybrid power systems containing SOFC-GT systems with respect to the cost and expenses [41]-[42],[45]. Also, several works have been done to optimize the power distribution system using PSO [43], [44]. In some applications PSO used to solve the optimization problem for power sharing and maximum load ability [36], [37]. Although there have been a lot of work in the area of the SOFC-GT system optimization there has not been more accurate researches in power sharing optimization to increase the efficiency of a systematical hybrid power plan. Therefore this effort tried to implement PSO algorithm to optimize the more accurate and complex SOFC-GT hybrid power system to achieve the high efficiency.

1.5 Summary of Contributions

Despite of many research in hybrid power systems combining SOFC and GT, more efforts to find a systematical model for in depth studies in this aria is necessary. In addition, as it was mentioned, it is important to design a good control system and select a process design with a suitable control structure which allows fast transient response and having less instability in all conditions.

To be able to design such a controlled structure and to analyze the dynamic behavior of the system, it is very useful to have simple and accurate models of components for the hybrid power system. Having a model like this for the system is valuable for online

optimization as well. Therefore in this project a detailed dynamic model for SOFC_GT and study the behavior of the system is investigated. Also, this research presents the developed version of previous proposed model to increase the flexibility of the system for power sharing as well as improvement the speed control. In this respect, the burner model which is used in the hybrid power system is improved and GT shaft speed is controlled to be constant by controlling either the injected fuel or air to the burner.

In addition some control strategies offered trying to improve the system performance based on specific desire goal such as fast transient response.

Considering the importance of optimization in hybrid power system, the other objective of this research has determined as optimizing the efficiency of the system. In this respect the objective function is introduced by simplifying the presented model. Considering all the advantage of PSO algorithm and complexity of the system, PSO algorithm is used to achieve the optimization goal.

The presented mathematical models have been simulated using Matlab Simulink. Also the PSO algorithm has been implemented using Matlab. The results of these simulations have been presented in chapter five.

1.6 Theses Outline

This thesis is organized as follows. Chapter two presents the model and structure of a SOFC-GT hybrid power system. In addition, the mathematical model for all components in the system is presented in this chapter. Chapter three explains the control system and different control strategies for the system. Chapter four presents the optimization method to optimize the hybrid power system in reaching maximum efficiency. Also in this chapter the PSO algorithm is introduced and is applied to optimize SOFC-GT

configuration. Chapter five describes simulation results for the modeling, control and optimization. Finally in Chapter six, the conclusion and future research directions are presented.

Chapter 2

Hybrid Power System Structure and Modeling

To determine the operating conditions and constraints of the physical system, a system simulation is usually helpful. Therefore, to study the hybrid power system performance it is easier to model and analyze it as a test bed consisting of its components.

In this chapter the hybrid system configuration is presented. In addition, the mathematical model for system components is explained in detail.

2.1 Structure of Fuel Cell/Gas Turbine Hybrid Power System

The hybrid power system in this study is a combination of a Gas Turbine (GT) with a Solid Oxide Fuel Cell (SFOC). Several significant advantages of SOFC lead us to consider it as a part of the hybrid power system. First of all, an SOFC operates at high temperatures. Also, the energy conversion efficiency of an SOFC stack can reach up to 65%; and its overall efficiency, when used in combined heat and power (CHP) applications, i.e., as an integrated SOFC combustion turbine system, can even reach up to 70%. Figure 2.1 describes the schematic of the system.

In the designed layout, the air is first pressurized by a compressor, and then passes through a heat exchanger which uses the exhaust gas from the turbine to be preheated.

The pressurized and preheated gas enters into the fuel cell. The chemical reaction between fuel and gas in the fuel cell produces the electricity. Meanwhile the temperature of the fuel cell increases to a high degree. The exhausted high temperature gas is injected from the fuel cell into the oxidizer (burner) and further heats up after burning with the fuel inside the burner. The mechanical power is produced by expansion of the high temperature gas in the turbine and it rotates the GT shaft which is coupled with a synchronous generator to generate electricity. Also, additional fuel is injected to the burner to control the power produced by the generator.

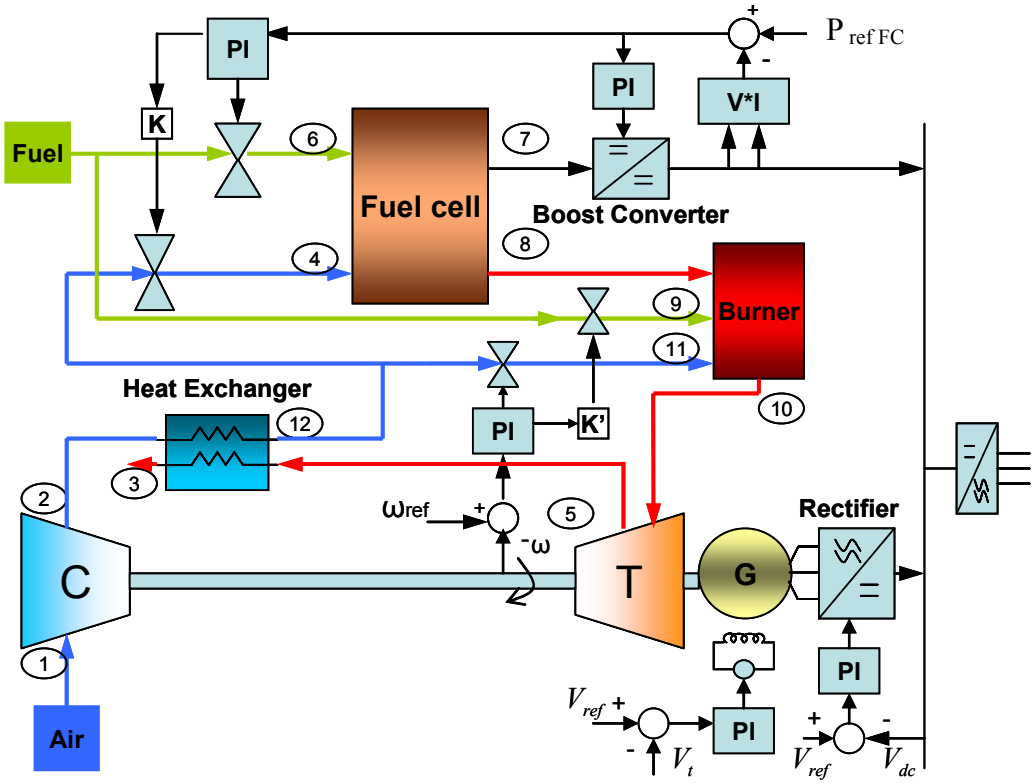

Figure 2.1 Schematic of a hybrid power system

2.2 Fuel Cell Description

Fuel cells are electrochemical devices which directly convert the chemical energy of a reaction into electrical energy. The basic physical structure of a fuel cell consists of an

electrolyte layer in contact with an absorbent anode and a cathode on either side. A schematic representation of a fuel cell with the reactant/product gases and the ion conduction flow directions through the cell is shown in Figure 2.2.

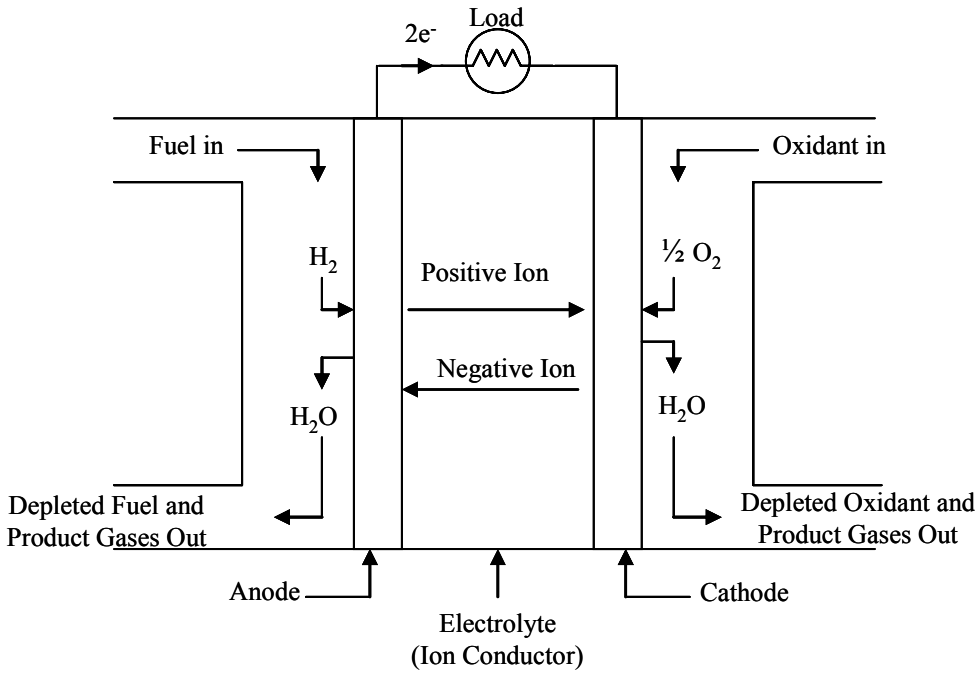

Figure 2.2 Schematic of a fuel cell

In a classic fuel cell, fuel is fed incessantly to the anode (negative electrode) side and an oxidant (i.e., oxygen from air) is fed continuously to the cathode (positive electrode) side. The hydrogen ions move across the electrolyte to the cathode while the electrons flow through an external circuit, resulting in a DC voltage that is produced because of the chemical reaction between hydrogen and oxygen.

Different kinds of fuel cells are in different steps of improvement. They can be classified into different categories. The most common classification of fuel cells is based on the type of electrolyte used in the cells which include:

1. Proton Exchange Membrane (PEM)
2. Alkaline fuel cell (AFC)

3. Phosphoric acid fuel cell (PAFC)

4. Molten carbonate fuel cell (MCFC)

5. Solid oxide fuel cell (SOFC)

The operating temperature is one of the important characters of a fuel cell. As mentioned one of the purposes of using a fuel cell in the hybrid power system is to increase the system efficiency. This efficiency would be achieved by using the high temperature exhausted gas from the fuel cell. Hence, in this research, the importance of high operating temperature leads us to choose SOFC in modeling of the hybrid power system. In fact, the operating temperature of a SOFC is around 1100 °k.

Figure 2.3 is a basic schematic model for a fuel cell which is used in this system to explain the input and output variables for this component.

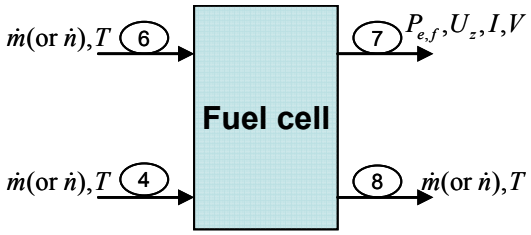

Figure 2.3 Schematic of a fuel cell

To describe the mathematical model of a SOFC, two models for each fuel cell can be considered: *electrical* and *thermal* models, which will be explained in the next section.

2.2.1 Electrical Model

The total output voltage of a stack can be expressed by using Equation (2-1) [7]:

$$V_{stack} = NE_0 - V_{act} - V_{\cos} - V_{ohm} \tag{2-1}$$

It is obvious from the equation that the voltage loss in the fuel cell is caused by the activation polarization (V_{act}), the ohmic polarization (V_{ohm}), and the mass transport loss or concentration polarization (V_{con}) which is the result of electrochemical reaction.

The V/I characteristic of a fuel cell can be divided into three regions. These three regions are displayed in Figure 2-4.

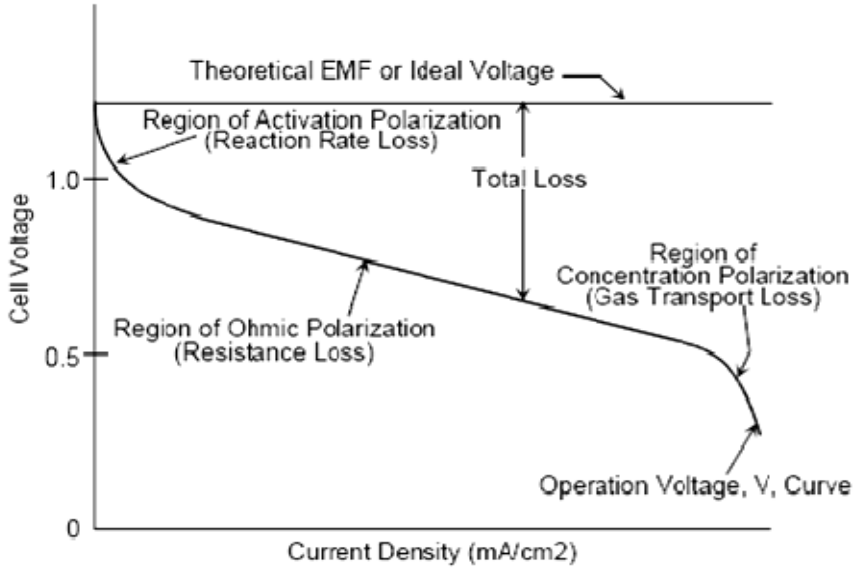

Figure 2.4 Typical V/I curve for a fuel cell

In low current densities, voltage changes have a logarithmic relationship with the current which can be explained by the activation polarization loss. However, in medium current densities, the voltage changes approximately linearly with the changes in current. The third part of the V/I curve for a fuel cell is related to concentration losses for high current operation.

Activation polarization loss

The V_{act} can be described by the formula below:

$$V_{act} = \begin{cases} \frac{RT_8}{4F}\frac{I_{cell}}{AJ_0} & \frac{I_{cell}}{A} \le J_0 \\ \frac{RT_8}{2F}\ln(\frac{I_{cell}}{AJ_0}) + \frac{RT_8}{4F}\frac{I_{cell}}{AJ_0} & \frac{I_{cell}}{A} > J_0 \end{cases} \quad (2\text{-}2)$$

Where T_8 is defined as the fuel cell temperature and I_{cell} is the cell current.

Ohmic Polarization

Electron transfer resistance from the anode to the cathode and proton movement through the electrolyte cause ohmic polarization, V_{ohm}. The ohmic resistance of a cell is approximately fixed. Following equation represents V_{ohm}..

$$V_{ohm} = r_{ohm} I_{cell} \quad (2\text{-}3)$$

Concentration Polarization

V_{con} occurs in all current densities, but is more evident in larger current densities and can be calculated using the equation below.

$$V_{con} = \frac{RT_8}{2F}\ln(1 - \frac{I_{cell}}{AJ_l}) \quad (2\text{-}4)$$

The cell current is dependent on the fuel flow rate and can be calculated from the following equation.

$$I_{stack} = \frac{2F\dot{n}_6}{N} = \frac{2F\dot{m}_6}{N \cdot M_{H_2}} \tag{2-5}$$

Where $\dot{n}$ is fuel molar flow rate, and M_{H2} is the hydrogen molar mass. The output power of the cell can be obtained by the next equation.

$$P_{e,f} = I_{cell} V_{stack} \tag{2-6}$$

2.2.2 Thermal Model

Regarding the air consistence of 21% oxygen and 79% nitrogen, the chemical reaction in the fuel cell can be explained as below.

$$2H_2 + O_2 + 3.76N_2 \rightarrow H_2O + 3.76N_2 \tag{2-7}$$

Therefore, for every 2 moles of hydrogen (fuel) we need one mole of oxygen and 3.76 moles of nitrogen. Based on this information, the next equation can describe the relationship between the fuel and air mass flow rate for the fuel cell where K is a constant.

$$\dot{m}_4 = K\dot{m}_6 \tag{2-8}$$

But in reality, not all of the hydrogen is consumed in a fuel cell. Fuel utilization is the ratio between the reacting fuel and the input fuel and can be defined as below [7].

$$U_z = (I_{satck} N/(2F))/(\dot{m}_6 / M_{H_2}) \tag{2-9}$$

Considering the utilization factor and ideal reaction, i.e., $\dot{n}_4 = \dot{n}_6/2$, the chemical reaction could be rewritten:

$$\dot{n}_6 H_2 + \frac{\dot{n}_6}{2} O_2 + \frac{\dot{n}_6}{2} 3.76\ N_2 \rightarrow \frac{\dot{n}_6}{2} U_z H_2 O + \dot{n}_6 (1 - U_z) H_2 + \frac{\dot{n}_6}{2} (1 - U_z) O_2 + \frac{\dot{n}_6}{2} 3.76\ N_2 \quad (2\text{-}10)$$

Therefore considering that the water is condensed, the exhaust of the fuel cell can be calculated by the equation below:

$$\dot{m}_8 = \frac{\dot{m}_6}{M_{H_2}} \left[(1 - U_z)(2M_{H_2} + M_{O_2}) + 3.76 M_{N_2} \right] \quad (2\text{-}11)$$

Where the M_{O2} is molecular mass for oxygen (32 g/mol) and M_{N2} molecular mass for nitrogen (28 g/mol)

The rest of the fuel is injected into the burner. The thermal power generated inside the fuel cell can be calculated by the following equation.

$$W_{gen} = W_{ch} - P_{e,f} \quad (2\text{-}12)$$

Where W_{ch} is the heat generated by the chemical reaction and could be determined as below.

$$\dot{W}_{ch} = U_z \left(\frac{\dot{m}_6}{M_{H_2}} \right) \Delta H_f \quad (2\text{-}13)$$

A portion of the thermal power released from the fuel cell is consumed and consequently increases the input air temperature (W_{air}) and stack temperature. The

remaining power is released to the environment. This state can be described using the following formula.

$$W_{gen} = C_{fc} m_{fc} \frac{dT_8}{dt} + W_{amb} + W_{air} \tag{2-14}$$

Where W_{amb} is the transferred power to the ambient and can be denoted as follows.

$$W_{amb} = A_{ex} h_{ex} (T_8 - T_{amb}) \tag{2-15}$$

The thermal power that increases the inlet air temperature, W_{air}, is explained by the equation below.

$$W_{air} = \dot{m}_4 C_p (T_8 - T_4) \tag{2-16}$$

The next component described in the following section is gas turbine. It is coupled to the fuel cell to maintain the required line power.

2.3 Gas Turbine

2.3.1 Basic Background of Gas Turbine (GT)

A basic gas turbine consists of a compressor, combustor and a turbine which work under the Brayton cycle in this study. The air-standard Brayton cycle is the ideal cycle for the simple gas turbine. The simple open cycle is made of four irreversible processes: 1-2 Isentropic Compression, 2-3 Constant Pressure heat addition, 3-4 isentropic expansion, and 4-1 Constant Pressure heat rejection (Figure. 2.5).

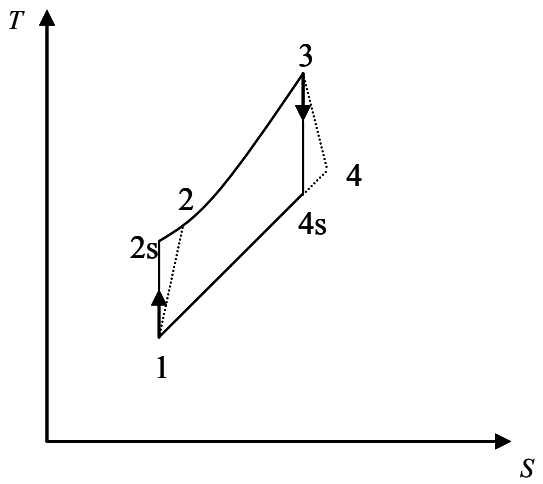

Figure 2.5 . A simple Brayton cycle

First, consuming mechanical power the air is compressed in the compressor. In this stage, the compressor does work to increase the pressure and temperature of the gas (processes 1-2). In the second stage, the compressed air is mixed with the fuel under constant pressure, either liquid or gas, and burned in the combustor (processes 2-3). Considering that the compression is ideally isentropic, a vertical line on the T-S diagram (from 1 to 2s) describes this process. In reality, the compression is not isentropic and the compression process line leans to the right because of the increase in entropy of the flow (1 to 2). The combustion process in the burner happens at constant pressure from station 2 to station 3. The temperature increase depends on the type of fuel that is used as well as the fuel-air ratio. The high temperature exhaust is then passed through the power turbine in which work is done by the flow from station 3 to station 4. Because the turbine and compressor are coupled with the same shaft, the output mechanical power is the difference between power generated from the turbine and consumed by the compressor. The physical model for this project is based on a simple single shaft GT with a heat

exchanger that increases the efficiency of the GT. Figure 2.6 shows the physical model of the GT designed for this project.

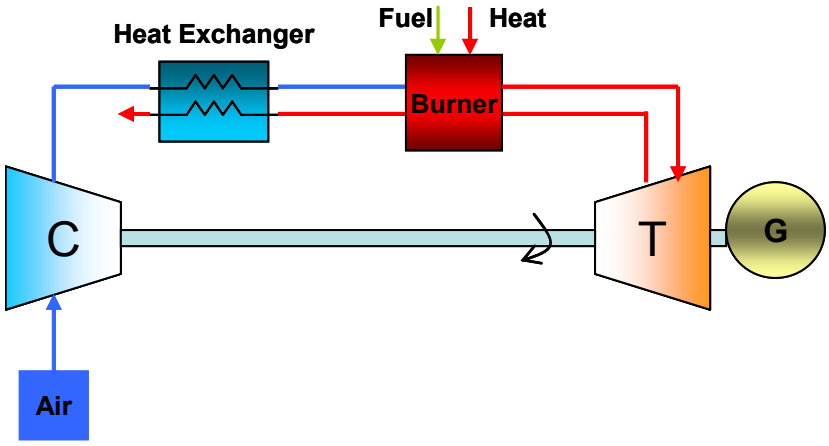

Figure 2.6 Physical model of the Gas Turbine system,

In the following section, each component of the gas turbine will be explained respectively.

2.3.2 Compressor and Heat Exchanger

The compressor is used to compress the air. The pressurized air passes through a heat exchanger to be preheated by recovering the heat from the exhaust gas from the turbine. Figure 2.7 explains the schematic of a simple compressor combined with a heat exchanger. $\dot{m}$ determines the mass flow rate and T shows the temperature of each point.

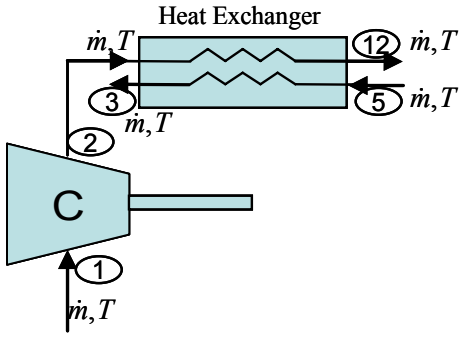

Figure 2.7 Compressor/Heat exchanger schematic

The consumed thermal power by the compressor, $P_{th,c}$, can be calculated via the following equation [67].

$$P_{th,c} = \frac{1}{\eta_{th,c}} \dot{m}_2 C_p (T_2 - T_1) \tag{2-17}$$

The following equation describes the relationship between input and output temperature of the compressor.

$$\frac{T_2}{T_1} = (PR_c)^{\frac{\gamma-1}{\gamma}} \tag{2-18}$$

Where PR_c is the constant pressure ratio for the compressor.

The essential mechanical power to pressurize the air can be expressed as a first order equation described as below [68].

$$\tau_c \frac{dP_{m,c}}{dt} = P_{m,c} - P_{th,c} \tag{2-19}$$

Based on the mass balance theory, the output mass flow rate is equal to the input mass flow rate.

$$\dot{m}_1 = \dot{m}_2 \tag{2-20}$$

The energy balance in the heat exchanger leads to the next equation.

$$\dot{m}_5 C_{p,gas} (T_5 - T_3) = \dot{m}_2 C_p (T_{12} - T_2) \tag{2-21}$$

The mass flow rate for the input and output of the heat exchanger can be considered using the Equations (2-22) and (2-23) below, respectively.

$$\dot{m}_2 = \dot{m}_{12} \tag{2-22}$$

$$\dot{m}_5 = \dot{m}_3 \tag{2-23}$$

Also, the temperature at points 1 and 3 in Figure 2.7 are equal to the ambient temperature.

2.3.3 Burner

In this model, a burner is used to burn the waste fuel exhausted from the fuel cell. Moreover, it can be used to control the shaft speed by fuel control methodology. Figure 2.8 demonstrates a simplified schematic for the burner.

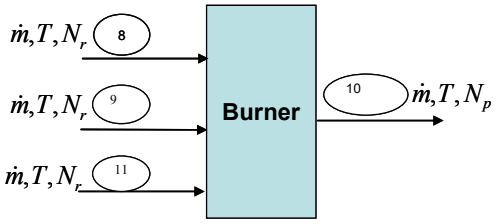

Figure 2.8 Figure 2-8. Schematic of a burner

Considering the following assumptions and Equation (2-24), the combustion reaction inside the burner can be described as Equation (2-25).

— Burner fuel is the preheated and pressurized hydrogen ,

— The combustion reaction in the burner assume to be ideal,

— The air consists of 21% oxygen and 79% of nitrogen,

$$T_9 = T_{11} = T_{12} \tag{2-24}$$

$$[(1-U_z)\frac{m_{f,f}}{M_{H_2}}(H_2+.5O_2+1.88\,N_2)]_{T_8}+[\frac{m_{f,b}}{M_{H_2}}(H_2+.5O_2+1.88\,N_2)]_{T_{12}}$$
$$\rightarrow [((1-U_z)\frac{m_{f,f}}{M_{H_2}}+\frac{m_{f,b}}{M_{H_2}})H_2O+1.88\,(\frac{m_{f,f}}{M_{H_2}}+\frac{m_{f,b}}{M_{H_2}})N_2]_{T_{10}} \quad (2\text{-}25)$$

The mathematical model of the burner is indicated as a first order equation based on energy balance. Equation (2-26) describes this model [30].

$$\frac{dT_{10}}{dt}=\frac{1}{C_b m_b}(\sum N_r(\bar{h}_f^\circ+\bar{h}(T_8)-\bar{h}^\circ)_r+\sum N_r(\bar{h}_f^\circ+\bar{h}(T_{12})-\bar{h}^\circ)_r-\sum N_p(\bar{h}_f^\circ+\bar{h}(T_{10})-\bar{h}^\circ)_p-A_x H_x(T_{10}-T_{amb})) \quad (2\text{-}26)$$

Where T is the temperature and N is the molar flow rate of inputs and outputs . By considering the mass balance, the output mass flow rate can be denoted as following Equation .

$$\dot{m}_{10}=\dot{m}_8+\dot{m}_9+\dot{m}_{11} \quad (2\text{-}27)$$

2.3.4 Turbine

A turbine is a rotary engine that converts thermal power energy to mechanical power.

Figure 2-9 is a simplified schematic for a turbine showing input and output variables.

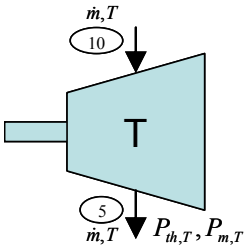

Figure 2.9 Figure 2-9. Turbine schematic

Using the mass balance theory above the relationship between input and output mass flow rate can be indicated by Equation (2-27).

$$\dot{m}_{10} = \dot{m}_5 \tag{2-28}$$

The output temperature of the turbine has a relationship with the pressure ratio of the turbine [67].

$$\frac{T_5}{T_{10}} = (PR_T)^{\frac{\gamma-1}{\gamma}} \tag{2-29}$$

The thermal power produced by the turbine can be calculated based on the following algebraic equation.

$$P_{th,T} = \eta_{th,T}\dot{m}_5 C_p (T_5 - T_{10}) \tag{2-30}$$

The following first order equation expresses a formula for converting thermal power to mechanical power [68].

$$\tau_T \frac{dP_{m,T}}{dt} = P_{th,T} - P_{m,T} \tag{2-31}$$

The output mechanical power from the gas turbine is defined as the difference between the mechanical power produced by the turbine and the power consumed in the compressor.

$$P_{m,gt} = P_{m,t} - P_{m,T} \tag{2-32}$$

2.4 Generator

An electrical generator is a device which converts mechanical energy to electrical energy. The operation of a generator depends on electromagnetic induction, which is described as the production of an electromotive force in an electric circuit by a change of magnetic flux passing through a circuit.

There are different kinds of sources to produce mechanical energy for a generator. The turbine steam engine, internal combustion engine, wind turbine, hand crank, sun or solar energy, are some examples of mechanical energy sources.

There are different kinds of generators that produce electricity. Induction generators and synchronous generators are two examples of these generators. Synchronous generators are widely used in a power generation system to convert the mechanical energy to electrical energy. The next sections are dedicated to the explanation of the performance and mathematical model of a synchronous generator.

Synchronous Generator

The operation of a synchronous generator is based on Faraday's law of electromagnetic induction. A synchronous machine refers to a rotating device that's speed is proportional to the system frequency under steady state conditions. Each synchronous machine consists of an armature and a rotor. The armature current produces a magnetic field that rotates at the same speed as the magnetic field created by the field current on the rotor.

Synchronous machines are commonly used as generators especially for large power systems such as turbine generators and hydroelectric generators in the grid power supply

Each synchronous machine consists of a rotor which is the rotating part, and a stator which is the fixed part. A conventional synchronous machine has an armature winding on the stator which is ordinarily a three phase winding. On the rotor there usually exists a field winding that is excited either by DC current or permanent magnets. Figure 2-10 shows a typical structure of a synchronous generator.

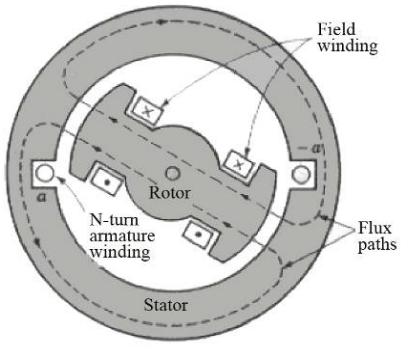

Figure 2.10 A typical structure of a synchronous generator

In a synchronous machine, the rotor poles are shaped such that the resultant *mmf* and flux density would distribute sinusoidally in the air gap, and thus the induced *emf* in the stator windings related to this flux will also be sinusoidal.

The equivalent circuit for the synchronous generator has been represented in Figure 2-11. For each phase, electrical equations are obtained by considering Kirchoff's voltage law for every winding, i.e. by equating the voltage at the winding's terminal to the sum of resistive and inductive voltage drops across the winding.

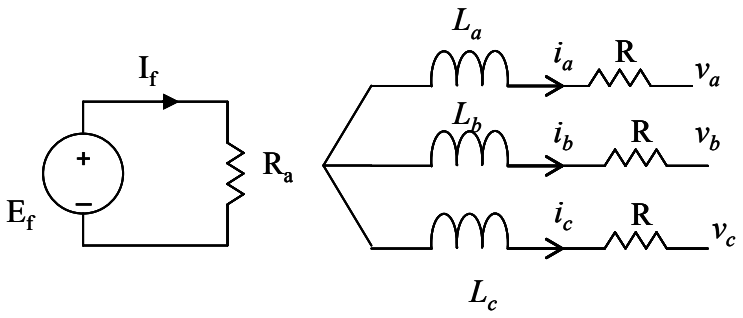

Figure 2.11 The equivalent circuit for the synchronous generator

To evaluate the inductive voltage drop across a winding correctly, total magnetic flux related to the winding must be calculated. This can be obtained by using an inductance matrix, which relates all flux linkages of the windings to their currents. As a result of this, an inductance matrix dependent on the rotor position will be obtained. This reliance is due to the magnetic asymmetry of the rotor; depending on the way the rotor of a synchronous machine is shaped, a preferable magnetic direction can be offered. This direction corresponds with the direction of the flux produced by the field winding, and is described as the machine's *d* axis. The machine's *q* axis is positioned at 90 electrical degrees (in a counterclockwise direction) with respect to the machine's *d* axis. Now, the rotor position can be identified by introducing an angle, named θ, between the magnetic axis of the armature's phase *a* and the rotor's *q* axis. Dependence of the inductance matrix on the rotor position signifies the main complexity in modeling the synchronous machine. One of the solutions to this problem is to modify the reference system, or frame, in which the machine's electrical and magnetic variables are expressed. Normally the reference frame used is the so-called stationary, or stator, or *abc* reference frame. In this frame, variables can be selected and measured in the machine; however the machine parameters are time variant (since θ is a function of time). It can be shown that the only reference frame that presents constant machine parameters is the rotor, or *dq*, reference

frame. This frame has been represented by Parks and others [75]. In this model, all variables are selected such that a hypothetical observer placed on the rotor could measure them. Transformation from the *abc* to the *dq* reference frame is given by the following transformation matrix [75].

$$T = \sqrt{\frac{2}{3}}\begin{bmatrix} \sin\theta & \sin(\theta - 2\pi/3) & \sin(\theta + 2\pi/3) \\ \cos\theta & \cos(\theta - 2\pi/3) & \cos(\theta + 2\pi/3) \end{bmatrix} \tag{2-33}$$

And θ is calculated as follows:

$$\theta(t) = \int_0^t \omega(\xi)d\xi + \theta_0 \tag{2-34}$$

If a generator operates in sinusoidal steady state, phase voltages can be written in the *abc* reference frame as:

$$v_a = V_p \cos\theta_v \tag{2-35}$$

$$v_b = V_p \cos(\theta_v - 2\pi/3) \tag{2-36}$$

$$v_c = V_p \cos(\theta_v + 2\pi/3) \tag{2-37}$$

Where θ_v is,

$$\theta_v = \omega_v t + \theta_{v0} \tag{2-38}$$

In steady state, clearly, $\omega_v = \omega$. However, in order to reach a steady state, the generator must go through a transient during which the rotor's electrical speed can differ from the terminal voltage's angular frequency.

The Park's Synchronous machine may be schematically shown as Figure 2-12.

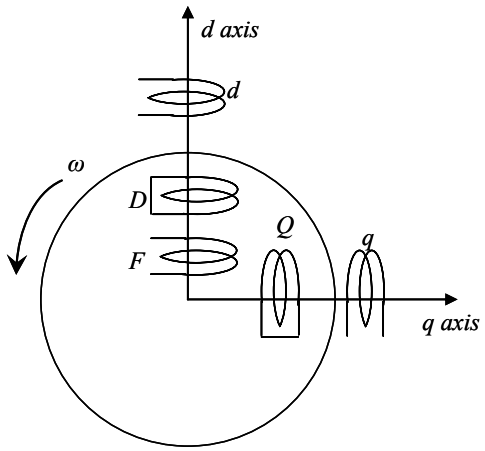

Figure 2.12 Park's Synchronous machine

There are three armature phase windings *a*, *b*, and *c* on the stator of the machine, which have been replaced by two equivalent armature phase windings on the *d* and *q* axis. There are two dampers winding on the rotor, D on the *d* axis and Q on the *q* axis, which are short-circuited.

Since there is no static coupling between *d*-axis and *q*-axis windings, a synchronous machine can be simply modeled in per unit of value using the following equations[70]:

$$v_{dg} = R_a(-i_d) + \dot{\psi}_d / \omega_b - \omega\psi_q \tag{2-39}$$

$$v_{qg} = R_a(-i_q) + \dot{\psi}_q / \omega_b - \omega\psi_d \tag{2-40}$$

$$v_F = R_F(-i_F) + \dot{\psi}_F / \omega_b \tag{2-41}$$

$$0 = R_D i_D + \dot{\psi}_D / \omega_b \tag{2-42}$$

$$0 = R_Q i_Q + \dot{\psi}_Q / \omega_b \tag{2-43}$$

In the equations above v, i, r, ψ, and ω, respectively, describe the voltage, current, resistance, flux linkage and speed, all per unit of value, and the subscriptions d, q, F, D, and Q signify the respective windings. The time derivative of ψ is $\dot{\psi}$ and $2\pi f$ radian per second is chosen as the base speed ω_b.

The d and q axis equivalent circuits of the synchronous machine are represented in the Figure 2-13 below.

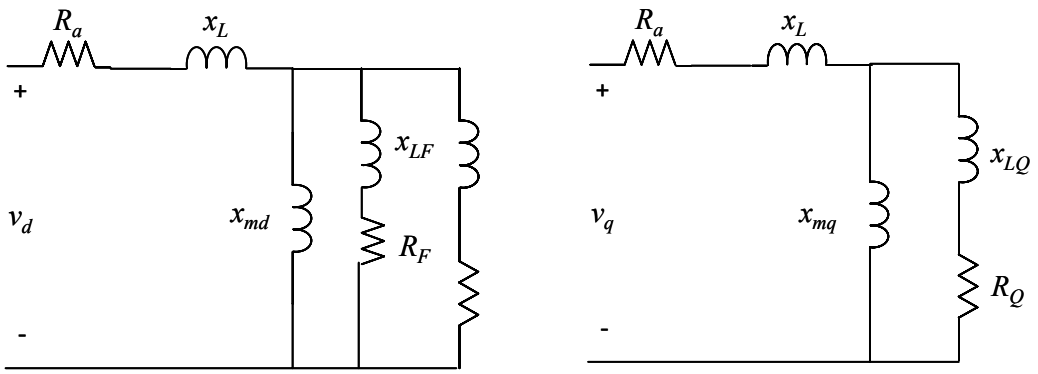

(a) d axis (b) q axis

Figure 2.13 The d and q axis equivalent circuits of the synchronous machine

Many synchronous models have been developed for dynamic studies. For this research, a third order model has been considered. Figure 2-14 demonstrates a schematic model of this generator to determine the input and output parameters of the generator. This model is based on the d-q axis model.

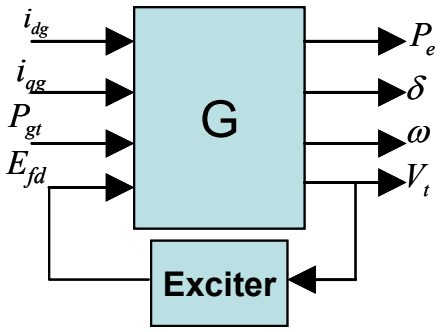

Figure 2.14 Generator schematic

There are many models which describe the dynamic behavior of a synchronous machine. The model which is used in this study is a second order synchronous generator model.

A phasor diagram for low-order synchronous generators in steady and transient states have been drawn as shown in Figure 2-15.

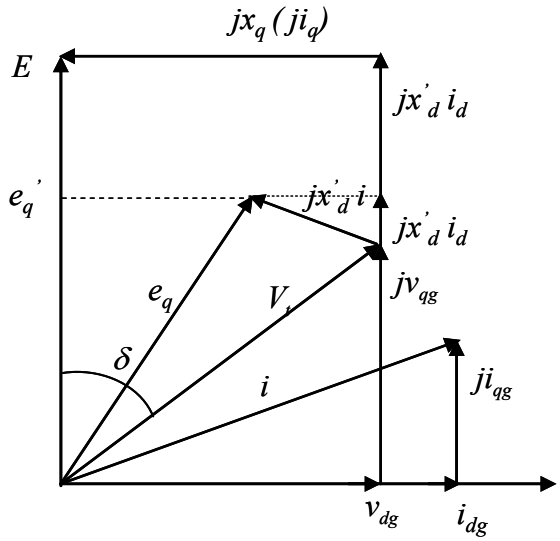

Figure 2.15 A phasor diagram for low-order synchronous generator

Considering ω of the equations (2-39) and (2-40) as approximation of synchronous speed ω_0 and by neglecting ψ_d, ψ_q and R_a, the next equations will be obtained for the armature windings [70]:

$$v_{qg} = e'_q - x'_d i_{dg} \tag{2-44}$$

$$v_{dg} = x_q i_{qg} \tag{2-45}$$

Based on Figure 2-13 the following reactance can be defined:

$$x_d \triangleq x_L + x_{md} \tag{2-46}$$

$$x_q \triangleq x_L + x_{mq} \tag{2-47}$$

$$x'_d \triangleq x_L + \frac{x_{md} x_{LF}}{x_{md} + x_{LF}} \tag{2-48}$$

$$x_F \triangleq x_{LF} + x_{md} \tag{2-49}$$

Also the following time constant can be defined based on Figure 2-13.

$$T'_{do} \triangleq \frac{x_F}{\omega_b r_F} \tag{2-50}$$

Considering Equation (2-41) the state variable is flux linkage ψ_F, which traditionally is replaced by a voltage and therefore the flux linkage equation is converted to a voltage equation. To approach this goal some new voltages are defined as follows:

$$e'_q \triangleq \frac{x_{md}}{x_F} \omega_0 \psi_F \tag{2-51}$$

$$E \triangleq x_{md} i_F \tag{2-52}$$

$$E_{fd} \triangleq \frac{x_{md} v_F}{r_F} \tag{2-53}$$

Substituting these equations in the equation (2-41) and considering the time constant T'_{do}, the following equation can be achieved:

$$\dot{e}'_q = \frac{de'_q}{dt} = \frac{1}{T'_{do}} (E_{fd} - E) \tag{2-54}$$

Considering the following equation, we can obtain the first order equation of the internal voltage e'_q.

$$e'_q = E - (x_d - x'_d) i_d \tag{2-55}$$

The following two first order equations can define the transient response of the synchronous generator. It must be mentioned that all values are defined in the per unit system.

$$\frac{de'_q}{dt} = \frac{1}{T'_{do}} (E_{FD} - e'_q - (x_d - x'_d) i_{dg}) \tag{2-56}$$

$$\frac{d\omega}{dt} = \frac{1}{J} (T_m - T_e - D\omega) \tag{2-57}$$

To calculate the real output power P_e and terminal voltage V_t, the following algebraic equation can be used:

$$V_t = \sqrt{v_{qg}^{\ 2} + v_{dg}^{\ 2}} \tag{2-58}$$

$$P_e = i_{dg} v_{dg} + i_{qg} v_{qg} \tag{2-59}$$

2.5 Power Conditioning Systems

It is necessary to control each generator in the hybrid power system to maintain the stable response to get the objective performance. In the presented hybrid power system, since the fuel cell output voltage is lower than the grid voltage it is necessary to boost it to the grid voltage. To achieve this goal boost a converter is used. Also, to maintain a stable DC voltage and minimize the reactive power generated by the synchronous generator an active rectifier is employed. Further details will be indicated in the following sections.

2.5.1 Active Rectifier

To convert the AC voltage produced by the synchronous generator, an active rectifier is used. In this section the system of an active rectifier will be described. The advantage of using an active rectifier is that it provides the ability to simultaneously control tow parameters. In this study, DC voltage and reactive currents are the two parameters which can be controlled by the active rectifier.

A three-phase boost rectifier and voltage source inverter are considered current bidirectional converters as they use the same switching cells which are current bidirectional. The switches that are used for these converters either have internal parallel diodes, for example IGBTs and MOSFETs, or have external parallel diodes, for instance, GTOs.

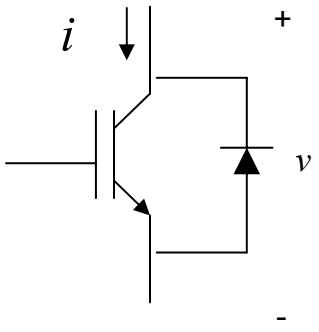

Figure 2.16 Symbolic representation of a current-bidirectional switching cell

A three-phase boost active rectifier equivalent circuit is shown in the following figure. As it shows it consists of six switching cells which conduct current from each phase prudicly.

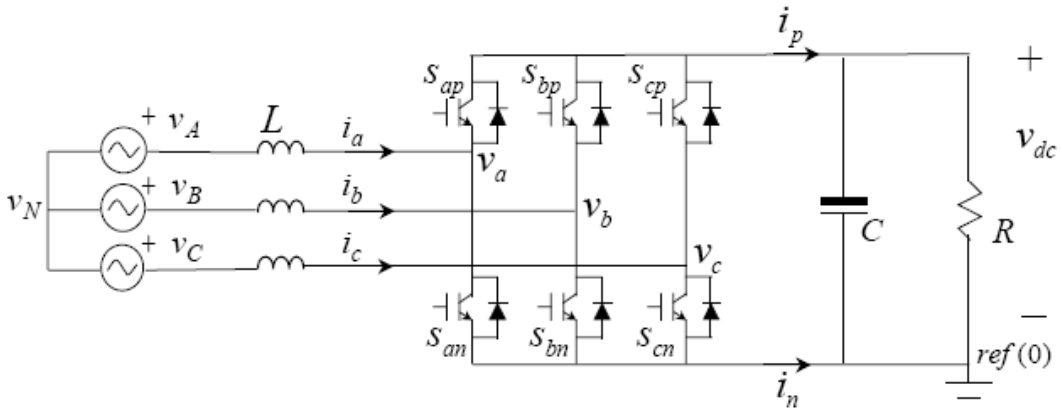

Figure 2.17 Three-phase boost active rectifier

The switching cell in Figure 2-17 can be described by a generic switch s, as shown in Figure 2-18.

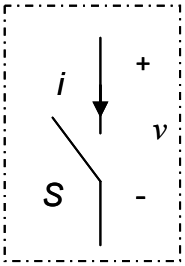

Figure 2.18 A generic switch

When *S* is open, none of the switch or the diode conducts, as referring to Figure 2-18, thus resulting in zero current *i*. When *S* is closed, either the switch itself or the diode conducts, therefore the voltage *v* is equal to zero. Therefore, a switching function S can be defined as follows:

$$S = \begin{cases} 0, & i = 0, \text{if switch S is open} \\ 1 & v = 0, \text{if switch S is closed} \end{cases} \tag{2-60}$$

The generic switching unit used in this study called a phase leg, can be described as shown in Figure 2-19. The phase leg consists of two switching cells, and has a voltage

source (or a capacitor) on one side and a current source (or an inductor) on the other side. These features cause the phase leg to be known as a generic switching unit [73].

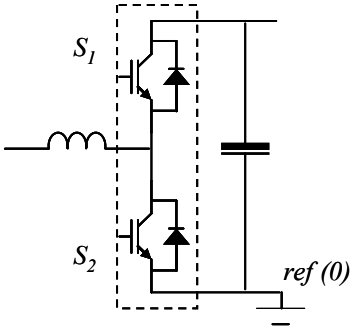

Figure 2.19 Generic phase leg in current-bidirectional converters.

There are switching limitations for the two switching cells. One of these limitations is that the voltage sources or capacitors cannot be short-circuited, and the other is that the current sources or inductors cannot be open-circuited. To avoid these limitations, it is required that the two switching cells be complementary. In other words, to prevent the voltage source (or the capacitor) from being short-circuited, only one of the two switching cells, S_1 or S_2, can be closed at any time. Meanwhile, to prevent the inductor from being open-circuited, one of the two switching cells has to be closed at any given time. Based on the switching function defined in equation (2-61), this complementary relationship can be described as:

$$S_1 + S_2 = 1 \tag{2-61}$$

As a result, the phase leg can be represented by a single-pole, double-throw switch, as shown in Figure 2-10.

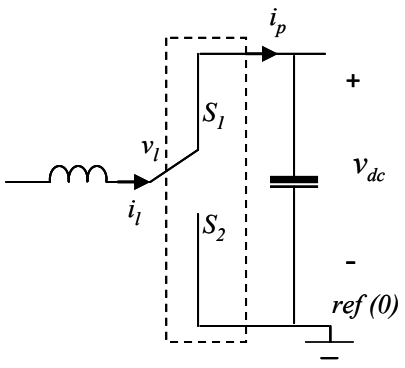

Figure 2.20 Phase leg represented as a single-pole, double-throw switch.

The PWM of the phase leg is shown in Figure 2-21, where T is the switching period and d is the duty cycle of the top switch S_1. The corresponding voltage and current waveforms are also shown in Figure 2-21.

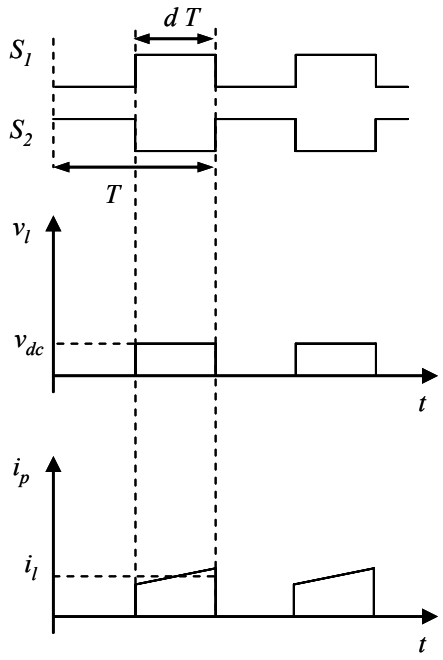

Figure 2.21 Phase leg PWM and corresponding current and voltage waveforms

Based on the waveforms, the average relationships for voltage and current can be obtained from Equation (2- 62) and (2-63), assuming the current i_λ and the voltage v_{dc} are continuous with small ripples.

$$v_l = d.v_{dc} \tag{2-62}$$

$$i_p = d.i_l \tag{2-63}$$

The average model of the phase leg is depicted in Figure 2-22.

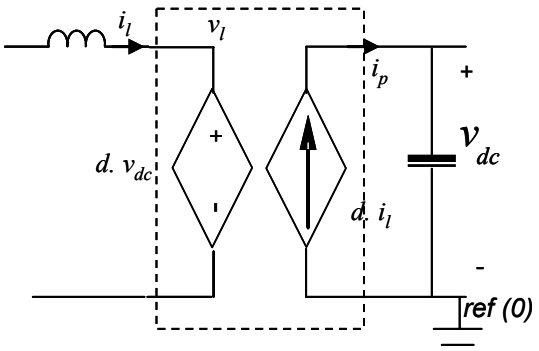

Figure 2.22 Phase leg's average model

Based on this model, the average model of a three-phase boost rectifier can be achieved by connecting three averaged phase legs and the rest of the circuit components, as shown in Figure 2-23,

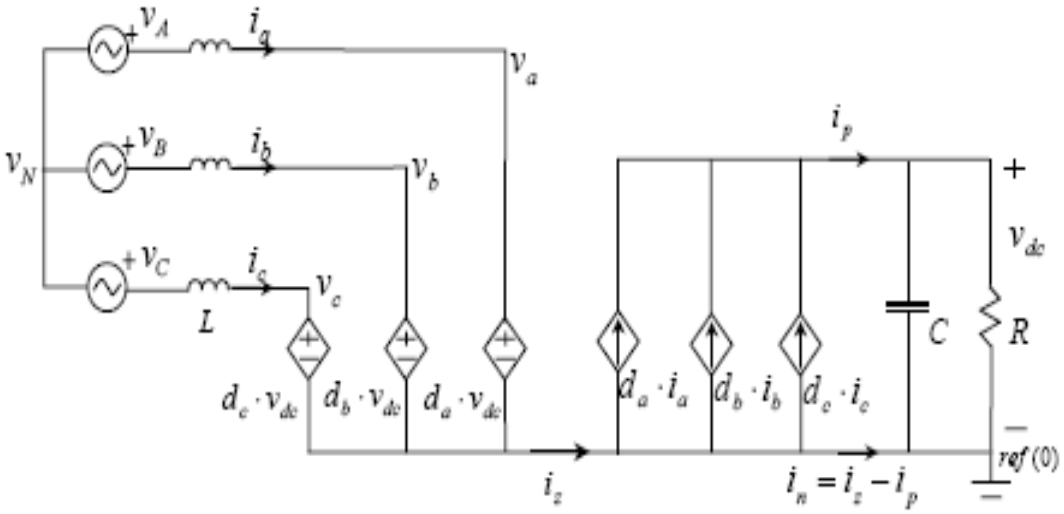

Figure 2.23 A three-phase boost rectifier

In this model i_z is equal to zero. This model can be described by the following equations [73]:

$$\frac{d}{dt}\begin{bmatrix} i_a \\ i_b \\ i_c \end{bmatrix} = \frac{1}{L}\begin{bmatrix} v_{AN} \\ v_{BN} \\ v_{CN} \end{bmatrix} + \frac{1}{L}\begin{bmatrix} v_N \\ v_N \\ v_N \end{bmatrix} - \frac{1}{L}\begin{bmatrix} d_a \\ d_b \\ d_c \end{bmatrix}.v_{dc} \tag{2-64}$$

$$\frac{dv_{dc}}{dt} = \frac{1}{C}\begin{bmatrix} d_a & d_b & d_c \end{bmatrix}\begin{bmatrix} i_a \\ i_b \\ i_c \end{bmatrix} \tag{2-65}$$

In the steady state condition, the output DC voltage v_{dc} is controlled by a constant value. The phase currents i_a, i_b, and i_c, are controlled to be sinusoidal and in phase with the corresponding input phase voltages v_{AN}, v_{BN} and v_{CN}, which are normally given, as follows:

$$\begin{bmatrix} v_{AN} \\ v_{BN} \\ v_{CN} \end{bmatrix} = \begin{bmatrix} V_m \cos(\omega t) \\ V_m \cos(\omega t - 2\pi/3) \\ V_m \cos(\omega t + 2\pi/3) \end{bmatrix} \tag{2-66}$$

In order to reach a DC steady-state operating point and linearize the system to design controllers, the model in the stationary coordinates is usually transformed into rotating coordinates (d-q axis). The transformation matrix is chosen as follows:

$$T = \sqrt{\frac{2}{3}}\begin{bmatrix} \cos\omega t & \cos(\omega t - 2\pi/3) & \cos(\omega t + 2\pi/3) \\ -\sin\omega t & -\sin(\omega t - 2\pi/3) & -\sin(\omega t + 2\pi/3) \\ 1/\sqrt{2} & 1/\sqrt{2} & 1/\sqrt{2} \end{bmatrix} \tag{2-67}$$

where ω is chosen as the same frequency as the AC line frequency, T is an orthogonal matrix. The variables in the stationary coordinates X_{abc} can be transformed into the rotating coordinates X_{dqz} using below.

$$X_{dqz} = T.X_{abc} \tag{2-68}$$

By applying (2-68) to (2-64)-(2-65), the average model of a single boost rectifier in the rotating coordinates will be obtained as follows:

$$\frac{d}{dt}\begin{bmatrix} i_d \\ i_q \\ i_z \end{bmatrix} = \frac{1}{L}\begin{bmatrix} v_d \\ v_q \\ v_z \end{bmatrix} + \frac{1}{L}\begin{bmatrix} 0 \\ 0 \\ 3v_N \end{bmatrix} - \begin{bmatrix} 0 & -\omega & 0 \\ \omega & 0 & 0 \\ 0 & 0 & 0 \end{bmatrix}.\begin{bmatrix} i_d \\ i_q \\ i_z \end{bmatrix} - \frac{1}{L}\begin{bmatrix} d_d \\ d_q \\ d_z \end{bmatrix}.v_{dc} \tag{2-69}$$

$$\frac{dv_{dc}}{dt} = \frac{1}{C}\begin{bmatrix} d_d & d_q & d_z/3 \end{bmatrix}\begin{bmatrix} i_d \\ i_q \\ i_z \end{bmatrix} \tag{2-70}$$

Where,

$$\begin{bmatrix} i_d \\ i_q \\ i_z/\sqrt{3} \end{bmatrix} = T.\begin{bmatrix} i_a \\ i_b \\ i_c \end{bmatrix}, \begin{bmatrix} v_d \\ v_q \\ v_z/\sqrt{3} \end{bmatrix} = T.\begin{bmatrix} v_{AN} \\ v_{BN} \\ v_{CN} \end{bmatrix}, \begin{bmatrix} d_d \\ d_q \\ d_z/\sqrt{3} \end{bmatrix} = T.\begin{bmatrix} d_a \\ d_b \\ d_c \end{bmatrix} \tag{2-71}$$

Since i_z is equal to zero, we can simplify the model as shown in Figure 2-24.

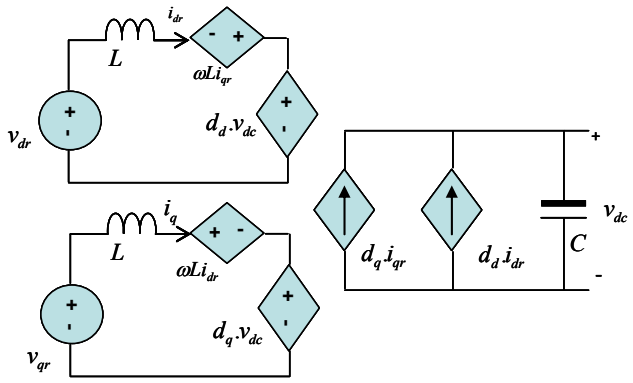

Figure 2.24 d-q axis model for active rectifier

Based on this figure, the mathematical model for this converter can be defined by three first order equations.

$$\frac{di_{dr}}{dt} = \frac{1}{L}v_{dr} + \omega i_{qr} - \frac{1}{L}d_d v_{dc} \tag{2-72}$$

$$\frac{di_{qr}}{dt} = \frac{1}{L}v_{qr} - \omega i_{dr} - \frac{1}{L}d_q v_{dc} \tag{2-73}$$

$$\frac{dv_{dc}}{dt} = \frac{1}{C}\left(d_d.i_{dr} + d_q i_{qr}\right) \tag{2-74}$$

The voltage and current of the rectifier can be calculated using the following equations:

$$V = v_{dr} + jv_{qr} \tag{2-75}$$

$$I = i_{dr} + ji_{qr} \tag{2-76}$$

Here, v_{dr} and v_{qr} are the *d-q* axis voltages and i_{dr} and i_{qr} are the *d-q* axis currents. I is the active rectifier output current. The real and reactive output power of the rectifier can be defined as:

$$S = P + jQ = 1.5 \cdot VI^{*} \tag{2-77}$$

$$P_{dc} = 1.5\,(v_{dr}\, i_{dr} + v_{qr}\, i_{qr}) \tag{2-78}$$

$$Q = 1.5(-v_{dr} i_{qr} + v_{qr} i_{dr}) \tag{2-79}$$

Since the *d-q* axis of the generator differs from the active rectifier, a transfer function is proposed here in order to allow the output current of the rectifier to be used for the input current of the generator. Hence, this model uses the output terminal voltage of the generator (V_t) as the input *d*-axis voltage of the rectifier (v_{dr}), thereby making them one. Also, v_{qr} is held at zero volts. Figure 2-25 displays this transfer function based on these explanations. The transfer function for the system can be expressed in the following equations:

$$\beta = \arctan(i_{qr} / i_{dr}) \tag{2-80}$$

$$I = \sqrt{i_{qr}^{\,2} + i_{dr}^{\,2}} \tag{2-81}$$

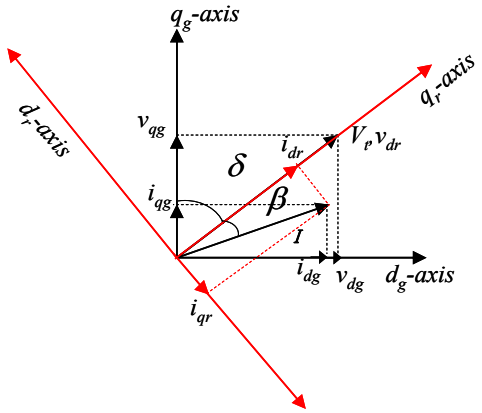

Figure 2.25 d-q axis model for active rectifier

To calculate the *d-q* axis current for the generator the following equations can be defined:

$$i_{dg} = I\sin(-\beta+\delta) \tag{2-82}$$

$$i_{qg} = I\cos(-\beta+\delta) \tag{2-83}$$

2.5.2 Fuel Cell Boost Converter

The boost converter is a well-known type of switched-mode DC-DC converter which is capable of boosting the input voltage to what is desired. Therefore, since fuel cell output voltage is less than the grid voltage, to control the output voltage of the fuel cell a boost converter is used. Figure 2-26(a) shows a practical realization of the switch, using MOSFET and diode.

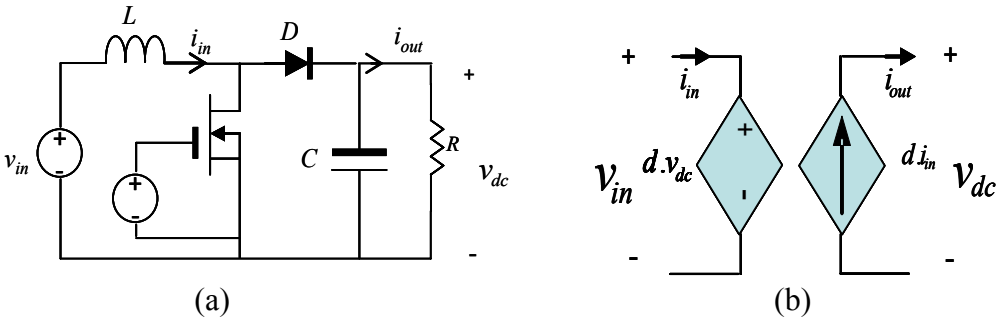

Figure 2.26 Boost Converter, (a) Practical realization using MOSFET and diode, (b) Electrical model for the boost converter

Also, based on the performance of the switch and analytical calculations [73], a boost converter can be simplified as an electrical model as presented in Figure 2-26(b).

The mathematical model for the boost converter can be defined by the following equations:

$$i_{out} = d.i_{in} \tag{2-84}$$

$$v_{dc} = (1/d)v_{in} \tag{2-85}$$

Chapter 3

Hybrid Power System Control Strategies

The Hybrid Power Control System (HPCS) can be considered a newly recognized branch in the power system industry. Power generation systems, including the SOFC-GT hybrid power system, have their best performance at a specific design condition. However considering the change in the demand power, they must be able to operate well under conditions that vary from the specific design condition. In the case of the SOFC-GT hybrid power system, the efficiency is significantly influenced by the change in power. Also, since the dynamic response of the SOFC to this change is quit slow, it is very important to select the best control strategy to achieve the best performance from the system. Therefore, in this chapter the control design systems and two different control strategies are presented and compared.

3.1 Control System Design

3.1.1 Fuel Controllers for Fuel Cell and Burner

There are four valves in the hybrid power system, which control the input fuel and air flow rates for the fuel cell and the burner. The proportional-integral (PI) algorithms are used to control these vales. Different power sharing strategies can be used to manage the valve controllers. The control system design for each valve may change based on different control strategies. In this paper, two different control strategies are introduced,

which will be explained in detail later.

In this research, the fuel valve injects fuel to the fuel cell stack to control the output power from the SOFC. Since the input air for the fuel cell has a linear relationship with the fuel, the amount of the air injected to the fuel cell is a proportion of the fuel. Figure 3.1 describes these control systems.

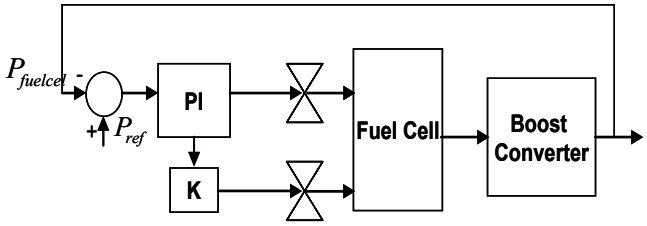

Figure3.1 Fuel cell fuel and air controller system for the first and second strategy

One of the control objectives is to have a constant shaft speed on the gas turbine. Achieving this goal would depend on the different system designs. If the hybrid system aims to utilize the waste fuel from fuel cells in the gas turbine without supplying fresh fuel, the control system could be designed to control the shaft speed by controlling the burner airflow rate. The schematic model of this control system is shown in figure 3.2

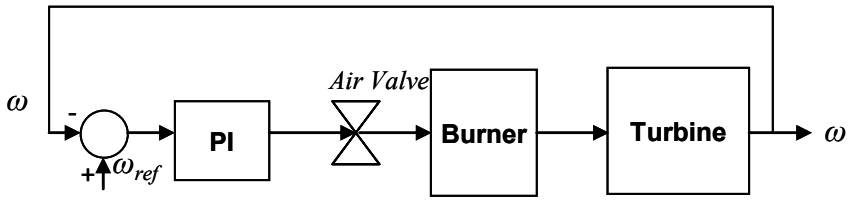

Figure3.2 Gas Turbine Shaft Speed control system for Strategy I.

Another control method is that the gas turbine shaft speed is maintained constant by controlling the fuel flow rate to the burner if the hybrid power system provides a mechanism to supply additional fuel to the gas turbine. The air flow rate to the burner is also proportional to its fuel flow rate. The schematic model of this control system is shown in Figure 3.3.

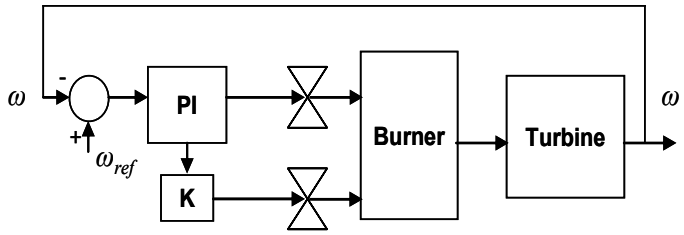

Figure3.3 Burner fuel and air controller system for the first and second strategy

3.1.2 Fuel Cell Power Controller

The fuel cell boost converter is used to control the output power of the fuel cell. The switching instant or duty cycle of the boost converter is controlled so that the SOFC output power follows the reference. Figure 3.4 represents the control diagram for the boost converter. The output from the PI compensator is used to produce a pulse width modulation (PWM) signal to drive the MOSFET switches.

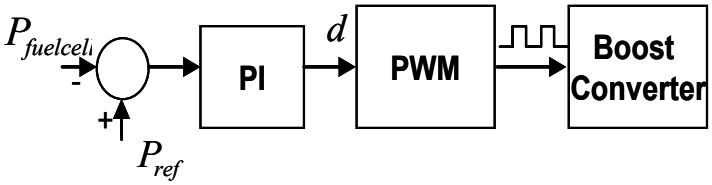

Figure3.4 **Fuel cell power control system.**

3.1.3 Generator Excitation Controller

The generator output voltage is regulated by the exciter control system. Figure 3.4 demonstrates the excitation control system for the generator [74].

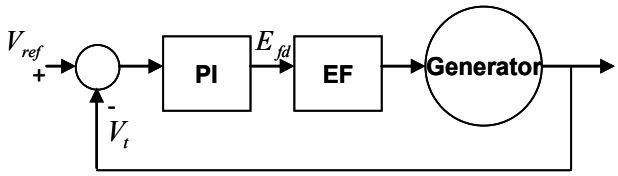

Figure3.5 Exciter control system

3.1.4 Rectifier Controller

The rectifier regulates the output DC voltage while it also controls the reactive current such that the reactive power generated is zero. The schematic model of the control system is shown in figure 3.6.

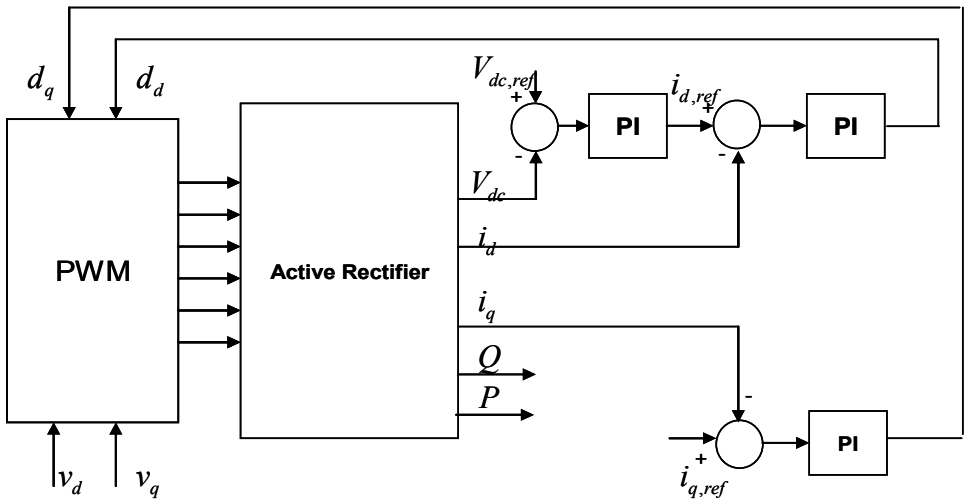

Figure3.6 **Rectifier control system**

3.2 Power Sharing Strategies

In the SOFC/GT hybrid power system, the efficiency is significantly influenced by load power changes. Since the dynamic response of the SOFC to these changes is quite slow, it is very important to select an efficient control strategy to achieve the optimal performance from the system. In this section, two different control strategies are studied to control the presented SOFC/GT hybrid power system.

3.2.1 Strategy I

In the first control strategy, the exhaust from the fuel cell that contains waste fuel is injected and burned in the burner. No additional fuel is supplied to the burner. The hot

oxidizer exhaust is expanded through the turbine, driving an electric generator. As the load power varies, the fuel cell output power changes and at the same time, the power produced from the gas turbine changes as well, as shown in Figure 3.7.

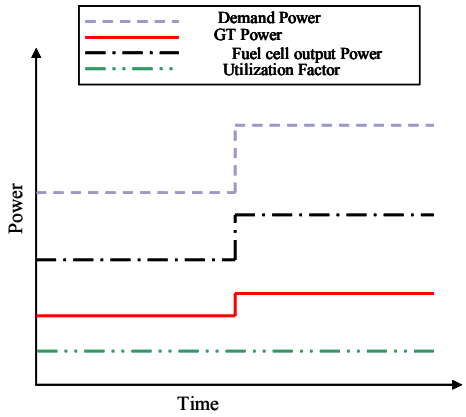

Figure3.7 Output power change of the SOFC/GT components in the passive fuel cell strategy

Figure 3.8 demonstrates the block diagram of the dynamic model and the controllers of the hybrid system. This control strategy is the simplest strategy to control the hybrid power system. Although, the design of the control system is simple, the flexibility of the system is limited. It means that the gas turbine performance depends on the fuel cell and the power sharing between the two generators is restricted since the power produced by gas turbine is dependent on the waste fuel and heat generated from the fuel cells.

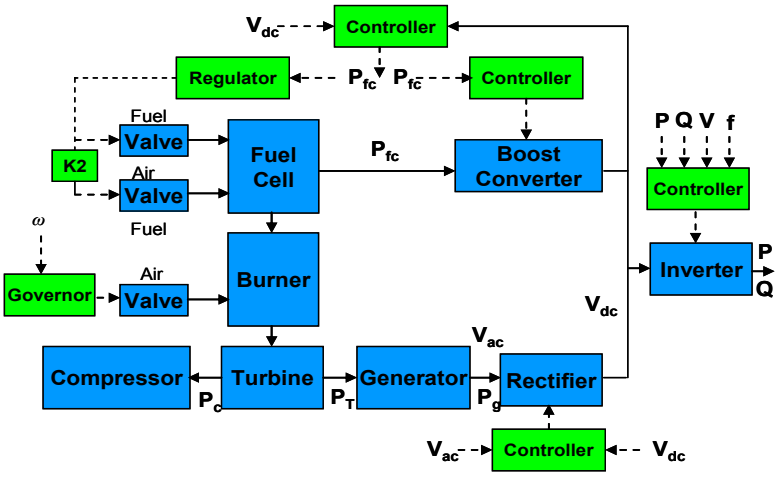

Figure3.8 Block diagram of the dynamic model and the controllers for the passive fuel cell strategy

3.2.2 Strategy II

In the second strategy, additional fuel is supplied to the burner in addition to the exhaust from the fuel cell stack. In this strategy, the power produced by the fuel cells is maintained constant by the controller. Of course this power setpoint can be changed during the run time. As a result, as the demand power changes, the gas turbine output power changes to produce remaining demand power. Figure 3.9 presents this control strategy.

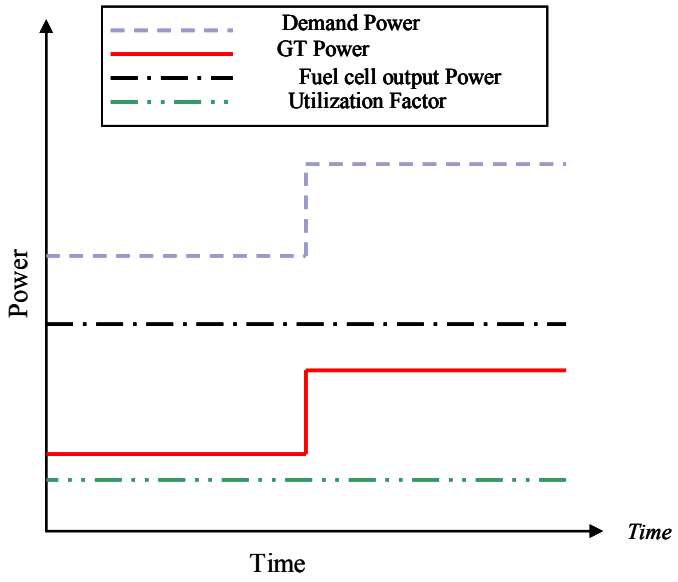

Figure3.9 Output power change of the SOFC/GT components in the constant fuel cell strategy

The block diagram of the dynamic model and controllers of the system is illustrated in Figure 3.10.

The advantage of this strategy is the rapid transient response of the hybrid system. Compared with SOFC, the transient response of the gas turbine is very fast. Therefore, keeping fuel cell output power constant during operation can help the system reach steady-state conditions rapidly. On the other hand, the complexity of the control system in this strategy is higher than the previous one. Also, considering that in some cases the

gas turbine generators have a lower efficiency, the total efficiency of the hybrid system could be reduced with this strategy.

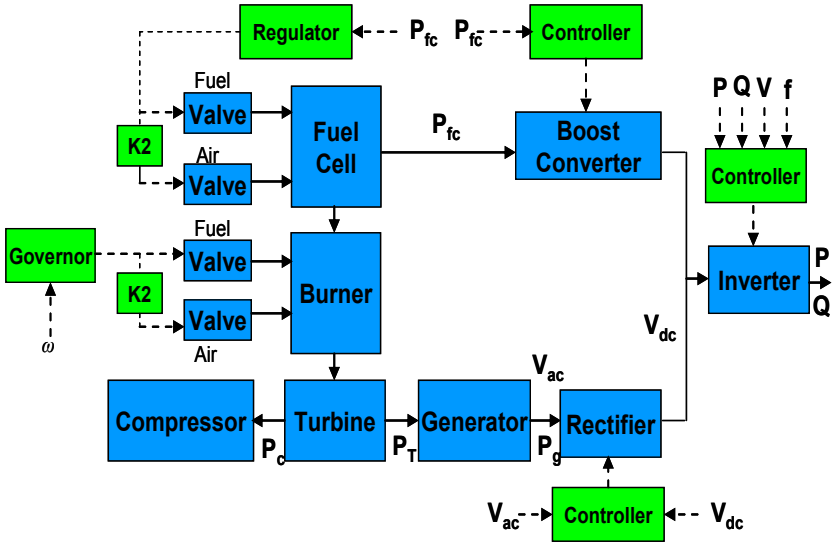

Figure3.10 Block diagram of the dynamic model and the controllers for the passive fuel cell strategy

The proposed control strategies are just some example of posbble one to control the hybrid power system. Considering the goal of the hybrid power system, more advanced and reliable control strategies may be proposed for control purpose.

Chapter 4

Particle Swarm Optimization

Power sharing is an important challenge in hybrid power systems. The demand output power is produced by the generators which make up the power system. Therefore to operate the system efficiently, the power sharing ratio should be determined appropriately. In this respect, the design of hybrid power systems can be regarded as an optimization problem. The feasible solution set of this problem must be obtained while the hybrid system should meet certain power and voltage requirements. Thus, determining the optimum power sharing in increasing the efficiency of the system is one of the focuses of this study.

To achieve this goal, some efforts have been devoted to finding appropriate optimization methods such as genetic algorithm (GA) and particle swarm optimization (PSO) for different kinds of hybrid generation systems. Compared with other optimization methods, the use of PSO and GA are growing recently. In comparison to GA however, using PSO has the following advantages:

- PSO is easy to implement
- It needs few parameters to adjust
- It has more effective memory capability
- It can be used for the nonlinear problem

As a result, to optimize the system, PSO has been used to achieve the most efficient hybrid system design.

4.1 PSO Background

Particle swarm optimization (PSO) is a population based stochastic optimization solution method. This optimization technique was developed by Eberhart and Kennedy in 1995. The idea behind the PSO originates from certain social behaviors observed in bird groups and fish schools. In PSO, the potential solutions called particles move across the problem space by following the current optimum particles based on a certain motion role.

PSO is very similar to evolutionary computation techniques such as Genetic Algorithms (GA). However, unlike GA, there are no evolution operators such as crossover and mutation in the PSO algorithm. In optimization literature, PSO has been successfully used in many areas such as function optimization, fuzzy system control, artificial neural network training, and in all operations where GA can be applied as well.

4.2 PSO Mechanism

As mentioned earlier, the PSO technique is used to optimize the hybrid power system. First, an initial population of particles is generated with preliminary speeds and positions. By operating the best positions encountered by itself and its neighbors, each particle updates its position according to its own flight experience and that of its companions (motion role). Assume x and v which determine a particle's position and its speed in the search space, respectively. Therefore, the i-th particle in the generation t can be represented as $x_i^t = [x_{i1}^t, x_{i2}^t, \ldots, x_{id}^t, \ldots, x_{iM}^t]$ in the M-dimensional space. During

the flight, each particle constantly records the best solution it has accomplished. This fitness value of the solution is called *pbest* . The best previous position for the i-th particle is denoted by $pbest_i = [\ pbest_{i1}\ , pbest_{i2}, \ldots, pbest_{id}, \ldots, pbest_{iM}\ ]$ and is stored in the memory. The global best *gbest* is the best particle of all particles in the swarm, which is the best value reached till that generation by all particles, is also tracked by the optimizer in the swarm. The velocity for particle *i* is represented by $v_i = (v_{i1}, v_{i2}, \ldots, v_{id}, \ldots, v_{iM})$. The velocity and position of each particle can be updated based on the current velocity and the distance from *pbest* to *gbest*. After all the generations, the PSO can find the best existing solution from memory. The velocity update of the particle e is graphically illustrated in Figure 4-1[76].

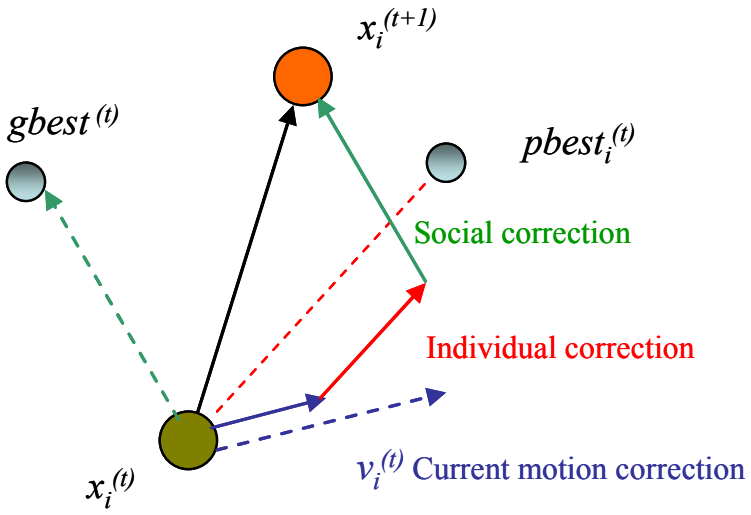

Figure 4.1 Graphical illustration of the mechanism of velocity update

Generally there are six steps for PSO algorithm as outlaid below and depicted in Figure 4-2.

Step 1: The position and velocity of the particle in the initial state for *n*-dimensional space are generated randomly.

Step 2: considering defined fitness function, the fitness value of the particle is well evaluated.

Step 3: *The Individual Perspective:* Here each particle will evaluate its performance by evaluating the fitness function. In the *t*-th generation, the present fitness $f(x^t_{id})$ value of the *i*-th particle is compared with the ones stored in $pbest_{id}^{(t)}$. If $f(x^t_{id}) > f(pbest_{id}^{(t)})$, then the algorithm sets $pbest_{id}^{(t+1)} = x^t_{id}$. By this method, a record of the best individual particle is kept for the velocity update.

Step 4: *The Social Perspective:* Here the particle considers the performance of the *entire* swarm. The best performance of *all* particles is stored in the global best *gbest*. The fitness value at the current generation is then compared to the one calculated at *gbest*, and the algorithm sets $gbest^t = x^t_{id}$ if $f(x^t_{id}) > f(gbest^t)$.

Step 5: The new velocities and positions of the particles for the next generation is determined according to equation (4-1) and equation (4-2).

$$v_{i_d}^{(t+1)} = w * v_{i_d}^{(t)} + c_1 * rand() * (pbest_{i_d} - x_{i_d}^{(t)}) + c_2 * Rand() * \left(gbest_d - x_{i_d}^{(t)}\right) \quad (4\text{-}1)$$

$$x_{i_d}^{(t+1)} = x_{i_d}^{(t)} + v_{i_d}^{(t+1)}, i = 1,2...,M, d = 1,2,...,N \quad (4\text{-}2)$$

Where *N* is the number of particles in a swarm, *M* is the number of members in a particle, *t* is the counter of generations (iteration), *w* is the inertia weight factor, c_1 and c_2 are weight factors, *rand()* and *Rand()* are uniform random values in a range [0, 1], $v_{i_d}^{(t)}$ is

the velocity of particle i in generation t, and $x_{i_d}^{(t)}$ is the current position of particle i in generation t.

Step 6: If the search satisfies the termination condition then it stops; otherwise, it returns to step 2.

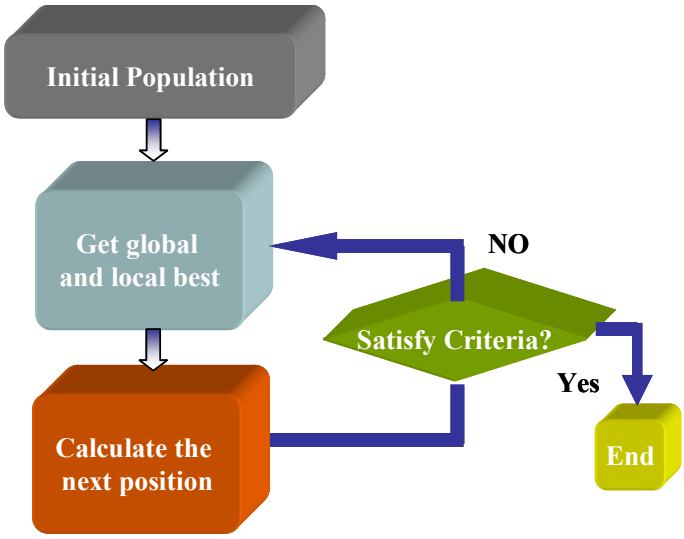

Figure 4.2 Flowchart of the PSO algorithm

In the following section the implementation methodology of PSO to achieve the high efficiency for the hybrid power system will be explained.

4.3 PSO Algorithm to Maximize the Efficiency

As mentioned, one of the important challenges in the hybrid power system is to reach a high efficiency of the system. Therefore the issue of finding the amount of the power generated by each generator in the hybrid power system to maximize the efficiency is formulated as an optimization problem. In this research, two types of configurations based on different assumptions have been studied to determine their optimum efficiency.

The first problem assumes that two generators of the hybrid power system, SOFC and GT, operate independently. In the second, these two generators are unilaterally connected. These two configurations will be explained as follows.

4.3.1 Hybrid Power System Containing Independent Generators

The hybrid system in this study consists of a SOFC operating at ambient pressure, and a gas turbine. Each power generator has its own efficiency curve, which is obtained from the experiments. The goal is determining the operating point for each generator in order to obtain maximum efficiency for the hybrid power system. Figure 4-3 illustrates the graphic representation of the model.

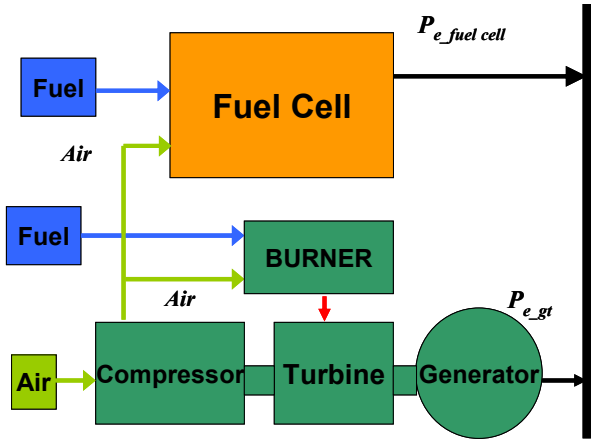

Figure 4.3 Hybrid power system model with independent generators

The total efficiency of the system is calculated from the following equation:

$$\eta(P_{gt}, P_{e,f}) = \frac{\eta(P_{gt}) \cdot (P_{gt} / P_{Load}) + \eta(P_{e,f}) \cdot (P_{e,f} / P_{Load})}{P_{Load}} \quad (4\text{-}3)$$

$P_{e,f}$ is the power produced by the fuel cell and P_{gt} is the power produced by the gas turbine. In addition, P_{load} is the total power of the system that is constant and is calculated from equation 4-5:

$$P_{Load} = P_{e,f} + P_{gt} \tag{4-5}$$

Moreover, each generator has a limitation to produce the eclectic power. These power limitations can be defined by the following inequality constraints:

$$P_{e,f\min} \le P_{e,f} \le P_{e,f\max} \tag{4-6}$$

$$P_{gt\min} \le P_{gt} \le P_{gt\max} \tag{4-7}$$

Therefore the objective function in this problem is the efficiency while the power output generated by the generators is considered as particles in the swarm in the PSO approach. The power output vector is defined as $x_i^0 = (P_{i1}^{(t)}, P_{i2}^{(t)})$. Here $P_{i1}^{(t)}$ represents the SOFC output power and $P_{i2}^{(t)}$ represents the GT output power in each iteration. Both quantities must be between the minimum and the maximum power for each generator [P_{min}, P_{max}]. The process of the modified PSO algorithm is as follows:

Step 1) Choose the initial set of variables randomly while satisfying the constraints

Step 2) Update *pbest* and *gbest* based on the fitness function (4-3)

Step 3) Update the velocity and position by using equation (4-1) while satisfying inequality constraints (4-6) and (4-7)

Steps 4) Return to Step 2 until the stopping criteria is satisfied

Initialization (Step 1): In this step a set of power quantities is generated randomly such that the vectors $x_i^0 = (P_{i1}^0, P_{i2}^0)$ satisfy the constraints by mapping them into the interval $[P_{\min}, P_{\max}]$. The initial velocity vectors, $v_i^0 = (v_{i1}^0, v_{i2}^0)$, are also randomly generated. The initial value of *pbest* is the same as the random initial positions, x_i^0, and the initial value of $gbest_d$ is vector x_j^0 for j which maximize the objective function, i.e. the efficiency.

Updating *gbest* and *pbest* (Step 2): In this step for each particle, $x_i^0 = (P_{i1}^0, P_{i2}^0)$, the fitness values, $\eta\ (\ p_{i1}^{(t)},\ p_{i2}^{(t)})$, is being calculated from the equation (4-3). These fitness values are then being compared to the fitness values based on the previous *pbest.* If $\eta\ (\ p_{i1}^{(t)},\ p_{i2}^{(t)}) > \eta\ (\ pbest_{i1}^{(t)},\ pbest_{i2}^{(t)})$, then the algorithm sets $pbest_{i1}^{(t+1)} = p_{i1}^{(t)}$ and $pbest_{i2}^{(t+1)} = p_{i2}^{(t)}$ respectively. In all other cases, the value of *pbest* remains uinchanged. The same comparison is being done to update the value of $gbest_d$.

Velocity update (Step 3): For the first generator, the position of each individual is modified based on the updated velocity of that individual using equation (4-1). The values of the parameters C_1 and C_2 in (4-1) and w_{min} and w_{max} (initial and final weights) in (4-8) are chosen such that the system reaches the optimum solution with the minimum number of iterations. The value of w then is calculated from equation (4-8).

$$w = w_{\max} - \frac{w_{\max} - w_{\min}}{Iter_{\max}} \times Iter \qquad (4\text{-}8)$$

Where $Iter_{max}$ is the maximum number of iterations and *Iter* is the number of current iteration. To update the position for each particle (i.e. updated power for each generator), this updated velocity is added to the previous position (equation (4-2)). This updated power must satisfy the inequality constrains (4-6) and (4-7). Therefore the finalized updated output power of the first generator in each iteration is

$$P_{i1}^{t+1} = \begin{cases} P_{i1}^{t} + v_{i1}^{t+1} & if \quad P_{1,\min} \le P_{i1}^{t} + v_{i1}^{t+1} \le P_{1,\max} \\ P_{1,\min} & if \quad P_{i1}^{t} + v_{i1}^{t+1} < P_{1,\min} \\ P_{1,\max} & if \quad P_{i1}^{t} + v_{i1}^{t+1} > P_{1,\max} \end{cases} \tag{4-9}$$

After finding the power output of the first generator in each iteration ($P_{i1}^{(t)}$), the power output of the second generator ($P_{i2}^{(t)}$) is found by deducting $P_{i1}^{(t)}$ from the demand power.

4.3.2 Hybrid Power System Containing Dependent Generators

The second configuration (hybrid power system consisting of an SOFC and a GT) is shown in figure 4-4. In this configuration, the first generator (SOFC) transmits its waste fuel as well as heat to the second one (GT). As explained in chapter 2, SOFC uses only a certain percentage of fuel calculated in utilization factor (U_z). Therefore, several studies have proposed sending the remaining of the fuel used in the fuel cell to the gas turbine. In addition to this unused fuel, since the SOFC works at high temperatures, the system efficiency can be increased by making a use of SOFC's high temperature exhaust in the gas turbine. Therefore, the gas turbine performance depends on the SOFC performance in this configuration.

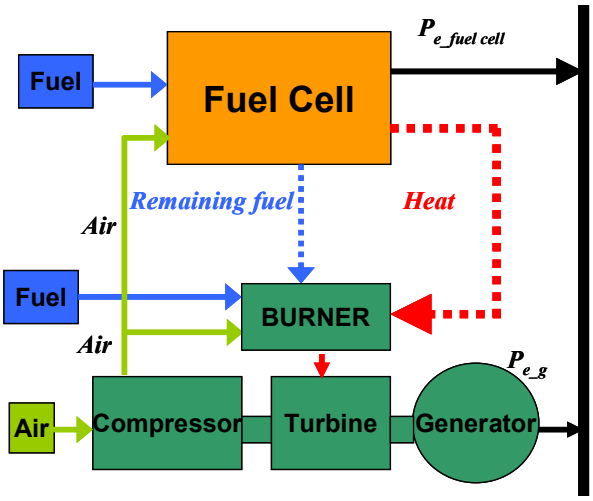

Figure 4.4 Hybrid power system model consisting dependent generators

To achieve the maximum efficiency of the system, each generator is modeled as described in chapter 2. The following equation describes the objective function for the optimization problem in this configuration.

$$\eta = \frac{P_{load}}{(m_{f,f} + m_{f,b}) \times LHV} \times 100 \tag{4-10}$$

Where η is the system efficiency, $m_{f,f}$ is the fuel mass flow rate of the fuel cell, $m_{f,b}$ is the fuel mass flow rate of the burner , P_{load} is the demand power, and LHV is the lower heating value of the fuel which is a constant.

To maximize the efficiency of the system, the total mass flow rate injected to the system, $m_{f,f}$ pluse $m_{f,b}$, should be minimized. In this optimization problem, $P_{e,f}$ and P_{gt} are introduced as particles in the swarm (in the PSO approach). $m_{f,f}$ *and* $m_{f,b}$ are evaluated by the power demanded from each generator. Therefore, based on the model presented in chapter 2, and equations (4-11) and (4-12), $m_{f,f}$ is a function of SOFC output power ($P_{e,f}$) and $m_{f,b}$ is a function of GT and SOFC output power ($P_{e,f}$ and P_{gt})

$$m_{f,f} = f(P_{e,f}) \tag{4-11}$$

$$m_{f,b} = f(P_{e,f}, P_{gt}) \tag{4-12}$$

Similar to the previous configuration, the total output power produced by two generators is constant here. Also, the power production limitations determine by inequalities (4-6) and (4-7) has to be satisfied all the time.

The PSO algorithm to solve this optimization problem can be summarized as following:

Step 1) Choose the initial set of output powers randomly for both generators while satisfying constraint (4-5).

Step 2) Determine $m_{f,f}$ and $m_{f,b}$ using (4-11) and (4-12)

Step 2) Update *pbest* and *gbest* based on fitness function (4-10)

Step 3) Update the velocity and positions using equation (4-1) while satisfying constraints enumerated by inequalities (4-6) and (4-7) .

Steps 4) Return to Step 2 until the stopping criteria is satisfied.

All these steps are executed in the same way explained in Section 4.3.1 with the only difference of using the objective function in equation (4-10) instead of (4-3).

Chapter 5

Simulation Results

In Chapter two, the modeling of the SOFC-GT hybrid power system was studied. The mathematical model for each component was introduced there. Also, those models had the capability to investigate the transient response of the system. Chapter three has presented different strategies that can be used to control the hybrid power system. In addition, the control design for each strategy has been explained. In Chapter four PSO has been introduced as the optimization method to improve the efficiency of the system. This method has been implemented for tow different problems. In the present chapter the results of simulation which has been done in the previous chapters is presented. MATLAB is the programming tool which is used to study the system. Since MATLAB has a powerful toolbox for runtime simulation, we use Simulink toolbox for modeling the hybrid power system and study the proposed control strategies. Also, it is used to programming the PSO algorithm for optimization module. In the following section the results of the simulation of the system modeling and controlling will be presented. Furthermore, the PSO algorithm behavior and the results of this method are shown.

5.1 Simulation Results and Discussions

The hybrid power system is tested on a standalone load supplied by a voltage source inverter. The SOFC consists of 600 cells and provides nominal output power 150 KW.

Gas turbine consists of compressor with pressure ratio (PR_c) 3, heat exchanger and a turbine with pressure ratio (PR_T) 3. The nominal power for gas turbine considered as 50 KW. The compressor input temperature in this simulation is ambient temperature. The generator is a two-pole generator working at 60 Hz by 50kW nominal power and 200V nominal voltage. During the simulation, SOFC provides 90kW power while the rest of the demanded power is supplied by gas turbine generator. The load power demand changes from 114 kW to 132 kW at 0.8s while the fuel cell output power reference changes to 95kW at 2s. The line voltage is kept constant at 600V. The schematic of the simulated hybrid power system in Matlab is presented in Figure 5.1

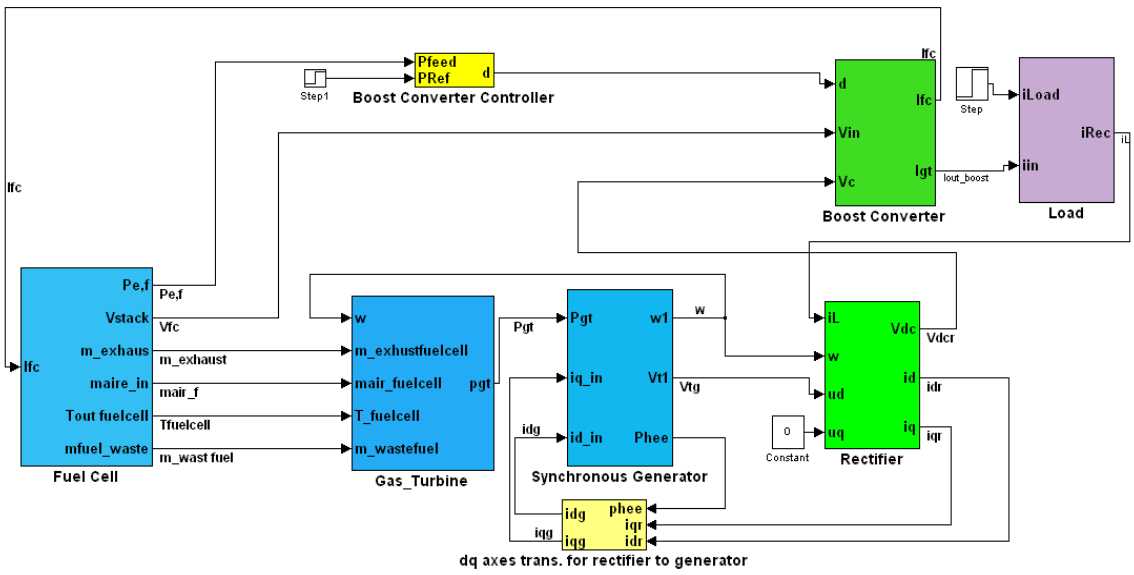

Figure 5.1. Matlab Simulink schematic

As it shows in the Figure 5.1 the waste fuel (m_wast fuel) and exhaust (m_exhast) from the fuel cell injects into the gas turbine. The mechanical output power of the gas turbine (P_{gt}) is connected to the generator to produce the electrical power in the synchronous generator. The generator terminal voltage (V_{tg}) is connected to the d axis

voltage of the rectifier. The d-q axis transfer function used to produce the generator d-q axis currents (i_{dg} , and i_{qg})from the rectifier d-q axis currents (i_{dr} , and i_{qr}) can be seen in figure 5.1. Also, from this figure it can be seen that the duty cycle of the fuel cell boost converter (d) is controlled by the fuel cell output power.

The gas turbine is considered as a subsystem in the Matlab Simulink which is demonstrated in Figure 5.2.

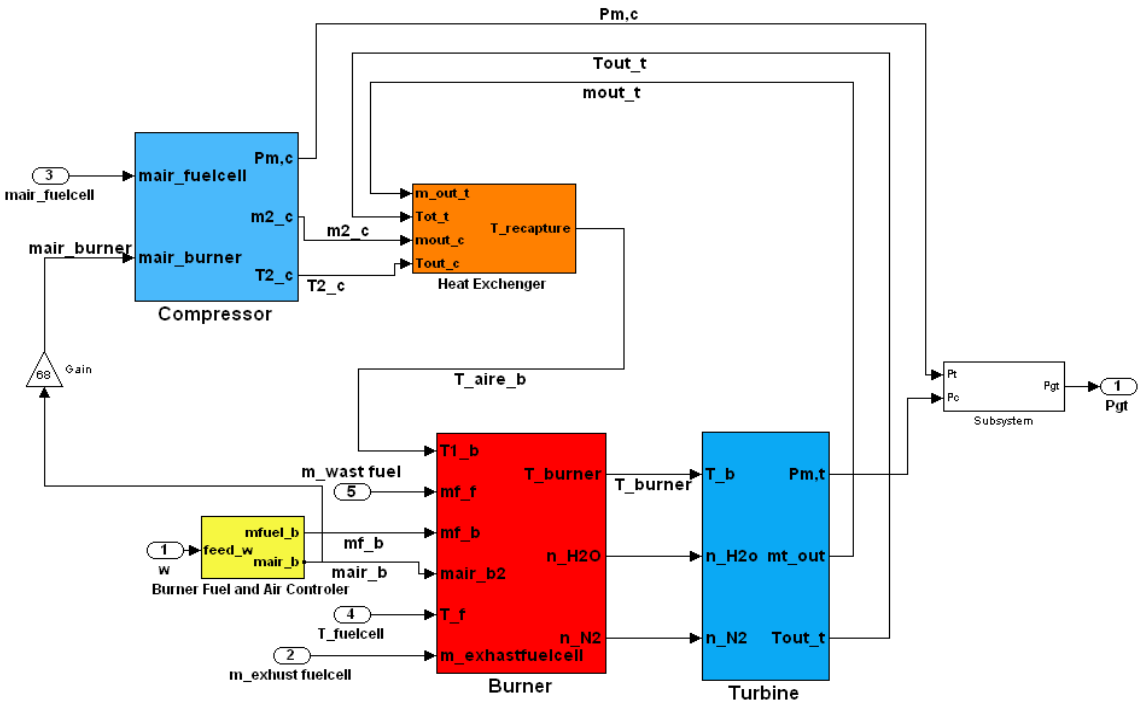

Figure 5.2. Gas turbine subsystem

As it can be seen from Figure 5.2 the burner input fuel flow rate (mf_b) air flow rate (mair_b) are controlled by shaft speed (w). Also, as it shows in this figure the fuel cell waste fuel (m_wast fuel) is injected to the burner. The input temperature of the turbine is the output temperature of the burner (T_burner). The output power of the gas turbine is the difference between of the power produced by the turbine (Pm,t) and power consumed by the compressor (Pm,c).The simulation results are are discussed in the follow. As it is

shown in Figure 5.3 when the demanded power is changed the DC bus voltage of the hybrid system remains almost unchanged with a slight disturbance.

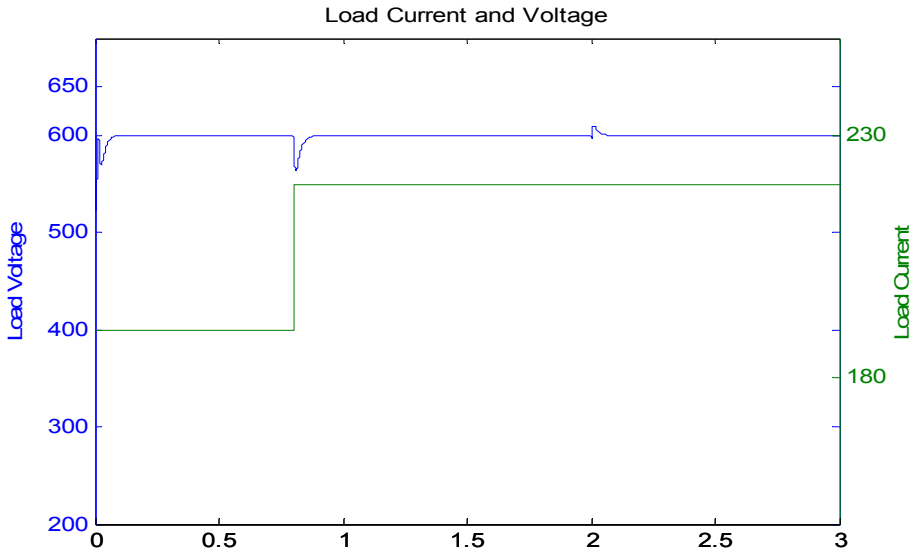

Figure 5.3. Load Current and Voltage

Also, the fuel cell output voltage and current do not change while the power produced by fuel cell is constant , but as the fuel cell output power increases at 2s, the stack current increases as well Fig. 5.4. Since the fuel flow rate of the fuel cell has a linear relationship with the current and power, it does not change before 2s and it increases at 2s.

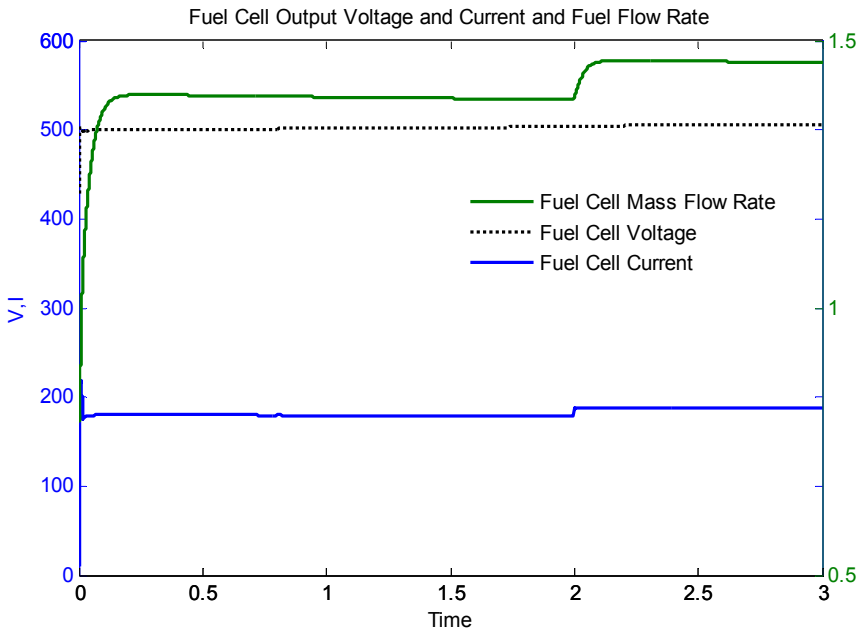

Figure 5.4. Fuel Cell Output Voltage and Current and Fuel Flow Rate

Figure 5.5 shows all the powers generated in the system. The output power of the fuel cell, as expected, remains unchanged before 2s, while the turbine, compressor and generator output powers increase by increasing the demand power of the system. But by increasing the fuel cell output power at 2s, since the total demand powers is constant, the generated power by gas turbine and generator decrease.

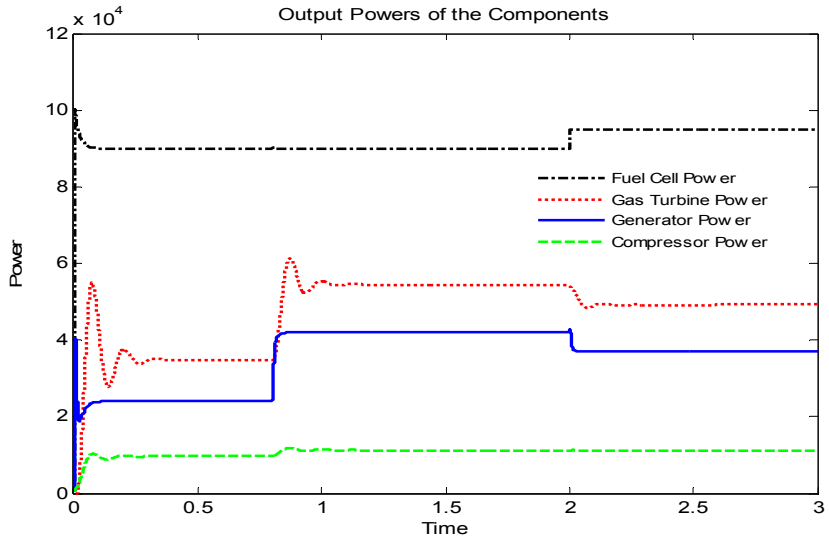

Figure 5.5. Output Powers for Turbine, Compressor, Generator and Fuel cell

Also, the gas-turbine generator output voltage is controlled by excitation control system, Fig. (5-4). The generator terminal voltage is maintained unchanged while the exciter voltage increases to generate more power as the load increases.

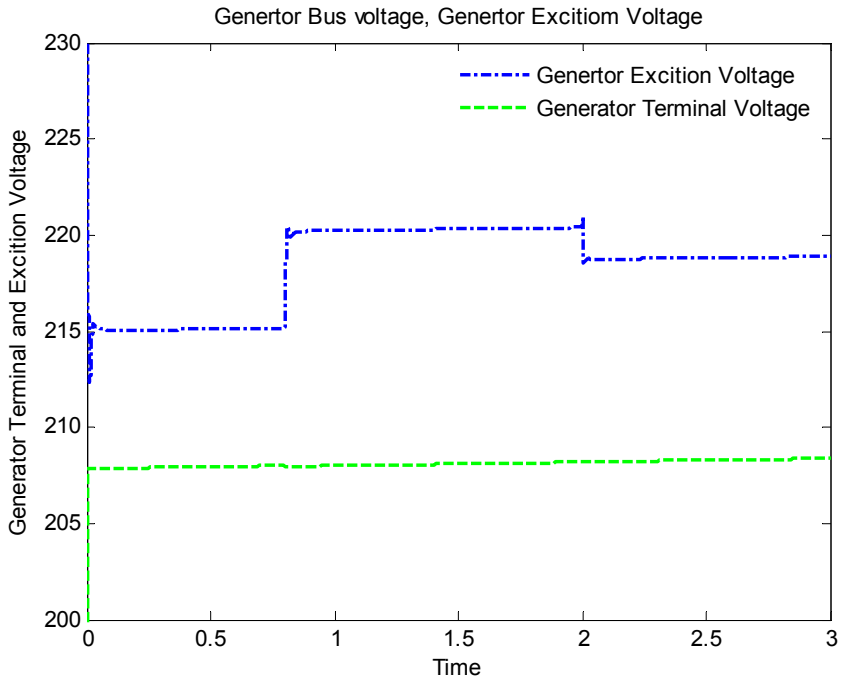

Figure 5.6. Generator Terminal Voltage and Excitation Voltage

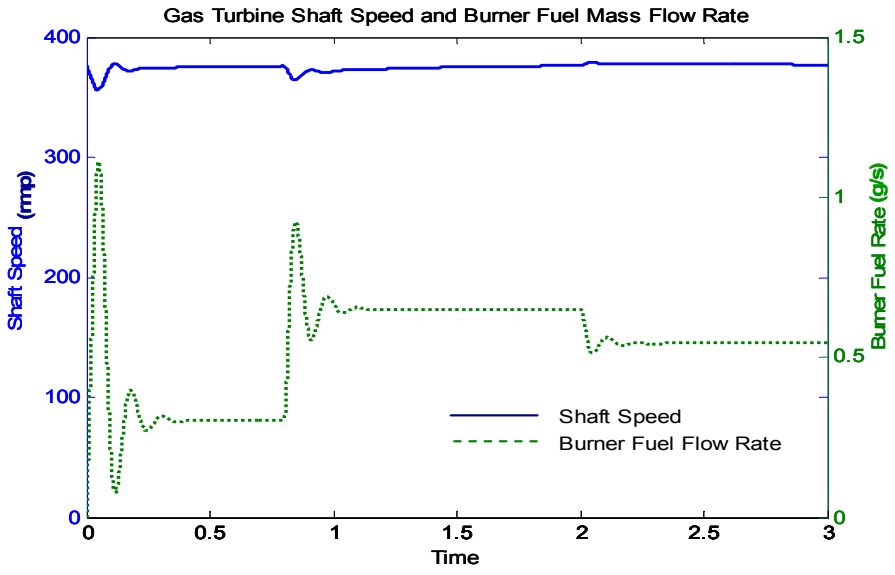

Figure 5.7. Gas Turbine Shaft Speed and Burner Fuel Flow Rate

The burner fuel flow rate changes while the shaft speed is almost constant, as shown in Figure 5.7. This is because the shaft speed is maintained constant by controlling the fuel flow rate of the burner. Moreover, as it can be seen in Figure 5.7 the shaft speed remains almost constant but the burner fuel flow rate increases as the load demand changes at 0.8s.

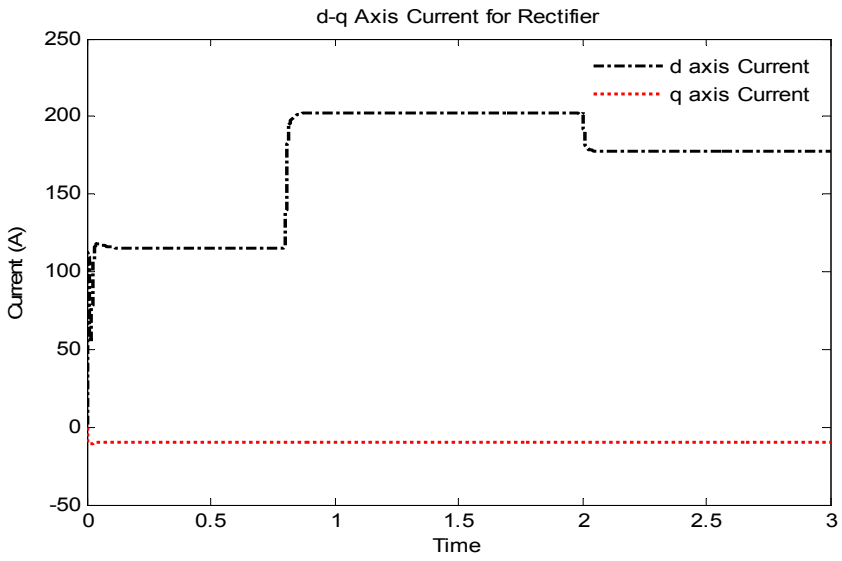

Figure 5.8. Rectifier d-q axis current

As it can be seen in the Figure 5.8, the rectifier q axis current is controlled to be constant at -10 (A). but the d axis current follows the change of the out power produced by the generator. The d-q axis current produced by generator changes also follows the output power generated by generator as it can be seen in the Figure 5.9

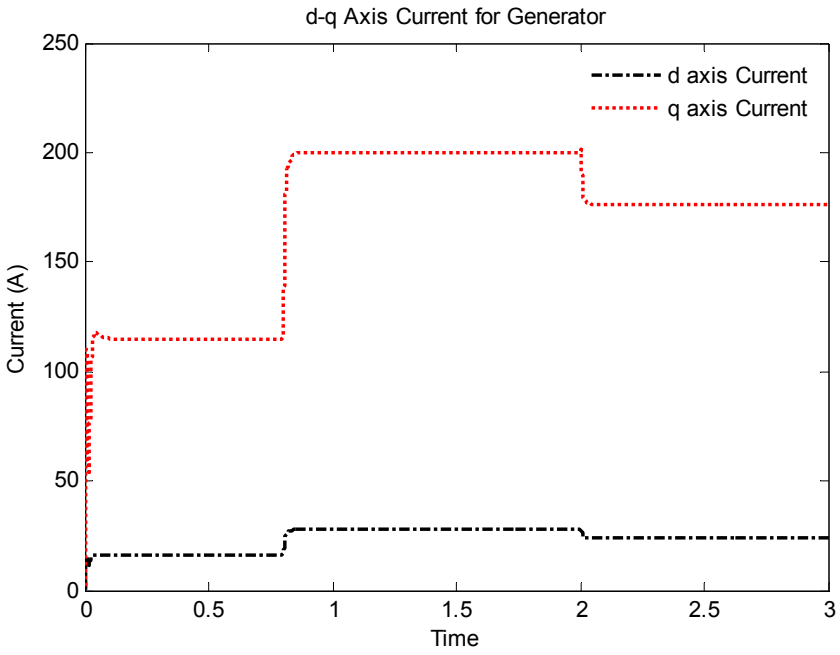

Figure 5.9. Generator d-q axis current

5.2 Comparison of Control Strategies

Two different strategies, as described in chapter 3, are investigated in the proposed hybrid power system. Simulation results with both strategies are presented as follow.

The rated power of solid oxide fuel cell stack is 150kW and contains of 600 cells. The gas turbine is operated at 24,000rpm (400Hz). The generator is a two-pole synchronous generator with a 100kW nominal power and 200V nominal voltage. The DC bus voltage is kept constant at 600V. The load power demand changes from 114 kW to 132 kW at 20s.

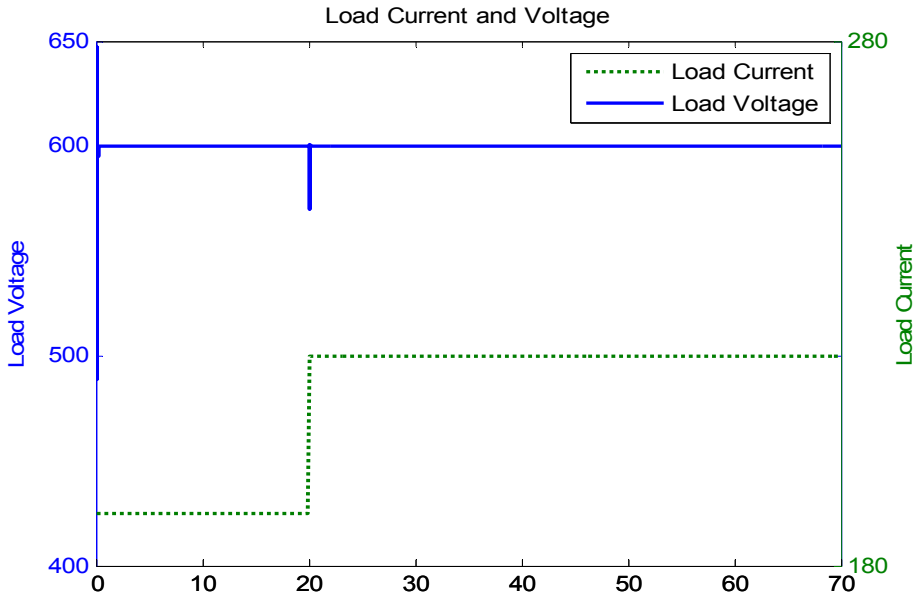

Figure 5.10. Load Current and Voltage

As shown in Figure 5.10, as the load demanded power is changed, the DC bus voltage of the hybrid system remains almost unchanged with a slight disturbance.

By increasing the demand power, the fuel cell output power increases, as can be seen in Figure 5.11. Besides, the gas turbine produced output power increases as the fuel cell produced more output power.

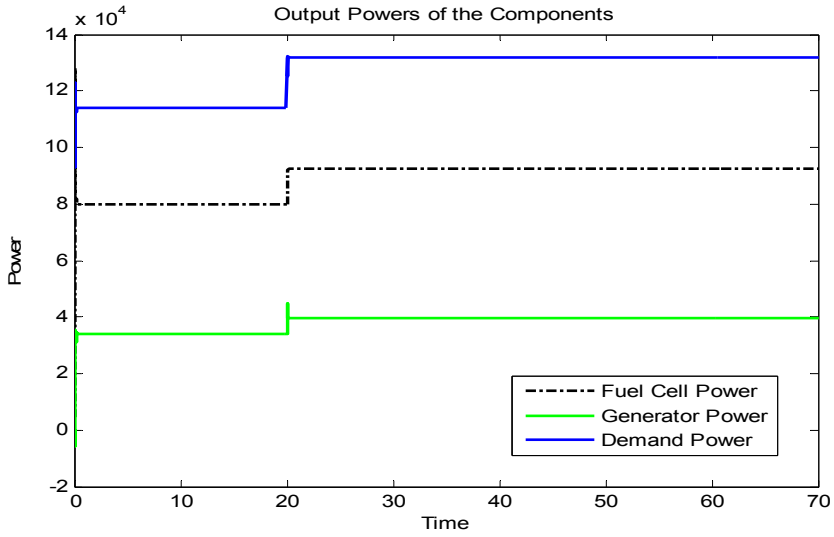

Figure 5.11. Output Powers and Demand Power

Since the output current of the fuel cell has a direct relationship with the output power and fuel flow rate, the fuel cell current and fuel flow rate both increase, as shown in Figure 5.12, while the fuel cell voltage decreases.

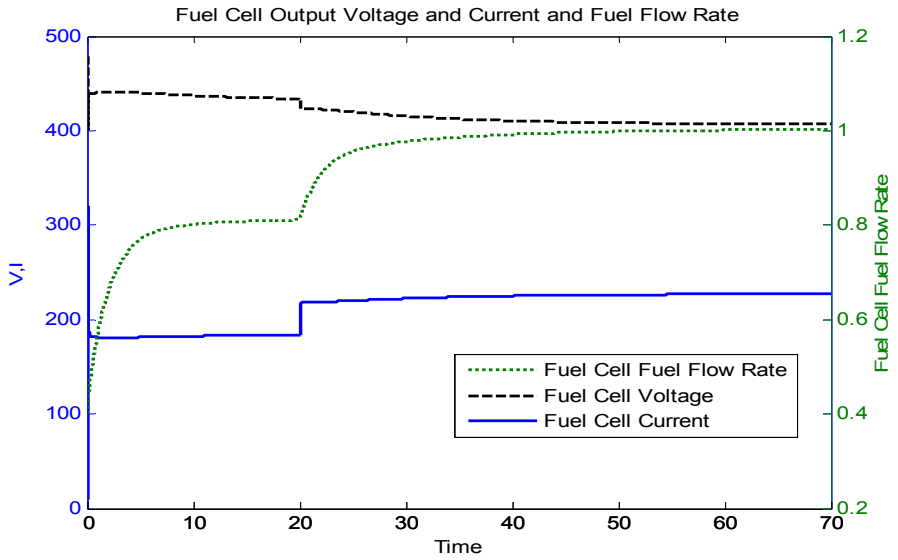

Figure 5.12. Fuel Cell Output Voltage and Current and Fuel Flow Rate

As the output power increases, the temperature of the fuel cell increases, as illustrated in Figure 5.13. Figure 5.12 shows the fuel cell and gas turbine output powers change correctly with respect to the demand power change, which is consistent with Figure 3.7.

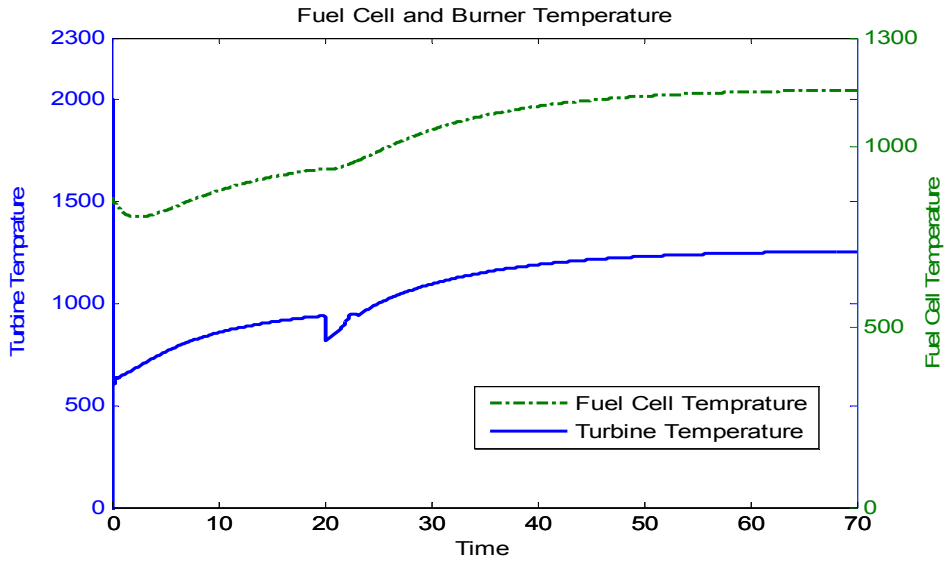

Figure 5.13. Fuel Cell and Burner Temperatures

The gas-turbine generator voltage is regulated by excitation control system. As shown in Figure 5.14, the generator terminal voltage is maintained unchanged while the exciter voltage increases to generate more power as the load increases.

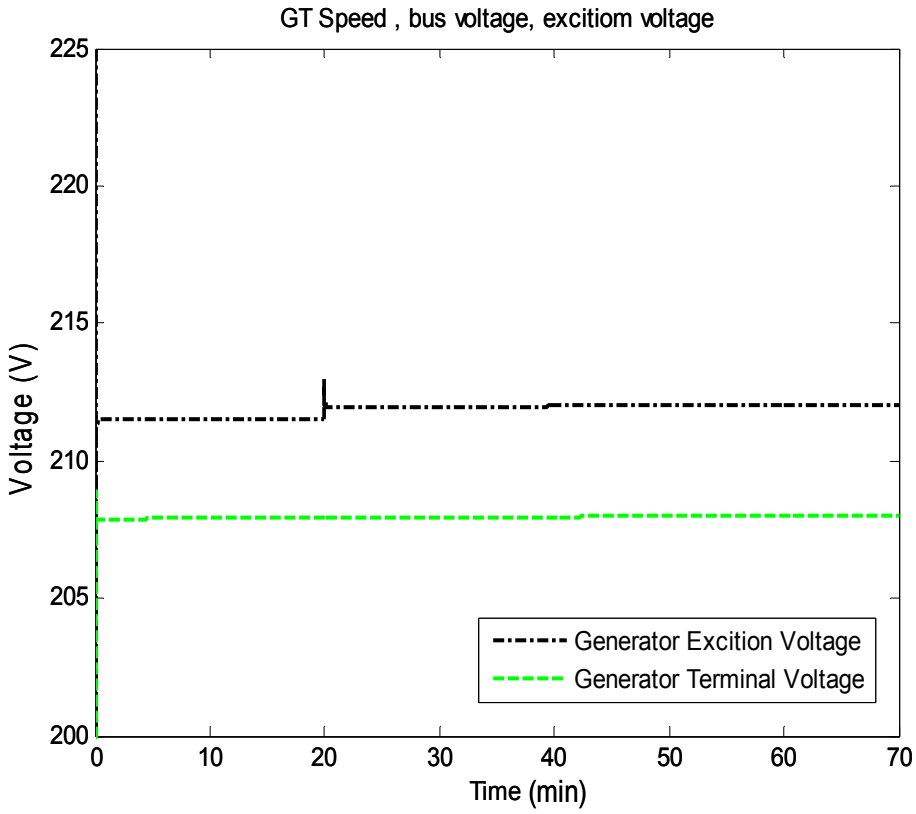

Figure 5.14. Generator Terminal Voltage and Excitation Voltage

Since no additional fuel is injected to the burner, the burner air flow rate changes while the shaft speed is almost constant, as shown in Figures 5.15 and 5.16. This is due to the fact that the shaft speed is maintained constant by controlling the burner air flow rate.

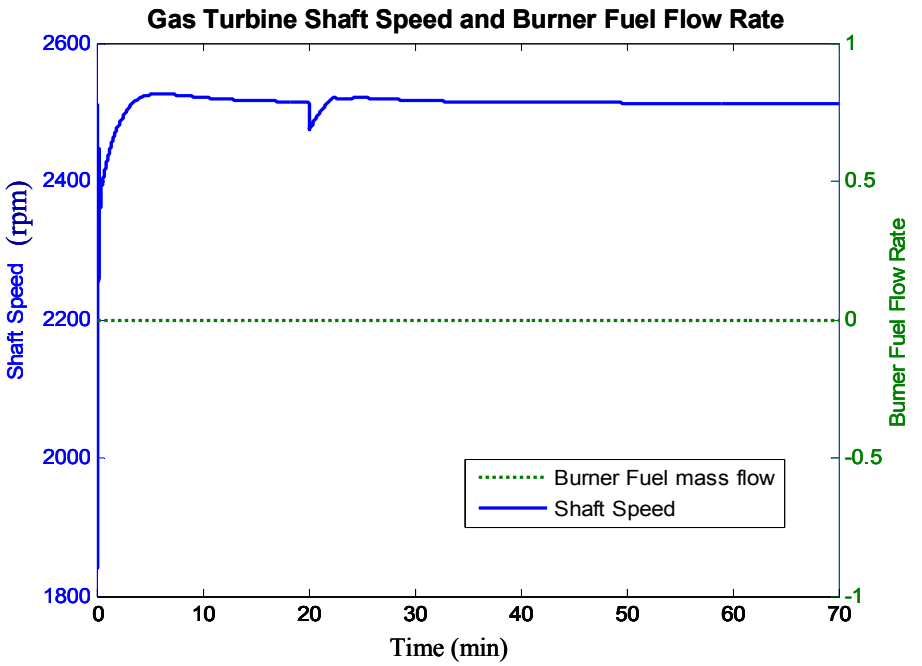

Figure 5.15. Gas Turbine Shaft Speed and Burner Fuel Flow Rate

The air flow rate for the fuel cell has a linear relationship with the fuel flow rate injects into the fuel cell. It can be seen from the Figure 5.16.

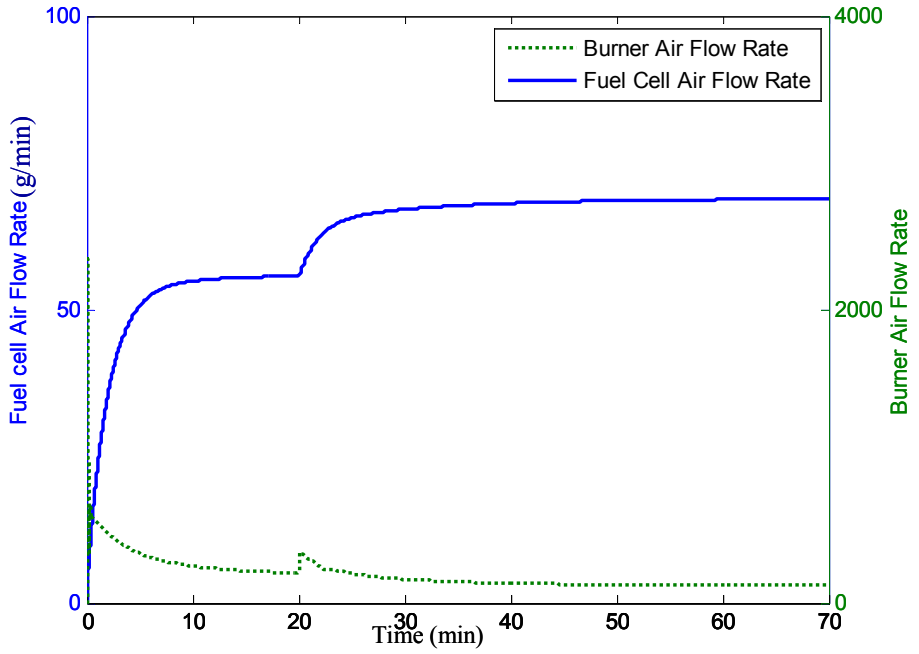

Figure 5.16. Burner and Fuel Cell Air Flow Rate

In the second strategy, the SOFC provides 90kW power constantly while the rest of the demand power is supplied by the gas turbine generator.

As shown in Figure 5.17, although the demand power is changed , the DC bus voltage of the hybrid system remains unchanged, like the first strategy.

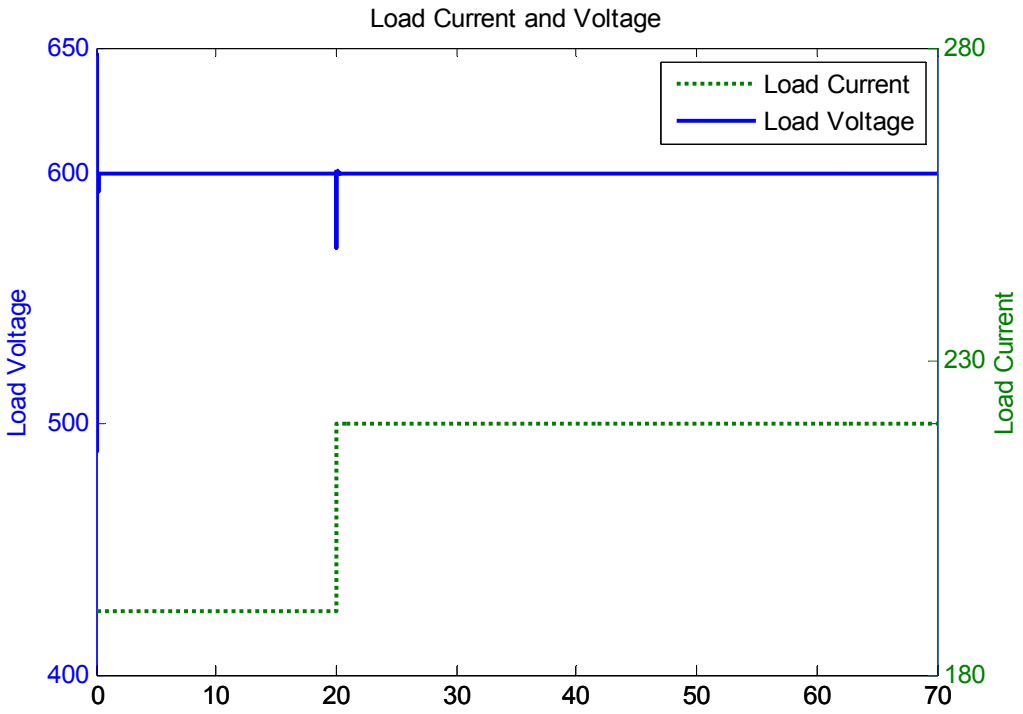

Figure 5.17. Load Current and Voltage

The fuel cell output voltage and current do not change, as shown in Figure 5.18, since its output power is regulated at a constant level.

As it can be seen since fuel flow has a linear relationship with current, it reaches to a constant level after a 7 minute and remain unchanged during the experiment.

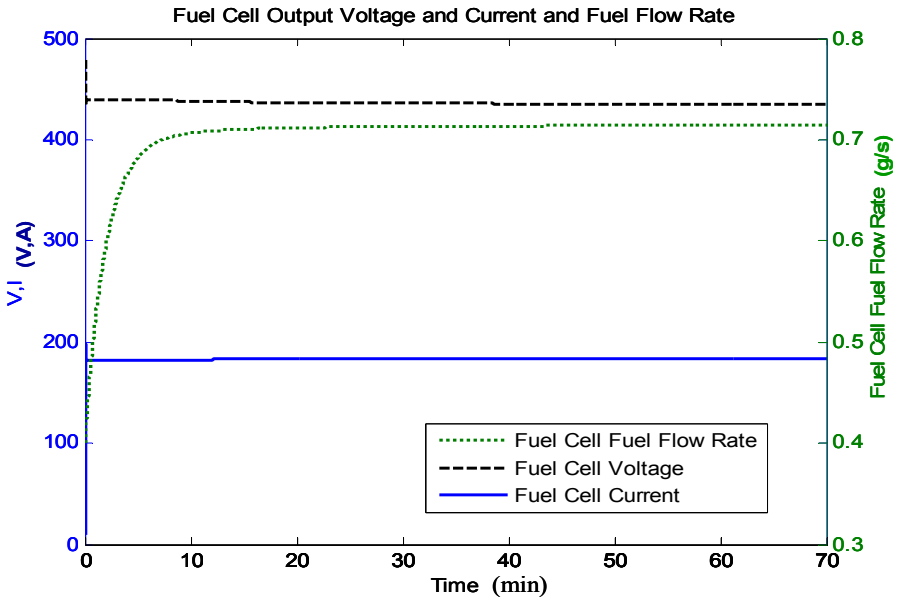

Figure 5.18. Fuel Cell Output Voltage and Current and Fuel Flow Rate

Figure 5.19 shows the power changes in different subsystems. The output power from the fuel cell remains unchanged, as expected, while the generator output power increases when increasing the demand power of the load. The fuel cell and gas turbine respond correctly to the load power change, which is consistent with Figure 3.9.

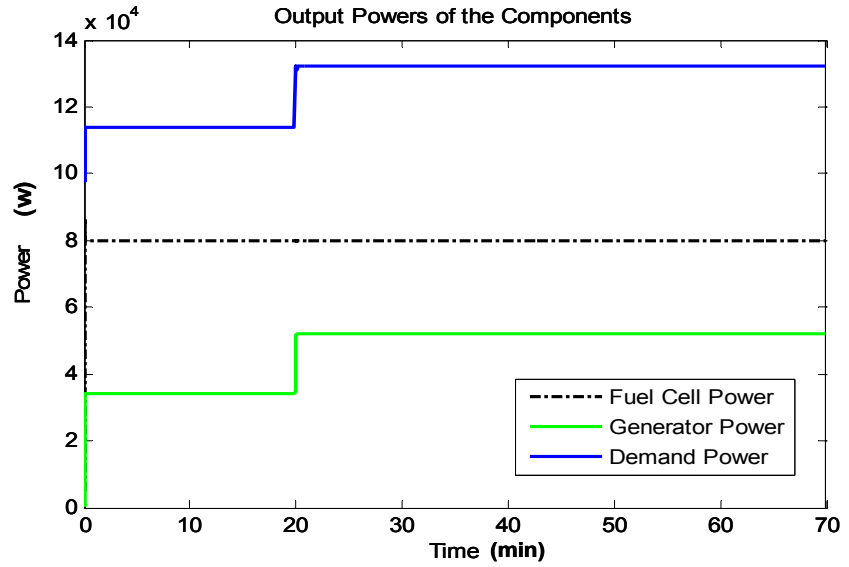

Figure 5.19. Output Powers and Demand Power

As shown in Figure 5.20, the generator terminal voltage is maintained unchanged while the exciter voltage increases to generate more power as the load power increases, like in the first strategy.

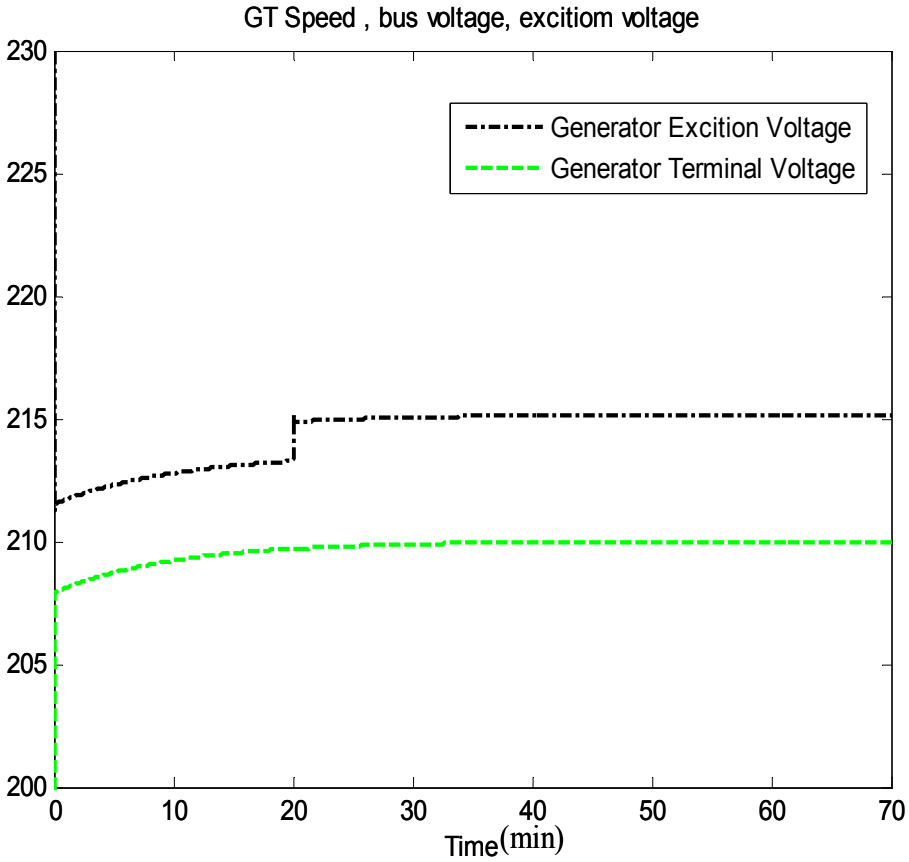

Figure 5.20. Generator Terminal Voltage and Excitation Voltage

The fuel flow rate of the burner changes with the load power while the shaft speed is almost constant, as shown in Figure 5.21. This is because fact that the shaft speed is maintained constant by controlling the burner fuel flow rate.

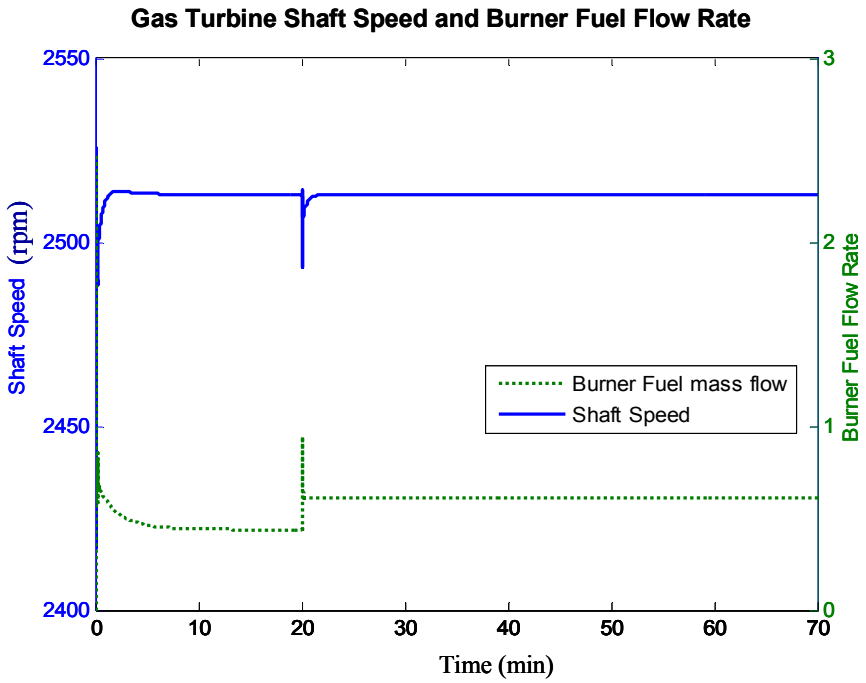

Figure 5.21. Gas Turbine Shaft Speed and Burner Fuel Flow Rate

The burner air flow rate in this strategy have a linear relationship with the burnr fuel flow rate as it can be seen in the Figure 5.22.

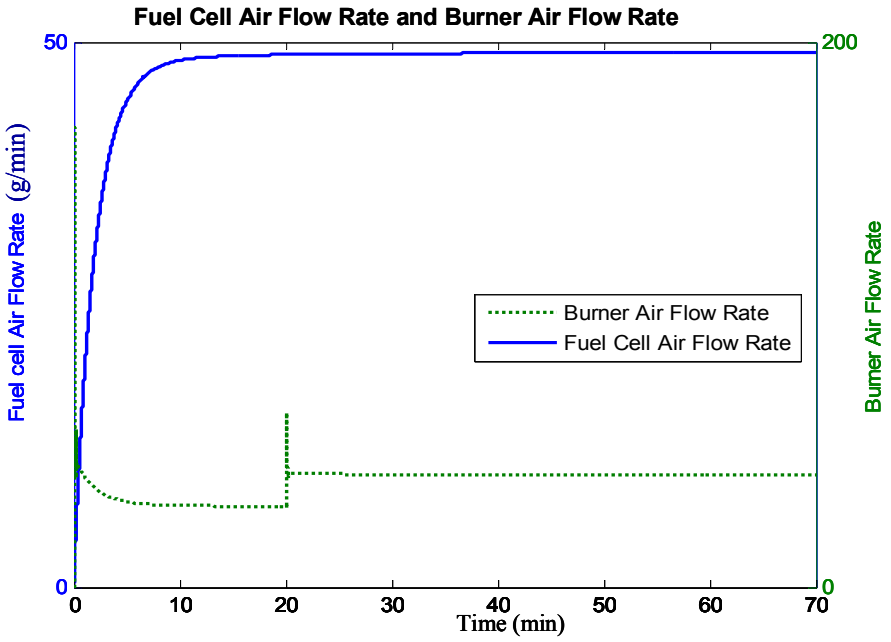

Figure 5.22. Burner and Fuel Cell Air Flow Rates

The fuel cell and burner temprature are shown in the Figure 5.23. The fuel cell temprature has a linear relationship with the fuel injected to the fuel cell and power produced by stack. Since the fuel flow rate and the power are fixed, the fuel cell temprature is unchaned after reaching to the study sate. But since the gas turbine changes by changing the demand power at 20s, while gas turbine output power changes, the shaft speed changes as well as the burner fuel flow rate. By changing the burner fuel flow rate its temprature changes as well as it is seen in Figure 5.23.

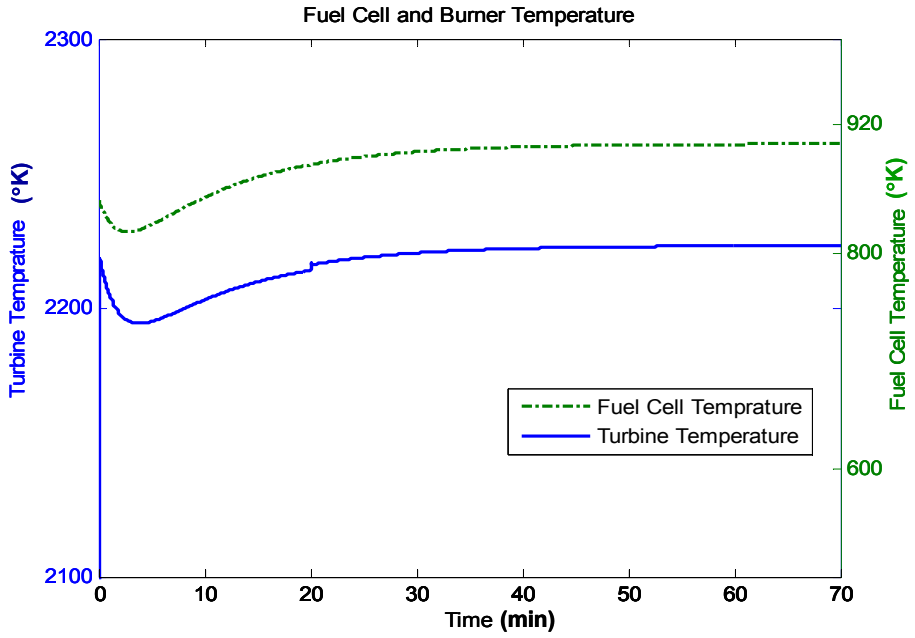

Figure 5.23. Fuel Cell and Burner Temperatures

5.3 Hybrid Power System Optimization Results

As it was mentioned in the optimization process of SOFC-GT, two different combination structures have been considered.

5.3.1 Hybrid Power System Containing Independent Generators

In the first experiment there is no interconnection between fuel cell and gas turbine. In this problem two generators introduced by their efficiency curves as it can be seen in the Figure 5.24.

The specifications of both generators are depicted in the Table (5-1). The demand power in this experiment is 300KW. The parameter that have been used for the PSO algorithm are presented in the Table (5-2). These parameters were chosen to reach the optimum solution for the efficiency in the shortest time.

Performance Index	SOFC	GT
Min Output Power	20Kw	20Kw
Max Output Power	320Kw	180Kw
Demand power	300 Kw	

Table 5.1. Hybrid Power System's generators Specifications

This data has been chosen based on general information about gas turbine and SOFC. The experiment consists of 45 iterations and there are 50 particles in the swarm. In the first iteration, the output powers are randomly initialized considering the output power limitations.

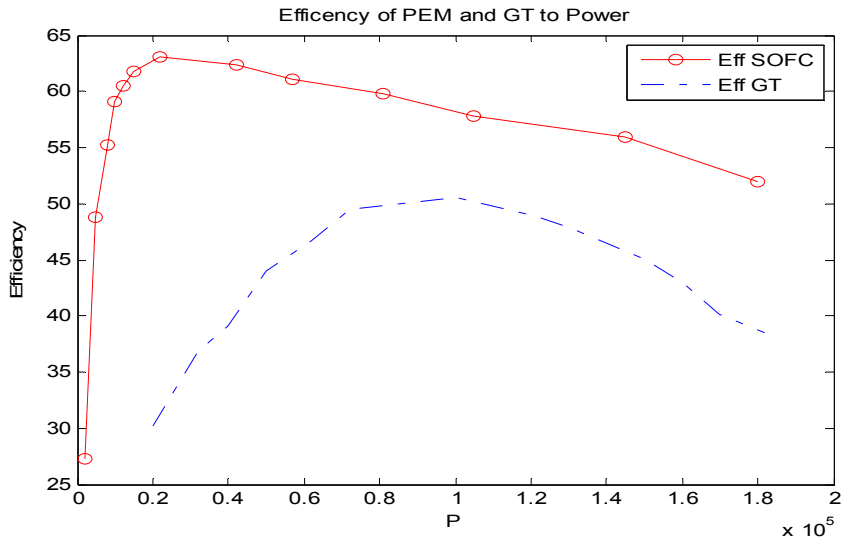

Figure 5.24. Efficiency curve for both generator in the Hybrid Power System

In the following iteration, all the particles are updated to reach the best value to maximize the efficiency.

w_{max}	0.6
w_{min}	0.1
C_1	2
C_2	2

Table 5.2. PSO Parameters

The particle movements in the swarm to reach the optimum solution for both generators are shown in the Figure 5.25. It can be seen that initial output powers meet the best position after 15 iterations.

In PSO algorithm as it was explained before, after initialization, particles update their velocity and their position respectively. As it is shown in Figure 5.25, the particles are updated in each iteration. Particles movement is going to converge to the optimum solution.

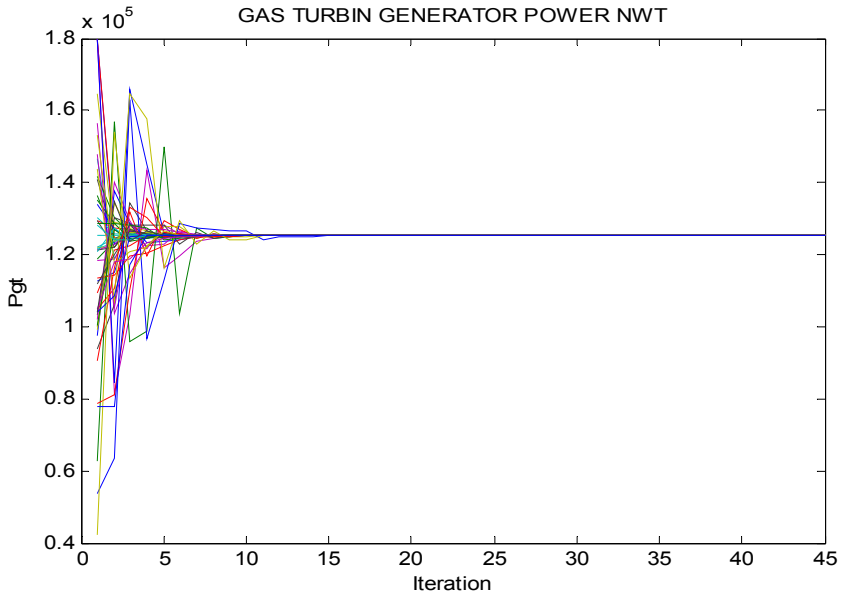

a)Output power for SOFC for different particles in the Swarm

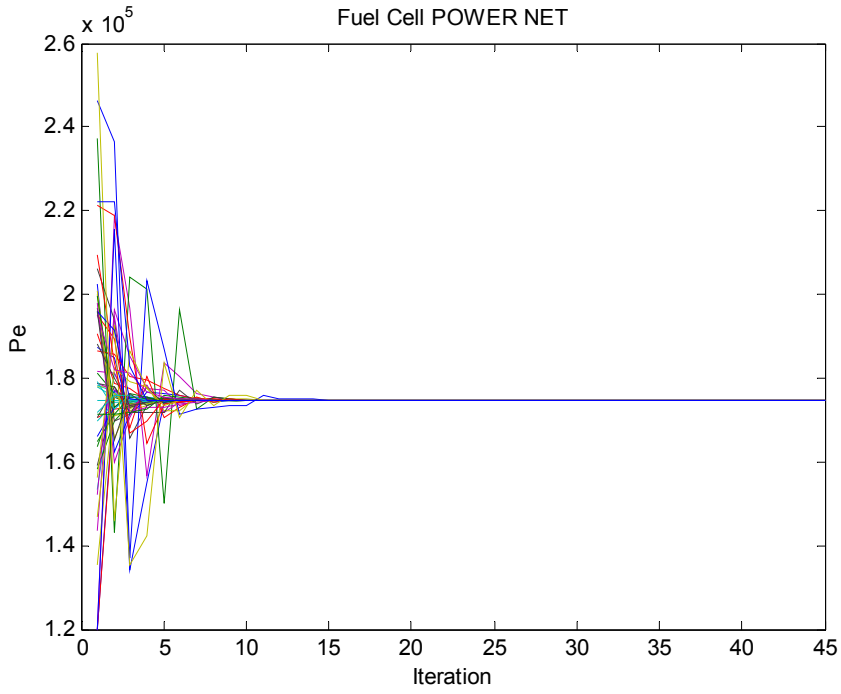

b)Output power for GT for different particles in the Swarm

Figure 5.25. Behavior of the system to find the best power output for each generators

The maximum efficiency can be reach in this problem is 50.85% as it seen in the Figure 5.26. as it was expected all the particles updated to converge to reach the maximum efficiency . In the algorithm if there is one individual which can improve the fitness function, then it will be considered as the best position in the swarm and all the movements go toward to that position (g_{best}). Therefore, to maximize the efficiency, all the particles move from the minimum amount to the best solution.

As it can be seen the efficiency for each particle is less than the maximum efficiency during in all iterations. This shows that the implied PSO algorithm is working properly.

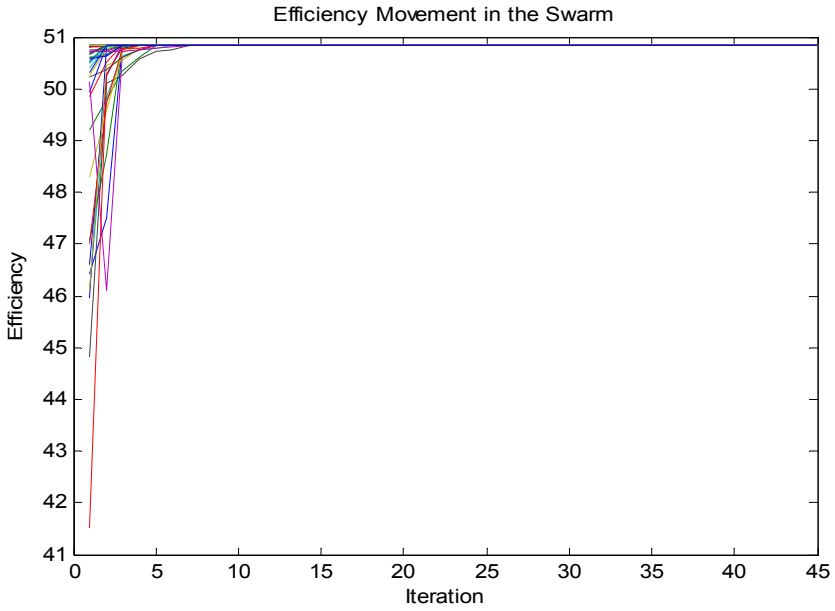

Figure 5.26. System efficiency

In Figure 5-27 the behavior of an individual (out of 50) during the PSO processing is depicted.

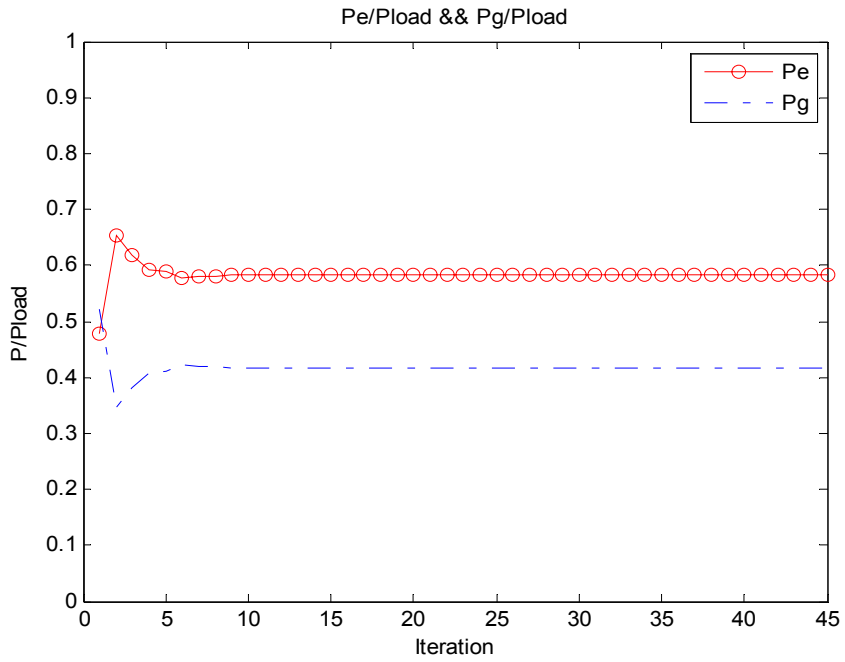

Figure 5.27. Power ratio for both Fuel Cell and GT for one particle

In next experiment, the hybrid power system had been optimized in power sharing for demand powers. The results as it shows in Figure 5.28 determine that by increasing the demand power, the efficiency of the system will be decreased.

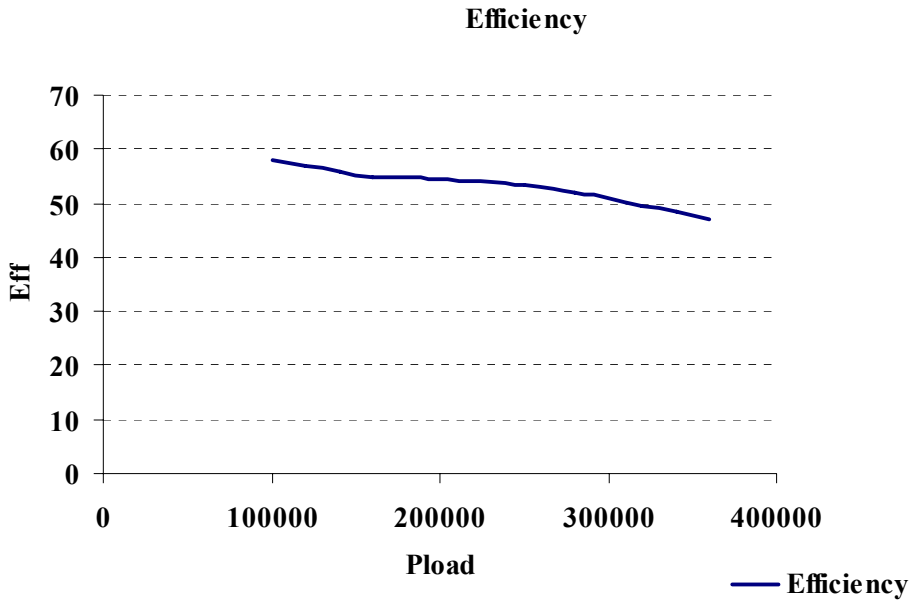

Figure 5.28. Efficiency based on different demand power

Also the power ratio after a specific demand power remains unchanged as it can be seen in Figure 5.29.

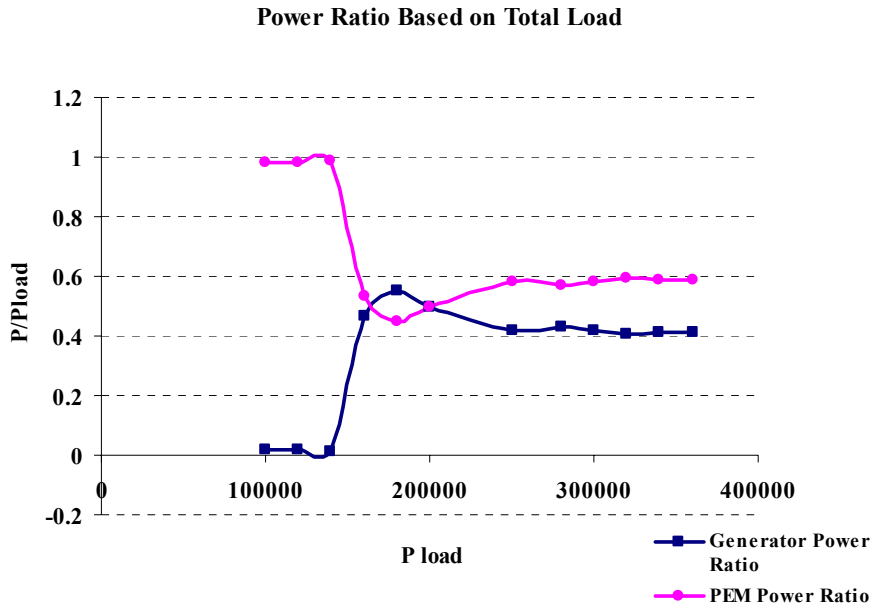

Figure 5.29. Power ratio based on different demand power

5.3.2 Hybrid Power System Containing Dependent Generators

In this configuration, the first generator (SOFC) transmits its waste fuel as well as the heat to the second one (GT). The maximum power that SOFC in this hybrid power system can produce is 80 KW. SOFC contains of 600 cells and works at around 500 V. The nominal voltage of gas turbine is 50KW and the total demand for the system is 110 KW. In this implementation the initial population size is 15 and the program stops after 20 maximum iterations.

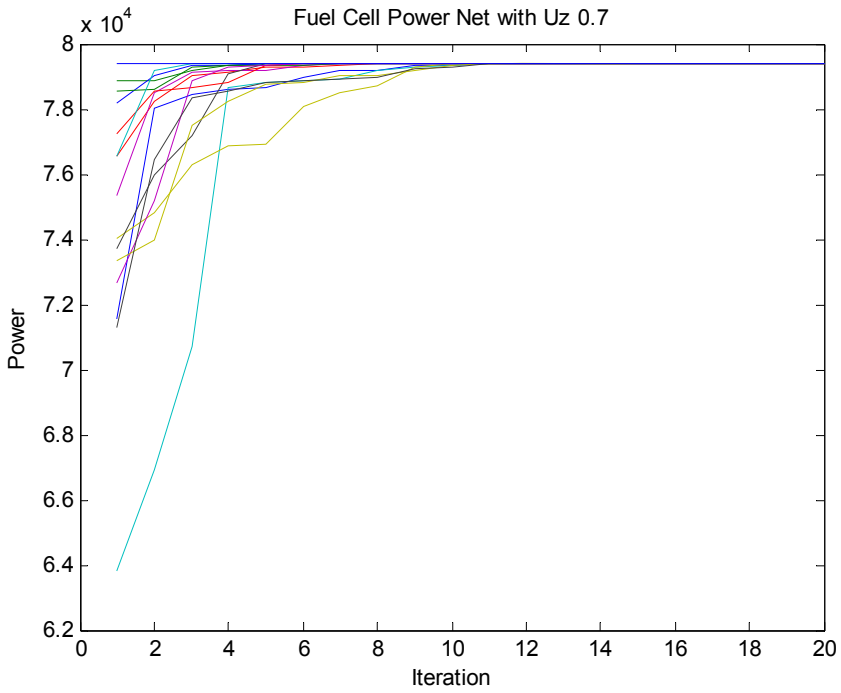

a) Fuel cell output power for different particles in the Swarm

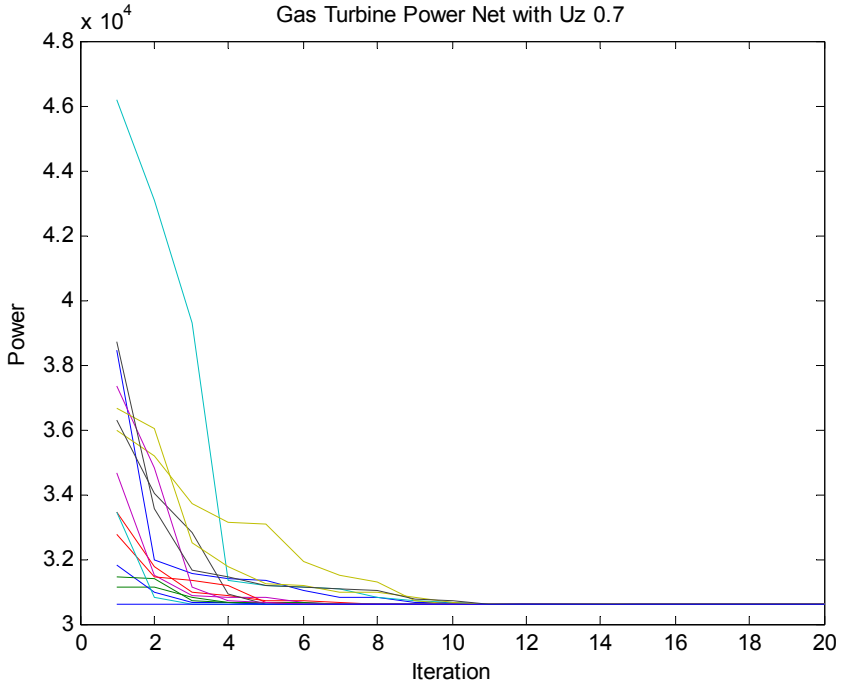

b)Gas turbine output power for different particles in the Swarm

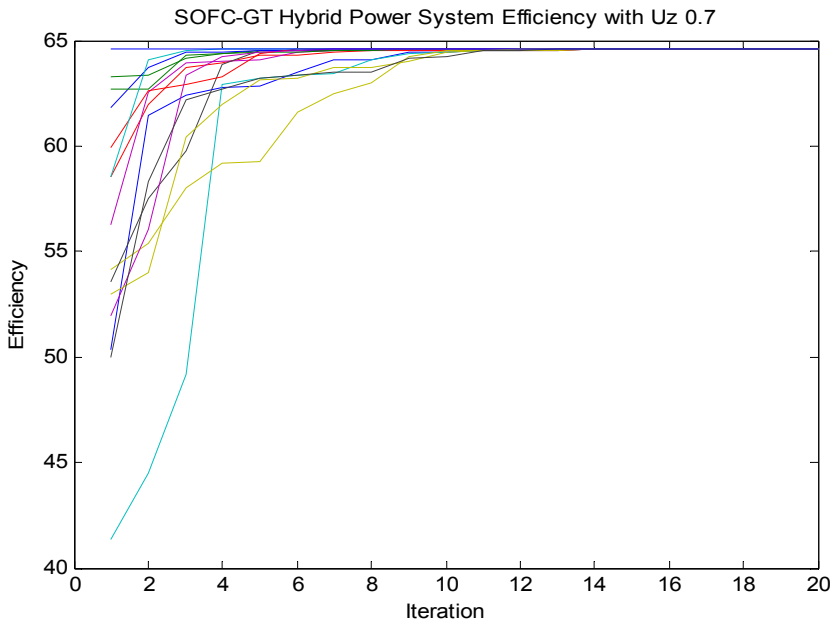

c) Optimum efficiency for the SOFC-GT hybrid power system with utilization factor 0.7

Figure 5.30. Optimum output power sharing and efficiency for the system with utilization factor 0.7

The simulation results for different utilization factor can be seen in the Figure 5.30. as it can be seen the efficiency for all the particles during the optimization process is less than the maximum efficiency, and it shows that PSO algorithm is properly applied to the problem.

The optimum efficiency in the hybrid power system with 0.7 utilization factor is around 65% as it shows in the Figure 5.30 (c).

Increasing the utilization factor has a very interesting impact on the system efficiency. The results of optimization of hybrid power system with utilization factor 0.8 and 0.9 are illustrated in the Figure 5.31 and Figure 5.31.

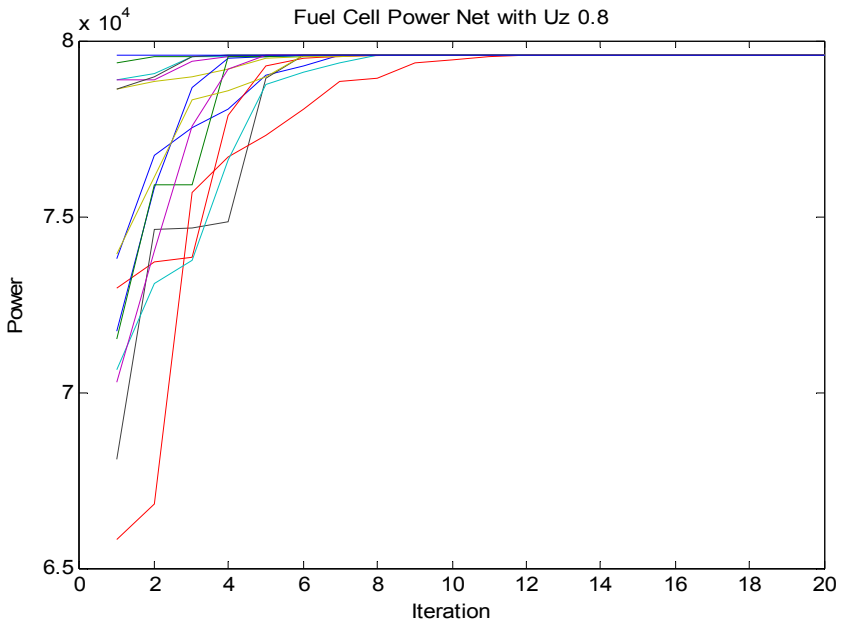

a) Fuel cell output power for different particles in the Swarm

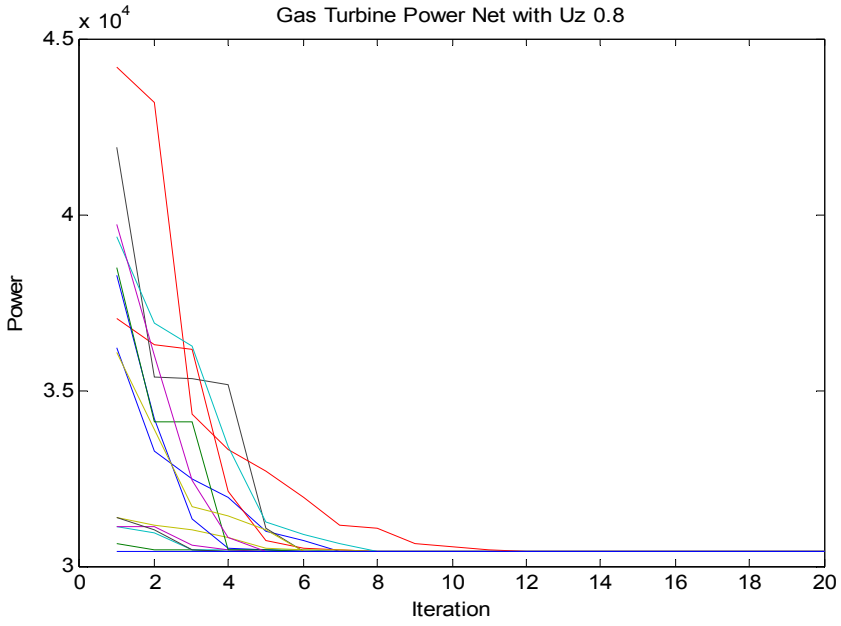

b)Gas turbine output power for different particles in the Swarm

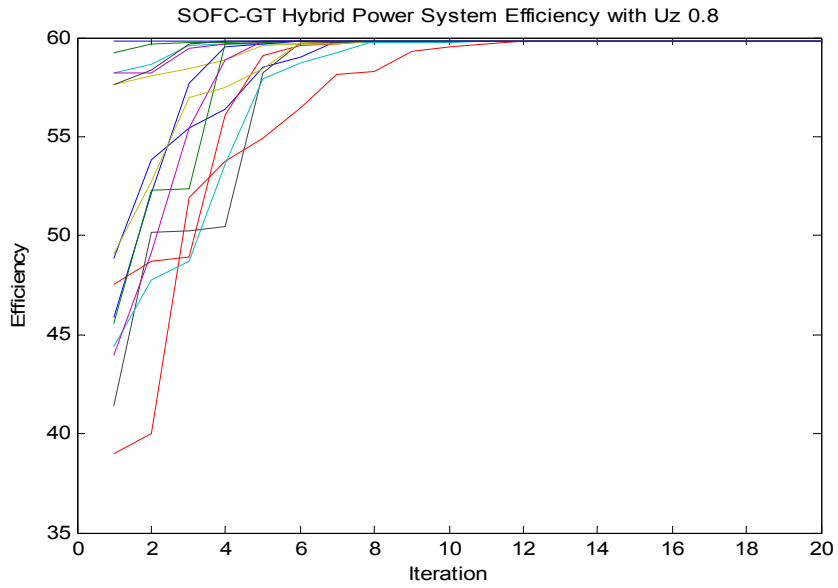

c) Optimum efficiency for the SOFC-GT hybrid power system with utilization factor 0.8

Figure 5.31. Optimum output power sharing and efficiency for the system with utilization factor 0.8

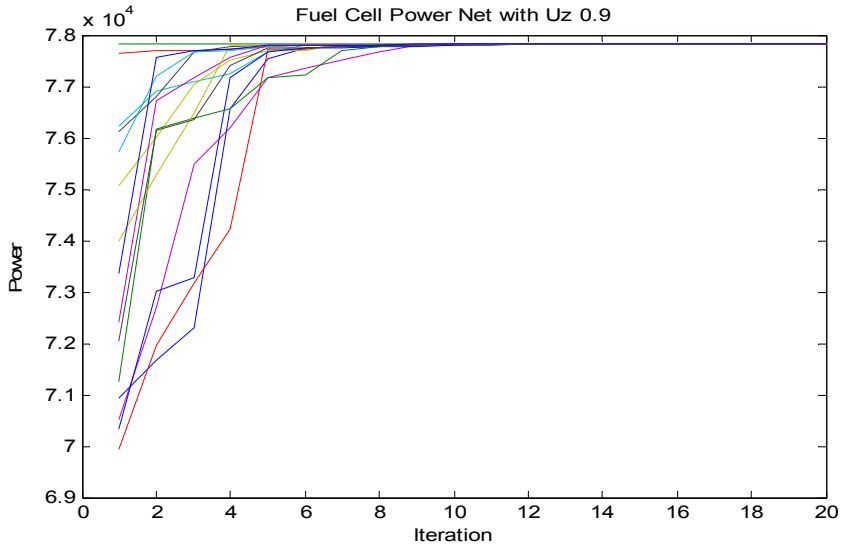

a) Fuel cell output power for different particles in the Swarm

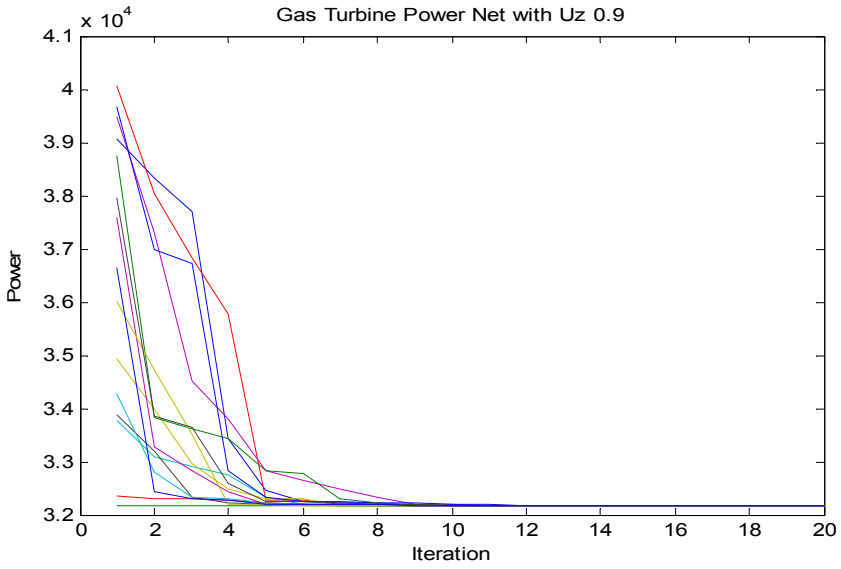

b)Gas turbine output power for different particles in the Swarm

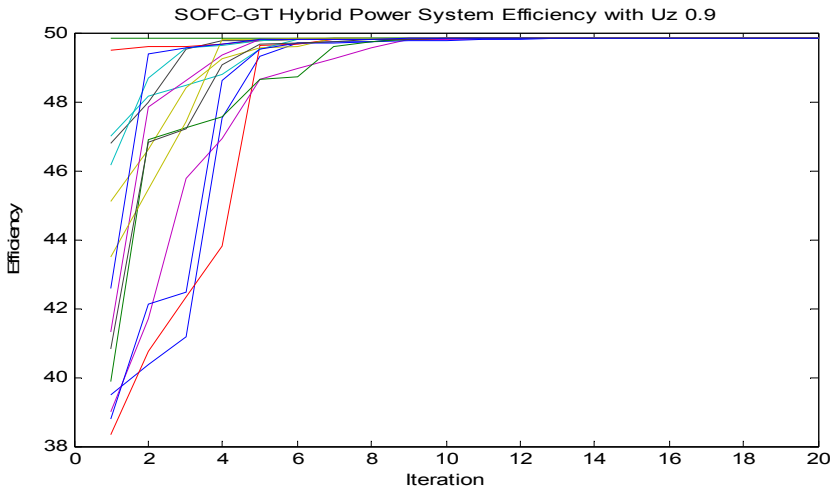

c) Optimum efficiency for the SOFC-GT hybrid power system with utilization factor 0.9

Figure 5.32. Optimum output power sharing and efficiency for the system with utilization factor 0.9

The result of these tree experiment are presented in table 5-3.

	GT	SOFC	GT	SOFC	GT	SOFC
Uz	0.7		0.8		0.9	
System Efficiency	64.9		59.8		49.8	
Fuel Flow rate	0.677	0.74	0.88	0.649	1.27	0.564
Power Sharing(KW)	30.597	79.402	30.398	79.602	32.178	77.822
Power Ratio	0.278	0.722	0.276	0.723	0.292	0.707

Table 5.3 PSO Parameters

As it is obvious from Figure 5.33,The system efficiency decreases by increasing the utilization factor.

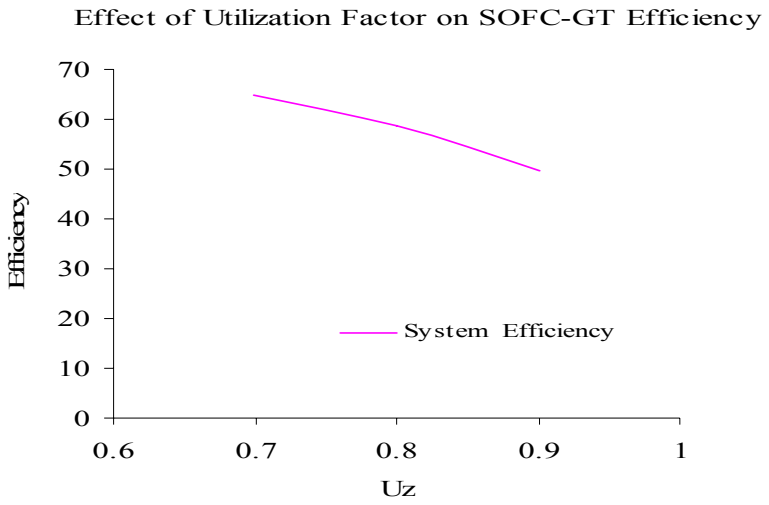

Figure 5.33. Hybrid power system eficiency based on utilization factor

As it can be seen in Figure 5.34, by increasing fuel cell utilization factor, while the power ratio for SOFC decreases, the gas turbine power ratio increases.

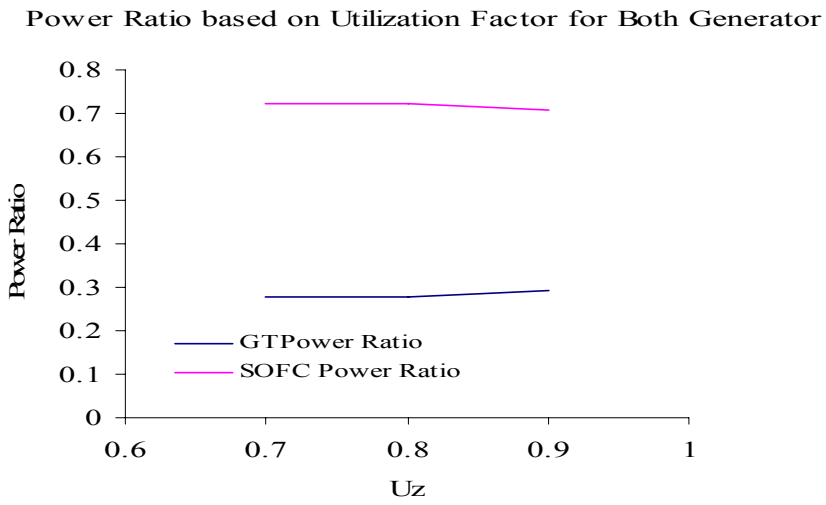

Figure 5.34. Power ratio based on utilization factor for both generator

Chapter 6

Conclusion

6.1 Summary

The fuel cell - gas turbine hybrid power system can utilize exhaust fuel and waste heat from fuel cells to increase the system efficiency. This research considers an internally reforming solid oxide fuel cell-gas turbine (SOFC-GT) hybrid system, where the anode exhaust, which contains the remainder of the fuel, is mixed with the cathode exhaust as well as an additional supply of fuel and compressed air and then burned in a catalytic oxidizer. The hot oxidizer exhaust is expanded through the turbine section, driving an electric generator. After leaving the gas turbine, the oxidizer exhaust passes through a heat recovery unit in which it preheats the compressed air that is to be supplied to the fuel cell and the oxidizer. The major conurbations in this research can be summarized as follow:

This study concentrates on multidisciplinary modeling and simulation of the fuel cell-gas turbine hybrid power system. The mathematical presented model has considered thermodynamic, electro mechanic, and electromagnetic characteristics of the system. Considering the dynamic model of the different component in the hybrid power system is one of the capabilities of this model, which provides the ability of studying the transient response of the hybrid system through time-domain simulation.

In the hybrid system, the control system plays a critical role in achieving the synergistic operation of various subsystems, improving the reliability of operation, and reducing the frequency and costs of maintenance. This work investigates different control strategies for the power sharing between the subsystems. An internally-reforming SOFC-GT hybrid power system is considered for the development of advanced control algorithms. The power electronic interfaces and controls for the hybrid power system are discussed in this research. Two different power sharing strategies are studied and compared. In the first control strategy, the exhaust from the fuel cell that contains waste fuel is injected and burned in the burner. No additional fuel is supplied to the burner. This control strategy is the simplest strategy to control the hybrid power system. Although, the design of the control system is simple, the flexibility of the system is limited. It means that the gas turbine performance depends on the fuel cell and the power sharing between the two generators is restricted since the power produced by gas turbine is dependent on the waste fuel and heat generated from the fuel cells. In the second strategy, additional fuel is supplied to the burner in addition to the exhaust from the fuel cell stack. In this strategy, the power produced by the fuel cells is maintained at a set point that can be changed during the run time by the controller. As a result, as the demand power changes, the gas turbine output power changes to produce remaining demand power. The advantage of this strategy is the rapid transient response of the hybrid system. Compared with SOFC, the transient response of the gas turbine is very fast. Therefore, keeping fuel cell output power constant during operation can help the system reach steady-state conditions rapidly. On the other hand, the complexity of the control system in this strategy is higher than the previous one. Also, considering that in some cases the gas

turbine generators have a lower efficiency, the total efficiency of the hybrid system could be reduced with this strategy. Simulation results are presented and analyzed. This study suggests that the hybrid power systems can be managed so as to achieve specified control objectives.

Power sharing is an important challenge in hybrid power systems. The demand output power is produced by the generators which make up the power system. Therefore to operate the system efficiently, the power sharing ratio should be determined appropriately. In this respect, having a reliable and simplified model for online optimization will help to improve the system optimality. The feasible solution set of this problem must be obtained while the hybrid system should meet certain power and voltage requirements. In this research PSO introduced as the optimization method for the hybrid power system. The objective of this optimization problem is to determine the optimum power sharing to increase the total efficiency of the system. PSO algorithm is implemented in Matlab and results have been presented in the previous chapter. In the optimization problem the effect of changing in the fuel cell utilization factor on the system efficiency has been studied. Based on the presented results in chapter 5, increasing the fuel cell utilization factor can cause the decrease in the system efficiency.

6.2 Future Work

Hybrid power systems have been introduced to the power industry to combine different property of various energy resources to achieve a global goal such as high power density, fast transient response, maximum efficiency, minimum emission, and minimum coast. Although the presented model can be a good reference for the study of

the hybrid power system it is not complete and there would be more work to improve the system. Also, putting more effort to study and optimize the system can help to achieve an economic and efficient system. Possible future developments, expansions, and improvements to our contributions are as follows:

The presented hybrid power system is a combination of fuel cell and gas turbine generator. The approach used here can be extended to study other hybrid power systems. For instance, an expanded hybrid power system can be introduced by adding a wind generator or solar cells.

In the modeling section the gas turbine dynamic model can be improved and studied in more detail. In the presented work the dynamic model of the heat exchanger has been not considered. Also, the generator which is used in this research is synchronous generator which needs excitation control system. Instead a permanent magnet generator can be used to reduce the complexity of the control system.

The control strategies introduced in this research are the simplest strategies for the system and have limitations. Considering different goals for the system more control strategy can be introduced. For instance, the life time live for the fuel cell is one of the aspects of study in the SOFC-GT hybrid power system. Therefore, temperature control can be one of the control strategies for this system. In this strategy the fuel cell power output will controlled in such way that the temperature would not increase more than a reference set point.

The optimization method which is used in this research can be used as the online optimization method to identify the power sharing ratio to increase the system efficiency.

Also the optimum objective function can be identified to optimize the cost and improve the economic feature of the hybrid power system.

Bibliography

[1] X. Zhang, J.li, G. Li, Z. Feng, "Dynamic Modeling Of Hybrid System Of The Solid Oxide,"

[2] R. Kandepu, L. Imsland, CH. Stiller, B. Foss, V. Kariwala, "Control-relevant Modeling and Simulation of a SOFC-GT Hybrid Power System,"

[3] Z. Chen, "High Pulse Power System Through Engineering Battery-Capacitor Combination," Energy Conversion Engineering Conference and Exhibit, 35th Intersociety, Volume 2, 24-28 July 2000 .

[4] E.A. Müller, A.G. Stefanopoulou, L. Guzzella, "Optimal Power Control of Hybrid Fuel Cell Systems for an Accelerated System Warm-Up," Control Systems Technology, IEEE Transactions on, Volume: 15, Issue: 2,2007.

[5] Eileen J. De Guire, "Solid Oxide Fuel Cells," Proquest, http://166.111.120.8/discoveryguides/fuecel/overview.php

[6] C. J. Hatziadoniu, A. A. Lobo, F. Pourboghrat, M. Daneshdoost,"A Simplified Dynamic Model of Grid-Connected Fuel-Cell Generators," IEEE Transactions On Power Delivery, VOL. 17, NO. 2, 2002

[7] C. Wang, and M.H. Nehrir, "A Physically Based Dynamic Model for Solid Oxide Fuel Cells," IEEE Transactions on Energy Conversion, VOL. 22, NO. 4, December 2007

[8] J. Padulle, G.W. Ault, J.R. McDonald, "An Integrated SOFC Plant Dynamic Model for Power Systems Simulation," Journal of Power Sources 86, 2000.

[9] M. Xu, C. Wang, Y. Qiu, B. Lu, F. C. Lee, "Control and Simulation for Hybrid Solid Oxide Fuel Cell Power Systems," Applied Power Electronics Conference and Exposition,, March 2006.

[10] Y. Qi, B. Huang , J. Luo, "Nonlinear State Space Modeling and Simulation of A SOFC Fuel Cell," American Control Conference, 2006 .

[11] D.J.Hall, R.G. Colclaser, "Transient Modeling and Simulation of a Tubular Solid Oxide Fuel Cell," IEEE Transactions on Energy Conversion, Vol. 14, No. 3, September 1999.

[12] P. Li, P. Degobert, B. Franvois, B. Robyns, "Modeling and Control of a as Micro Turbine Generator by Using a Causal Ordering Graph," IMACS Multi conference on Computational Engineering in Systems Applications(CESA), 2006.

[13] P. Zhu, H. I. H. Saravanamuttoo, "Simulation of an Advanced Twin-Spool Industrial Gas Turbine," Transactions of the ASME, 180/Vol. 114, April 1992.

[14] L J. Kerr ,T. S. Nemec, G. W. Gallops "Real-Time Estimation of Gas Turbine Engine Damage Using a Control-Based Kalman Filter Algorithm," Journal of Engineering for Gas Turbines and Power, Vol. 114/187, APRIL 1992.

[15] Kunitomi, K. Kurita, A. Okamoto, H. Tada, Y. Ihara, S. Pourbeik, P. Price, W.W. Leirbukt, A.B. Sanchez-Gasca, "Modeling frequency dependency of gas turbine output," Journal of Power Engineering Society, Volume 2, 2001

[16] B. Pongr´acz1, P. Ailer, K. M. Hangos, G. Szederk´enyi1, "Nonlinear reference tracking control of a gas turbine with load torque estimation," International Journal Of Adaptive Control And Signal Processing ,2007.

[17] Y. Zhu1 and H. C. Frey, "Simplified Performance Model of Gas Turbine Combined Cycle Systems," Journal Of Energy Engineering, 2007.

[18] V. Y. Arkov ,G. G. Kulikov , 'T. V. Breikin, P J Fleming, "Dynamic Model Identification Of Gas Turbines," UKACC International Conference on Control, 1998.

[19] C. J. Steffen, J. E. Freeh, L.M. Larosiliere ,"Solid Oxide Fuel Cell/Gas Turbine Hybrid Cycle Technology for Auxiliary Aerospace Power," American Society of Mechanical Engineers, Reno, Nevada, 2005

[20] J. E. Freeh, C. J. Steffen, L. M. Larosiliere, "Off-Design Performance Analysis of a Solid-Oxide Fuel Cell/Gas Turbine Hybrid for Auxiliary Aerospace Power," NASA/TM—2005.

[21] S. Samuelsen, "Fuel Cell/Gas Turbine Hybrid Systems," ASME International Gas Turbine Institute, 2004.

[22] K. Sedghisigarchi, "Dynamic and Transient Analysis of Power Distribution Systems with Fuel Cells—Part I: Fuel-Cell Dynamic Model," IEEE Transactions on Energy Conversion, vol. 19, no. 2, June 2004.

[23] S.h. Chan, H.K. Ho, Y. Tian, "Modeling Of A Simple Hybrid Solid Oxide Fuel Cell and Gas Turbine Power Plant," J Power Sources 109, pp. 111–120, 2002.

[24] S.H. Chan, H.K. Ho, Y. Tian, "Modeling For Part Load Operation Of Solid Oxide Fuel Cell–Gas Turbine Hybrid Power Plant," J Power Sources 114 ,2003.

[25] S.H. Chan, H.K. Ho, Y. Tian, "Multi-Level Modeling Of Sofc-Gas Turbine Hybrid System," Int. J Hydrogen Energy 28, 2003.

[26] S.H. Chan, K.A. Khor, Z.T. Xia, "A Complete Polarization Model of A Solid Oxide Fuel Cell and Its Sensitivity To The Change Of Cell Component Thickness," J Power Sources 93, 2001.

[27] A. Bejan, G. Tsatsaronis, M. Moran, "Thermal Design and Optimization," Wiley, New York (1996).

[28] S.H. Chan, C.F. Low, O.L. Ding, "Energy and Exergy Analysis Of A Simple Solid-Oxide Fuel Cell Power System," J Power Sources 103, 2002.

[29] F. Calise, M. Dentice d'Accadiaa, A. Palomboa, L. Vanolib, "Simulation And Exergy Analysis Of A Hybrid Solid Oxide Fuel Cell (SOFC)–Gas Turbine System," Energy 31, 2006.

[30] Y. A. Qengel, M. A. Boles, "Thermodynamics an Engineering Approach," McGraw-Hill, New York, 2002.

[31] Jong-Bae Park, Ki-Song Lee, Joong Rin Shin, Kwang Y.Lee, "A Particle Swarm Optimization For Economic Dispatch With Nonsmooth Cost Function," IEEE Transactions On Power System, Vol. 20, No. 1, pp. 34-42, February 2005.

[32] Jong-Bae Park, Ki-Song Lee, Joong-Rin Shin, Kwang Y. Lee, "A Particle Swarm Optimization for Economic Dispatch With Nonsmooth Cost Functions," IEEE Transactions On Power Systems, Vol. 20, No. 1, 2005.

[33] S. Naka, T. Genji, T. Yura, Y. Fukuyama, "A Hybrid Particle Swarm Optimization for Distribution State Estimation," IEEE Transactions on Power Systems, Vol. 18, No. 1, 2003.

[34] Y. W. Jeong, W. N. Lee, J.-R. Shin, J.B. Park "An Improved Particle Swarm Optimization for Economic Dispatch Problems with Non-Smooth Cost Functions," IEEE, 2006.

[35] The U.S. Department of Energy, "Vision 21 Program Plan – Clean Energy Plants for the 21st centuary," 1999.

[36] A.A. EL-Dib, H.K.M. Youssef, M.M. EL-Metwally, Z. Osman, " Maximum load ability of Power Systems Using Hybrid Particle Swarm Optimization," Electric Power Systems Research, Vol 76, Issues 6-7, pp.485-492, April 2006.

[37] Huseyin Hakan Balci, Jorge F, "Scheduling Electric Power Generators Using Particle Swarm Optimization Combined With The Lagrangian Relaxation Method," Int. J. Appl. Math. Comput. Sci., 2004, Vol. 14, No. 3, 411–421

[38] Karl O. Jones, André Bouffet, "Comparison Of Bees Algorithm, Ant Colony Optimisation And Particle Swarm Optimisation For Pid Controller Tuning," International Conference on Computer Systems and Technologies - CompSysTech'08

[39] Ziegler, J.G. and Nichols, N.B. 1942. "Optimum settlings for automatic controllers," ASME Transactions, (Vol. 64) , pp. 759-768.

[40] Y. Fukuyama, et al , "A Particle Swarm Optimization For Reactive Power And Voltage Control Considering Voltage Security Assessment," IEEE Trans. Power Syst., vol. 15, pp. 1232–1239, Nov. 2000.

[41] M. Y. El-Sharkh, ,M. Tanrioven A. Rahman,M. S. Alam, "A Study of Cost-Optimized Operation of a Grid-Parallel PEM Fuel Cell Power Plant," IEEE Transactions On Power Systems, Vol. 21, No. 3, August 2006

[42] Lingfeng Wang; Singh, C. "PSO-based Hybrid Generating System Design Incorporating Reliability Evaluation and Generation/Load Forecasting," Power Tech, 2007 IEEE Lausanne 1-5 July 2007 Page(s):1392 - 1397

[43] Shigenori Naka, Takamu Genji, Toshiki Yura, and Yoshikazu Fukuyama, "A Hybrid Particle Swarm Optimization for Distribution State Estimation," IEEE Transactions On Power Systems, Vol. 18, No. 1, February 2003

[44] W. H. E. Liu, et al., "A Practical State Estimation Algorithm For Distribution Management Systems," in Proc. 13th Power Syst. Comput. Conf., June 1999.

[45] Yaofan Yi, Ashok D. Rao, Jacob Brouwer and G. Scott Samuelsen, "Analysis and optimization of a solid oxide fuel cell and intercooled gas turbine (SOFC–ICGT) hybrid cycle," Journal of Power Sources, 132, 77–85, 2004.

[46] I. Jadric, "Modeling and Control of a Synchronous Generator with Electronic Load," Master thesis, Virginia Polytechnic Institute and State University, January 5, 1998.

[47] P. M. Anderson, B. L. Van Agrawal and J. E. Ness, "Sub synchronous Resonance in Power Systems," IEEE Press, New York, 1989.

[48] R. P. Schulz, "Synchronous Machine Modeling," IEEE Symposium on Adequacy and Philosophy of Modeling, IEEE Publications,75CH0970-4-PWR, pp. 24-28.

[49] S. B. Papaefthimiou, "Simulation And Control Of A Variable Speed Wind Turbine With Synchronous Generator," Diploma Thesis, NTUA, September 2005.

[50] Y. Yu, "Electric Power System Dynamics," New York: Academic Press, 1983.

[51] Enrique L. Carrillo Arroyo, "Modeling And Simulation Of Permanent Magnet Synchronous Motor Drive System," Master These, University Of Puerto Rico,2006.

[52] Zhenhua Jiang, "Design of Power System Stabilizers Using Synergetic Control Theory," Power Engineering Society General Meeting, IEEE Publication, 2007.

[53] Z. Ye, "Modeling and Control of Parallel Three-phase PWM Converters," PHD Dissertation, Virginia Polytechnic Institute and State University, Sep 2000.

[54] W. Shao, Z. Xu, "Excitation System Parameter Setting for Power System Planning", IEEE Power Engineering Society Summer Meeting, July 2002.

[55] P.J.H. Wingelaar, J.L. Duarte, M.A.M. Hendrix ,"Dynamic Characteristics of PEM Fuel Cells," Power Electronics Specialists Conference, June 2005

[56] A. Giustiniani, G. Petrone, C. Pianese, M. Sorrentino, G. Spagnuolo, M. Vitelli, "PEM Fuel Cells Control by means of the Perturb and Observe Technique," IEEE Industrial Electronics, IECON, 2006.

[57] M. Kirkman, "The Use Of Simulation In The Design Of Modern Gas Turbine Control Systems," Integrated Systems in Aerospace, Digest No: 1997/015, IEEE Colloquium, 1997.

[58] K. Sedghisigarchi,.A .Feliachi, A. Fernandes, K. Schoder, "Gas Turbine Control and Load Sharing for Shipboard Power Systems," Power Engineering Society General Meeting, 2007.

[59] EG&G Technical Services, Inc, "Fuel Cell Handbook (Seventh Edition)," Under Contract No. DE-AM26-99FT40575, November 2004.

[60] F. Calise, M. Dentice d'Accadiaa, L.Vanoli, M. R. Spakovsky, "Full Load Synthesis/Design Optimization of a Hybrid SOFC–GT Power Plant," Energy 32: 446–458, 2007.

[61] J. Palsson, A. Selimovic, L Sjunnesson, "Combined Solid Oxide Fuel cell and Gas Turbine Systems for Efficient Power and Heat Generation," Journal of Power Sources;86:442–8, 2000.

[62] F. Calise, M. Dentice d'Accadia, A. Palomboa, L. Vanoli, "Simulation and Exergy Analysis of a hybrid Solid Oxide Fuel Cell (SOFC)–Gas Turbine System," Energy Volume 31, Issue 15, December 2006.

[63] S. Chan, H. Ho, Y. Tian, "Modeling For Part Load Operation Of Solid Oxide Fuel Cell–Gas Turbine Hybrid Power Plant," J Power Sources, 114:213–27. 2003.

[64] S. Chan, H. Ho, Y. Tian, "Multi-Level Modeling Of Sofc-Gas Turbine Hybrid System," Int'l Journal of Hydrogen Energy 28:889–900, 2003.

[65] M. Xu, C. Wang, Y. Qiu, B. Lu, F. C. Lee, "Control and Simulation for Hybrid Solid Oxide Fuel Cell Power Systems," Center for Power Electronics Systems, 2006.

[66] K. Sedghisigarchi, "Dynamic and Transient Analysis of Power Distribution Systems with Fuel Cells—Part I: Fuel-Cell Dynamic Model," IEEE Transactions on Energy Conversion, vol. 19, no. 2, June 2004.

[67] R. E. Sonntag, and G. V. Wylen, "Introduction to Thermodynamics classical & Statistical," New York: John Wiley & Sons, 1982.

[68] P. Li, P. Degobert, B. Franvois, B. Robyns, "Modeling and Control of a as Micro Turbine Generator by Using a Causal Ordering Graph," IMACS Multiconference on Computational Engineering in Systems Applications"(CESA), 2006.

[69] M. Fleming, A. Hiskens, "Dynamics of a Microgrid Supplied by Solid Oxide Fuel Cells," iREP Symposium Charleston, South Carolina, USA, Aug 2007.

[70] P. Buasri, and Z. M. Salameh , "An Electrical Circuit Model for A Proton Exchange Membrane Fuel Cell (PEMFC) ," Power Engineering Society General Meeting, IEEE Vol. , Iss. , 18-22, June 2006.

[71] Z. Jiang, R. A. Dougal, S. Liu, S. A. Gadre, A. D. Ebner, J. A. Ritter, "Simulation of a Thermally Coupled Metal-hydride Hydrogen Storage and Fuel Cell System," Journal of Power Sources, 142, 92–102, 2005.

[72] Y. Yu, "Electric Power System Dynamics," New York: Academic Press, 1983.

[73] Z. Ye, "Modeling and Control of Parallel Three-phase PWM Converters," PHD Dissertation, Virginia Polytechnic Institute and State University, Sep 2000.

[74] W. Shao, and Z. Xu, "Excitation System Parameter Setting for Power System Planning," IEEE Power Engineering Society Summer Meeting, July 2002.

[75] I. Jadric, "Modeling and Control of a Synchronous Generator with Electronic Load," Master thesis, Virginia Polytechnic Institute and State University, 1998.

[76] S. M. Mikki ,A. A. Kishk, " Particle Swarm Optimization: A Physics-Based Approach," Morgan & Claypool Publishers, 2008.

[77] M.G. Pangalis, R.F. Martinez-Botas, N.P. Brandon, "Integration of Solid Oxide Fuel cells into Gas Turbine Power Generation Cycles. Part I: Fuel Cell thermodynamic Modeling," Journal Power and Energy, 2002.